6-2019

Investigation of ceria-nickel containing aerogels for catalytic converter applications

Xiao Peng Li
Union College - Schenectady, NY

Investigation of ceria-nickel containing aerogels for catalytic converter applications

By

Xiao Peng Li

****

Submitted in partial fulfillment
of the requirements for
Honors in the Department of Chemistry

UNION COLLEGE

June, 2019

ABSTRACT

LI, XIAO PENG Investigation of ceria-nickel containing aerogels for catalytic converter applications. Department of Chemistry, June 2019.

ADVISOR: Professor Mary K. Carroll

Aerogels have physical properties that make them appealing for automotive exhaust catalysis: they are highly porous with low density and high surface area. Current catalytic converter technology uses precious metals (Pt, Pd and Rh) to oxidize CO and unburned hydrocarbons and reduce NO. Catalytic-metal-containing aerogel can potentially be a less expensive alternative for use in catalytic converters. Prior work with nickel-alumina aerogels indicated promise for this application; the goal of including ceria is to increase oxygen storage and thereby enhance catalytic ability. Here, cerium- and nickel-containing aerogels, with an alumina backbone and silica backbone, are fabricated using an epoxide-assisted recipe and characterized for this application. The precursors for the aerogel, hydrated salts of aluminum chloride, cerium(III) chloride and nickel (II) nitrate, are dissolved in reagent-grade ethanol, to which propylene oxide is added. Wet gels are prepared with different molar ratios of cerium to nickel (25:75, 50:50, 75:25). Following solvent exchange, the metal-containing wet gels are processed into aerogels using a rapid supercritical extraction method and calcined at 800˚C for 24 h. Physical characterization of the aerogels before heat treatment, after heat treatment, and after UCAT testing involved FTIR, XRD, SEM, and EDX. Catalytic testing of the aerogels is performed using an in-house-constructed catalytic testbed under exposure to simulated automotive exhaust.

ACKNOWLEDGEMENTS

I want to thank my advisor, Professor Mary Carroll for her guidance and knowledge throughout the research and writing of this thesis. I want also like to thank Professor Ann Anderson and Professor Bradford Bruno for their support and assistance throughout this research project. This project would not have been made possible without the Professors' dedicated involvement.

I want to thank the members of the Aerogel Lab, particularly Christ Avanessian for his assistance in the SEM and EDX imaging and Ryan Puglisi, Matt LaRosa, and Christopher O'Brien for their assistance in the UCAT tests.

TABLE OF CONTENTS

TABLE OF FIGURES

TABLE OF TABLES

1. Introduction

1.1. Thesis Goals

The goal of the research is to fabricate, physically characterize, and catalytically test alumina and silica-based aerogels containing cerium oxide (ceria) and nickel nitrate. These aerogels will be prepared using the Union College patented Rapid Supercritical Extraction (RSCE) technique.[1] Physical characterizations that will be performed include bulk density, BET surface area, X-ray powder diffraction, infrared spectroscopy, and scanning electron microscopy (SEM). The aerogels will be catalytically tested in the Union College Aerogel Testbed (UCAT) to assess the reduction of nitrogen oxides (NO) and oxidation of hydrocarbons (HC) and carbon monoxide (CO). The long-term goal is that these metal-containing aerogels can potentially replace the precious metals, platinum, palladium, and rhodium in current catalytic converters.

1.2. Catalytic Converters

A catalytic converter is a device that performs redox reactions to convert toxic gases such as NO, HC, and CO into less harmful gases such as carbon dioxide (CO_2), nitrogen gas (N_2), and water vapor (H_2O). Toxic gases such as NO when released in air can react with other organic compounds in air, forming smog.[2] Additionally, the NO can react with sulfur dioxide in the air to produce acid rain, which is destructive because acid rain can corrode infrastructures. CO and HC gas are poisonous to humans. exposing the human body to HC gas can lead to nervous system impairments and cardiovascular problems.[2] In a catalytic converter, approximately 98% of the harmful causes are converted to less harmful gases.[2] There are five major components in a catalytic

converter: the substrate, the support, the stabilizers, the base metal promoters, and platinum group metals.[3] A typical composition of a catalytic converter is a metal housing with ceramic honeycomb-like interior with insulating layers.[2] The honeycomb-line interior has an aluminum oxide washcoat on the surface.[2] The aluminum oxide washcoat is porous and increases surface area.[2] The porosity and high surface area of the washcoat aid in increasing the redox reactions in the catalytic converters. The chemistry behind the catalytic converters is that nitrogen oxides are reduced to elemental nitrogen and oxygen, carbon monoxide is oxidized to carbon dioxide, and hydrocarbons are oxidized to carbon dioxide and water vapor.[2] Representative gas-phase chemical equations can be found in eq. 1, 2, and 3.

$$2NO \rightarrow N_2 + O_2 \qquad (\mathbf{1})$$

$$CO + O_2 \rightarrow CO_2 \qquad (\mathbf{2})$$

$$C_3H_8 + 5O_2 \rightarrow 3CO_2 + 4H_2O \qquad (\mathbf{3})$$

Catalytic converters are currently found in almost every device/vehicle that has an internal combustion engine.[2] Some examples of devices/vehicles that have an internal combustion engine are generators, buses, trucks, and trains.[2] The problem with the current catalytic converters is that the precious metals platinum, rhodium, and palladium are environmentally damaging to mine, and they are expensive. In a catalytic converter, the precious metals inside can easily be sold for $200 apiece, and the metals can be salvaged for as much as $1000 in a single catalytic converter.[4] Therefore, inexpensive metal-containing aerogels can be a more environmentally friendly, and less expensive alternative to the current precious metals used in catalytic converters.

Less expensive metal catalysts such as cerium and nickel have pros and cons. The losses of inexpensive metals are more tolerable in an industrial process, which can eliminate recycling steps currently used for salvaging precious metals from catalytic metals.[5] Inexpensive metals are not widely used today for several reasons. For example, inexpensive metals have not been widely studied, and the selectivity of inexpensive metal catalysts may not be as good as to the precious metals.[5] To increase the reactivity of inexpensive metals, the concentration of the metals can be increased and/or the loading capacity of the catalysts can be increased.[6] However, a higher catalyst loading can result in negating the cost advantage of inexpensive metals.[5]

1.3. Aerogels

Aerogels are highly porous, amorphous materials that are 90-99% air by volume. The benefits of aerogels are that they have high surface area, low density, and low thermal conductivity. These physical features of aerogels allow for their use in heterogeneous catalysis applications.[7] For example, high surface area is important because it contributes to high reactivity.[8] Aerogel was first discovered in the 1930's by Kistler.[9]

Currently, aerogels are synthesized using the sol-gel method. For certain aerogels, to create a wet gel, first the precursors are hydrolyzed by having their alkoxide groups replaced with hydroxyl groups. Then polymerization occurs, and an acid or base is added to the mixture to catalyze the polymerization. If the solvents are removed from the pores of the sol-gel matrix without collapsing the matrix, one produces an aerogel. One method to remove the solvents is through supercritical extraction, whereby the solvents in the

pores of the wet gel are transformed from liquid to supercritical fluid and extracted from the matrix without pore collapse. Supercritical CO_2 extraction is the conventional way to do this, but that method requires solvent exchanges prior to extraction method. However, the disadvantages of the supercritical extraction method were the time required and solvent waste produced during the solvent exchange process.[10] The supercritical extraction method can take a few days to prepare an aerogel.

The method to produce aerogels in this experiment is to use the RSCE method patented by Union College. This method uses a hydraulic hot press to make an aerogel.[1] In the RSCE method, the precursor mixture or wet gels are placed into a steel mold. The mold is then sealed in the hot press using graphite, Kapton or stainless-steel foil. The hydraulic press applies high temperature and high pressure over a course of ~4 h to produce an aerogel.[1] During the process, the solvent mixture in the wet gels are brought above its critical point, and the solvents are extracted from the pores of the wet gel in the supercritical phase, leaving an aerogel. The RSCE method is faster and environmentally safer method, due to reducing the time and product waste, to make an aerogel compared to the supercritical CO_2 method.

The types of aerogels that will be focused on in this research are ceria- and nickel-containing aerogels. Ceria-containing materials have been shown to undergo rapid change between oxidation states Ce^{4+} and Ce^{3+}, which means ceria-containing aerogels are potentially good for automotive catalysis.[10] Cerium has already been implemented in alumina washcoats to enhance thermal stability of the current catalytic metals in catalytic converters.[11,12] The redox reaction of cerium oxides usually takes place at high temperature (>600°C) and/or at low oxygen partial pressure. Studies have shown that

oxygen atoms can be released by electrical fields in cerium oxide, which can also result in decreasing the operation temperature.[13]

Previous studies in the Union College Aerogel Laboratory with catalytic-containing aerogels involved one type of metal in the aerogels. For example, ceria-containing aerogels were physically characterized and catalytically tested in a thesis by Luisa Fernanda Posada.[10] The catalytic testing results from ceria-containing alumina aerogels reached a 50% conversion of NO at 450°C, and NO has a 99% conversion at 600°C.[10] CO reached a 50% conversion at 350°C and 100% conversion at 600°C.[6] HC has a 50% conversion at 550°C and 84% conversion at 650°C.[10] Therefore, ceria-containing alumina aerogels showed promising NO and CO conversions, but not HC conversion.

Another metal that will be focused on in this research is nickel. Nickel is a transition metal that has a good catalytic performance and moderate reaction conditions. It has been shown before that Ni-based catalysts deactivate at temperature above 600°C; therefore, to improve the stability of Ni-based catalysts, different metal oxides can be used, such as aluminum oxide and cerium oxide.[14] Nickel-alumina aerogels have proven to show reactivity for CO and NO conversion.[15] Nickel-alumina aerogels have been studied at Union by Nicholas Dunn and Stephen Juhl previously. Dunn performed physical characterization of nickel-alumina aerogels with FTIR, XRD, SEM, EDX, and GC-MS.[16] However, Dunn did not catalytically test the performance of nickel-alumina aerogels. Juhl also worked with nickel-alumina aerogels, where he physically characterized and catalytically tested them under different conditions than are currently employed in the UCAT system. The catalytic testing results from nickel-containing

alumina aerogels reached a 50% conversion of NO conversion at 600℃.[17] CO reached a 50% conversion at 450℃ and 80% conversion at 600℃.[6] HC has an 8% conversion at 600℃.[17] Since nickel-alumina aerogels have proven to show reactivity for CO and NO conversion, nickel-containing aerogels may be promising in acting as a heterogeneous catalysis in catalytic converters.

Ceria-containing aerogels and nickel-containing aerogels have shown promising NO and CO conversions. In this thesis, I focus on incorporating these two metals into aerogels in hope of increasing conversion rate at a lower temperature. This research will contribute to the growing library of the physically characterized and catalytically tested metal-containing aerogels.

References

1. Ben M. Gauthier, Smitesh D. Bakrania, Ann M. Anderson, and Mary K. Carroll. "Simplified Technique for Fabricating Aerogel Monoliths Using Fast Supercritical Extraction." *J. Non-Cryst. Solids* (2004) 350, 238.

2. Raph H. Petrucci, William S. Harwood, and Geoff E. Herring. "General Chemistry: Principles and Modern Applications." 9th ed. *Upper Saddle River: Prentice Hall*, 2006.

3. John S. Howitt. "Thin Wall Ceramics as Monolithic Catalyst Supports". S.A.E. Paper No. 800082, 1980.

4. Elizabeth Donlon

5. B. J. Cooper, W. D. J. Evans, and B. Harrison. "Catalysis in Automotive Pollution Control", ed. A. Oucq and A. Frennet, Elsevier, 1987.

6. Khalil T. Hassan, Jiabin Wang, Xiao Han, Jon J. Sharp, Gaurav A. Bhaduri, Vladimir Martis, and Lidija Siller. "Catalytic Performance of Nickel Nanowires Immobilized in Silica Aerogels for the CO2 Hydration Reaction." *ACS Omega* (2019) *4* (1), 1824-1830 DOI: 10.1021/acsomega.8b03361

7. Theodore F. Baumann, Alex E. Gash, and Joe H. Satcher. "A Robust Approach to Inorganic Aerogels: The Use of Epoxides in Sol-Gel Synthesis." In *Aerogels Handbook*. Ed. Michel A. Aergerter, Nicholas Leventis, and Matthias M. Koebel. *New York: Springer* (2011): 155-170. Print.

8. Connie M. Y. Yeung, Kai Man K. Yu, Qi Jia Fu, David Thompsett, Michael I. Petch, and Shik Chi Tsang. "Engineering Pt in Ceria for a Maximum Metal−Support Interaction in Catalysis." *Journal of the American Chemical Society* (2005) *127* (51), 18010-18011. DOI: 10.1021/ja056102c

9. Samuel S. Kistler. "Coherent Expanded Aerogels." *J. Phys. Chem*. 36, 52-64

10. Luisa F. Posada, Mary K. Carroll, Ann M. Anderson, Bradford A. Bruno, "Inclusion of ceria in alumina- and silica-based aerogels for catalytic applications." In press, J. Supercrit. Fluids https://doi.org/10.1016/j.supflu.2019.05.004

11. Grigorios C. Koltsakis and Anastasios M. Stamatelos. "Catalytic Automotive Exhaust Aftertreatment." *Prog. Energy Combust. Sci.* (1997) 23: 1-39.

12. Harrison B., Diwell A. F., Hallet, C. “Promoting Platinum Metals by Ceria Metal-Support Interactions in Autocatalysts.” *Platinum Metals Rev.* (1988), 32, (2).

13. Peng Gai, Zhenchuan Kang, Wangyang Fu, Wenlong Wang, Xuedong Bai, and Enge Wang. “Electrically Driven Redox Process in Cerium Oxides.” *J. AM. CHEM. SOC. (*2010) 132: 4197-4201.

14. Binying Gao, I-Wen Wang, Lili Ren, Thomas Haines, and Jianli Hu. “Catalytic Performance and Reproducibility of Ni/Al2O3 and Co/Al2O3 Mesoporous Aerogel Catalysts for Methane Decomposition.” *Industrial & Engineering Chemistry Research* (2019) *58* (2), 798-807 DOI: 10.1021/acs.iecr.8b04223

15. S. Krompiec, J. Mrowiec-Bialon, K. Skutil, A. Dukowitz, L. Pajak, and A.B. Jarzebski, 2004. “Nickel-alumina composite aerogel catalysts with a high nickel load: a novel fast sol-gel synthesis procedure and screening of catalytic properties.” *J. Non-Cryst. Solids* 315, 297-303

16. Nicholas J. H. Dunn. “Alumina-Based Aerogels by Rapid Supercritical Extraction for use in Green Automotive Catalysis.” Senior Thesis, Union College, June 2011

17. Stephen Juhl. “Morphosynthesis and Characterization of Alumina-Based Aerogels for Automotive Catalysis.” Senior Thesis, Union College, June 2012.

2. Experimental

2.1. Materials

The precursors for the aerogel were aluminum chloride hexahydrate ($AlCl_3 \bullet 6H_2O$), cerium (III) chloride heptahydrate ($CeCl_3 \bullet 7H_2O$), nickel (II) nitrate hexahydrate ($Ni(NO_3)_2 \bullet 6H_2O$), and tetramethyl orthosilicate (TMOS). All the precursors were purchased from Sigma-Aldrich. The solvents used were reagent-grade ethanol (EtOH, 99%) from Fisher Scientific, absolute ethanol from Pharmco-AAPER, HPLC grade methanol (MeOH) from Fisher Scientific, and in-house deionized water (DI water). The catalysts used for gelation were propylene oxide (>99%) from Sigma-Aldrich and 1.5-M ammonia. The 1.5-M ammonia were made by diluting concentrated ammonia purchased from Sigma-Aldrich to 1.5 M with DI water. All other chemicals were used without further purification.

The alumina-based gels were prepared by tweaking the sol-gel fabrication recipe listed in Posada's thesis paper.[1] The complete alumina recipe can be found in Table 1.

Table 1. Recipes for alumina-based sol-gel fabrication.

Aerogel Type*	$AlCl_3$•$6H_2O$ (g)	$CeCl_3$•$7H_2O$ (g)	$Ni(NO_3)_2$•$6H_2O$ (g)	Reagent EtOH (mL)	Propylene Oxide (mL)
50:50 CeNiAl	4.52	1.08	0.843	40	8
75:25 CeNiAl	4.52	1.62	0.422	40	8
25:75 CeNiAl	4.52	0.540	1.26	40	8
3x50:50 CeNiAl	4.52	3.24	2.53	40	8
NiAl	4.52	---	1.69	40	8

*50:50, 75:25, 25:75 are the mole ratios of ceria to nickel salt respectively. The total moles of metal salt in each aerogel batch is 0.0058 moles. 3x50:50 indicates that the sample contains three times the amount of ceria and nickel at a 50:50 ratio of ceria and nickel salt, respectively.

The parameters for the hydraulic hot press can be found in Table 2.

Table 2. The hot press parameters for the gels.[2]

Step #	**Temperature**		**Rate of Temperature**		**Force**		**Rate of Force**		**Time (hr:min:s)**
	℉	**℃**	**℉/min**	**℃/min**	**kips**	**kN**	**kips/min**	**kN/min**	
1	90	32	500	278	45	200	600	2669	01:01:00
2	480	250	4	2.2	45	200	1	4.5	00:30:00
3	480	250	200	111	1	4.5	1	4.5	00:15:00
4	100	38	4	2.2	1	4.5	600	2669	00:01:00
5 (End)	0	0	0	0	0	0	0	0	0

2.2. 50% Ceria 50% Nickel Alumina Aerogel (50:50)

A 40-mL batch of 50% ceria 50% nickel alumina wet gel was prepared by dissolving 4.52 g $AlCl_3 \bullet 6H_2O$, 1.08 g (0.00290 moles) of $CeCl_3 \bullet 7H_2O$, and 0.843 g (0.00290 moles) of $Ni(NO_3)_2 \bullet 6H_2O$ in 40 mL of reagent-grade ethanol. After all the solutes are completely dissolved, 8 mL of propylene oxide was added to the solution. The solution gelled within 5 min, and the wet gel was aged for 24 h. After 24 h, three solvent exchanges, each of 40 mL absolute ethanol, were performed over the course of three days. After the solvent exchanges, the 50:50 ceria-nickel-alumina wet gel was put into a steel mold, and then the hydraulic hot press.

The steel mold was sealed with a 0.001”-thick stainless steel foil sheet on top of the steel mold, and then a 0.08”-thick graphite sheet on top of the aluminum foil. The parameters for the hydraulic hot press were inputted, and that information can be found in Table 2. The resulting aerogel samples were placed in crucibles and heat-treated in a Thermolyne furnance at a constant 800°C for 24 hr. The aerogel was characterized before heat treatment and after heat treatment.

2.3. 75% Ceria 25% Nickel Alumina Aerogel (75:25)

A 40-mL batch of 75% ceria 25% nickel alumina wet gel was prepared by dissolving 4.52 g $AlCl_3 \bullet 6H_2O$, 1.62 g (0.00435 moles) of $CeCl_3 \bullet 7H_2O$, and 0.422 g (0.00145 moles) of $Ni(NO_3)_2 \bullet 6H_2O$ in 40 mL of reagent-grade ethanol. After the solids dissolved, 8 mL of propylene oxide was added to the solution. The solution gelled within 5 min, and the rest of the procedure to create an alumina aerogel is the same as **50:50**. The aerogel was characterized before heat treatment and after heat treatment at 800˚C.

2.4. 25% Ceria 75% Nickel Alumina Aerogel (25:75)

A 40-mL batch of 25% ceria 75% nickel alumina wet gel was prepared by dissolving 4.52 g $AlCl_3 \bullet 6H_2O$, 0.540 g (0.00145 moles) of $CeCl_3 \bullet 7H_2O$, and 1.26 g (0.00435 moles) of $Ni(NO_3)_2 \bullet 6H_2O$ in 40 mL of reagent-grade ethanol. After the solids dissolved, 8 mL of propylene oxide was added to the solution, and the solution gelled within 5 min. The rest of the procedure to create an alumina aerogel is the same as for the **50:50** aerogels. The aerogel was characterized before heat treatment and after a 24-h heat treatment at 800˚C.

2.5. 3x-50% Ceria 50% Nickel Alumina Aerogel (3x50:50)

A 40 mL batch of 3x-50% ceria 50% nickel alumina wet gel was prepared by dissolving 4.52 g $AlCl_3 \bullet 6H_2O$, 3.24 g (0.00870 moles) of $CeCl_3 \bullet 7H_2O$, and 2.53 g (0.00870 moles) of $Ni(NO_3)_2 \bullet 6H_2O$ in 40 mL of reagent-grade ethanol. After the solids dissolved, 8 mL of propylene oxide was added to the solution, and the solution gelled within 5 min. The rest of the procedure to create an alumina aerogel is the same as for the **50:50** aerogels. The aerogel was characterized before heat treatment and after a 24-h heat treatment at 800˚C.

2.6. Nickel Alumina Aerogel (NiAl)

A 40-mL batch of nickel-alumina wet gel was prepared by dissolving 4.52 g $AlCl_3 \bullet 6H_2O$, 1.69 g (0.00579 moles) of $Ni(NO_3)_2 \bullet 6H_2O$ in 40 mL of reagent-grade ethanol. After the solids dissolved, 8 mL of propylene oxide was added to the solution, and the solution gelled within 5 min. The rest of the procedure to create an alumina

aerogel is the same as for the **50:50** aerogels. The aerogel was characterized before heat treatment and after a 24-h heat treatment at 800˚C.

2.7. 50% Ceria 50% Nickel Silica Aerogel (50:50SI)

The **50:50SI** gel recipe is different than the alumina based gels. The recipe was modified based on Lusia Posado's recipe, and the total mole of the ceria and nickel salt is 0.01338 mole.[1] A 40-mL batch of 50% ceria 50% nickel silica wet gel was prepared by initially dissolving 2.495 g (0.00669 moles) of $CeCl_3 \bullet 7H_2O$ and 1.945 g (0.00669) of $Ni(NO_3)_2 \bullet 6H_2O$ in 20 mL of reagent-grade ethanol and 1.97 mL of water. In a separate container, 8.5 mL of TMOS, 8.5 mL of reagent-grade ethanol, 0.153 mL of DI water, and 5.35 of propylene oxide were mixed. Then, the mixtures were combined together and 3 more mL of propylene oxide was added to the combined mixture. After gelation, the rest of the procedure to create an alumina aerogel is the same as for the **50:50** aerogels. The aerogel was characterized before heat treatment and after a 24-h heat treatment at 800˚C.

2.8. Infrared Spectroscopy (IR)

The infrared spectra were taken using a Nicolet iS5 FT-IR Spectrometer with an iD5 Attenuated Total Reflection (ATR) accessory. IR spectra were taken pre- and post-heat-treatment for all the aerogels. The EZ OMINC program was used to collect the spectra using 32 scans and 4 cm^{-1} resolution. The spectra were exponentially smoothed by adding an exponential trend line using Excel.

2.9 X-ray Powder Diffraction (XRD)

The X-ray powder diffraction patterns were obtained with a Phillips PW-1840 X-ray with a copper radiation source. XRD patterns were taken pre- and post-heat-treatment for all the aerogel samples. The aerogels samples were placed in a silicon type sample holder, and the XRD patterns were taken from 2 to 90 degrees at a rate of 0.2 degrees per minute with a tube voltage of 45 keV and a 40 mA. The patterns were smoothed by adding an exponential trend line using Excel.

2.10. Scanning Electron Microscopy (SEM).

Scanning electron microscopy (SEM) images were collected using a Zeiss EVO50. SEM images were taken pre- and post-heat-treatment for all the aerogel samples at voltages between 12-15 kV and with a spot size of 429. The images were taken ranging from 300 nm to 100 micrometers.

2.11. Electron-Dispersive X-ray Spectroscopy (EDX)

Electron-Dispersive X-ray spectra were obtained using a Bruker Quantax 200 EDX system with a Peltier-cooled XFlash silicon drift detector attachment. EDX images were taken pre- and post-heat treatment for all the aerogel samples. The primary elements of focus were aluminum, cerium and nickel.

2.12. Union Catalytic Aerogel Testbed

Catalytic tests were performed using the Union Catalytic Aerogel Testbed (UCAT) under two conditions: with air (with oxygen) and without air (without oxygen).[2] The tests was performed post-heat treatment, usually three times, for the aerogel samples. The aerogels samples were put into a steel sample holder, and a mixture of NO, C_3H_8, CO, CO_2, and N_2 was flowed through the sample holder between 200℃ to 600℃ in increments of 50℃. The gas pollutant concentrations can be found in Table 3 and the UCAT inputs and test parameters can be observed in Table 4.

Table 3. The gas pollutant concentrations used during catalytic testing.[3]

Gas	Partial Pressure
NO	2.52
C_3H_8	1.02
CO	7.54_5
CO_2	68.5
N_2	$101._5$

Table 4. UCAT user inputs and test parameters.[3]

Input	Values
Reactor Volume	Varies
Space Velocity	20
Standard Temperature (K)	298
Air Blend Ratio	0.017
Temperature Range (°C)	200-600
ΔT (°C)	50

The concentration of each gas at the inlet and outlet of the UCAT test section was measured with an Infrared Industries FGA4000XDS Gas Analyzer five-gas analyzer. The partial pressure values of the gas pollutants are hand recorded at the varying test temperatures. A table of percent conversion vs. temperature ℃ was plotted for each aerogel sample and the total percent conversion of HC, NO, CO was calculated using Excel. The light-off temperature is defined as the temperature at which the percent conversion of the gas pollutants for each aerogel sample reaches 50%.

References

1. Luisa F. Posada, Mary K. Carroll, Ann M. Anderson, Bradford A. Bruno, "Inclusion of ceria in alumina- and silica-based aerogels for catalytic applications." In press, J. Supercrit. Fluids https://doi.org/10.1016/j.supflu.2019.05.004

2. Bradford A. Bruno, Ann M. Anderson, Mary K. Carroll, Paul Brockmann, Thomas Swanton, Isaac A. Ramphal, Timothy Palace. "Benchtop Scale Testing of Aerogel Catalysts." *SAE Technical Paper*, 2016, 2016-01-920.

3. Jiaer Xu and Allison King. "UCAT 3.0 Test Procedure (As of June 2018)". Laboratory Manual, Union College, June 2018.

3. Results & Discussion

3.1. Aerogel Samples

Ceria-nickel-containing alumina aerogels at varying mole ratios were successfully synthesized. In Figure 1, the images of the 50:50 CeNiAl wet gel, the aerogel, the aerogel before heat treatment, and the aerogel after heat treatment can be observed.

(a) (b) (c) (d)

Figure 1. Images of (a) 50:50CeNiAl wet gel, (b) 50:50CeNiAl aerogel, (c) 50:50 CeNiAl aerogel before heat treatment, and (d) 50:50CeNiAl aerogel after heat treatment.

As can be seen in Figure 1a, the 50:50 CeNiAl wet gel had a green color to it. After processing in the hydraulic hot press, the aerogel came out beige in color. The aerogel color is homogenous throughout. As can be observed by the difference between Figure 1c and Figure 1d, the aerogel shrank more than half in volume after heat treatment.

In Figure 2, the images of the 75:25 CeNiAl wet gel, the aerogel, the aerogel before heat treatment, and the aerogel after heat treatment can be observed.

(a) (b) (c) (d)

Figure 2. Images of (a) 75:25 CeNiAl wet gel, (b) 75:25 CeNiAl aerogel, (c) 75:25 CeNiAl aerogel before heat treatment, and (d) 75:25 CeNiAl aerogel after heat treatment.

The 75:25 CeNiAl wet gel was more yellow than green (Fig. 2a), and the aerogel came out beige as observed in Figure 2b, which is similar in color to the 50:50 CeNiAl aerogel in Figure 1b. Like the other alumina aerogels, after heat treatment, the aerogel shrank more than half in volume. The sample does not appear to be homogenous in color after heat treatment as observed in Figure 2d.

In Figure 3, the images of the 25:75 CeNiAl wet gel, the aerogel, the aerogel before heat treatment, and the aerogel after heat treatment can be observed.

(a) (b) (c) (d)

Figure 3. Images of (a) 25:75CeNiAl wet gel, (b) 25:75CeNiAl aerogel, (c) 25:75CeNiAl aerogel before heat treatment, and (d) 25:75CeNiAl aerogel after heat treatment.

As observed in Figure 3a, the 25:75CeNiAl wet gel sample was a light green color. After putting the wet gel sample in the hydraulic hot press, the aerogel was a dirty, green color, as observed in Figure 3b. Additionally, the sample also changed to a teal color after heat treatment as observed in Figure 3d. Like the other alumina aerogel samples, the 25:75 CeNiAl shrank more than half in volume after the heat treatment.

In addition to synthesizing 50:50 CeNiAl, 3x 50:50 CeNiAl were also made. The 3x-50:50 CeNiAl samples have three times as much Ce and Ni salt compared to the 50:50 CeNiAl sample, but with the same molar ratio, and photographs of these materials can be observed in Figure 4.

(a) (b) (c) (d)

Figure 4. Images of (a) 3x-50:50 CeNiAl wet gel, (b) 3x-50:50 CeNiAl aerogel, (c) 3x-50:50 CeNiAl aerogel before heat treatment, and (d) 3x-50:50 CeNiAl aerogel after heat treatment.

As observed in Figure 4a, the wet gel is a light green color. Unlike the wet gel, the 3x-50:50 CeNiAl aerogel is a whitish, light beige color (Figure 4b). It can be observed in Figure 4c and Figure 4d that after the aerogel samples were heat-treated, the aerogels shrunk to more than half of their volume. The aerogel sample changed from a white color to a non-uniform beige color after heat treatment (Figure 4d).

Similar to the other alumina aerogels, the NiAl aerogels shrunk after heat treatment (see Figures 5a and 5b). A shrinkage test was done on the NiAl to find the potential loss in mass and volume. It was calculated that the NiAl lost approximately 30% percent by mass and 70-75% by volume.

(a) (b)

Figure 5. Images of NiAl aerogel (a) before heat treatment and (b) after heat treatment.

In Figure 5a, the NiAl aerogel before heat treatment is a light bluish, green color. After heat treatment, the aerogel turned into a teal color as observed in Figure 5b.

In Figure 6, the images of the 50:50 CeNiSi wet gel, the aerogel, the aerogel before heat treatment, and the aerogel after heat treatment can be observed.

(a) (b) (c) (d)

Figure 6. Images of (a) 50:50 CeNiSi wet gel, (b) 50:50 CeNiSi aerogel, (c) 50:50 CeNiSi aerogel before heat treatment, and (d) 50:50 CeNiSi aerogel after heat treatment.

The 50:50 CeNiSi wet gel are greenish, yellow (Fig. 6a), and the aerogel came out murky, grey with a beige, powdered coating as observed in Figure 6b. Like the other alumina aerogels, after heat treatment, the aerogel shrank, but the silica-based aerogels did not shrink more than the alumina-based aerogels. After heat treatment, the overall color became darker compared to the sample before heat treatment.

Although the RSCE method was supposed to extract the solvents within the pores of the aerogels without shrinkage, there may potentially be solvent still left in the pores in the aerogels or the solvent was adsorbed from the atmosphere in the laboratory. Therefore, when the aerogels were heated in an 800℃ furnace, the evaporation of the solvent may have caused the pores in the aerogel to collapse. The removal of adsorbed solvent from the pores and/or the structural change that involves decomposition of the aerogel will result in the loss of mass and volume.

3.2. Infrared Spectroscopy (IR)

IR spectra were taken for all the aerogel samples. The IR spectra of 50:50 CeNiAl aerogel as prepared and after heat treatment can be observed in Figures 7 and 8, respectively.

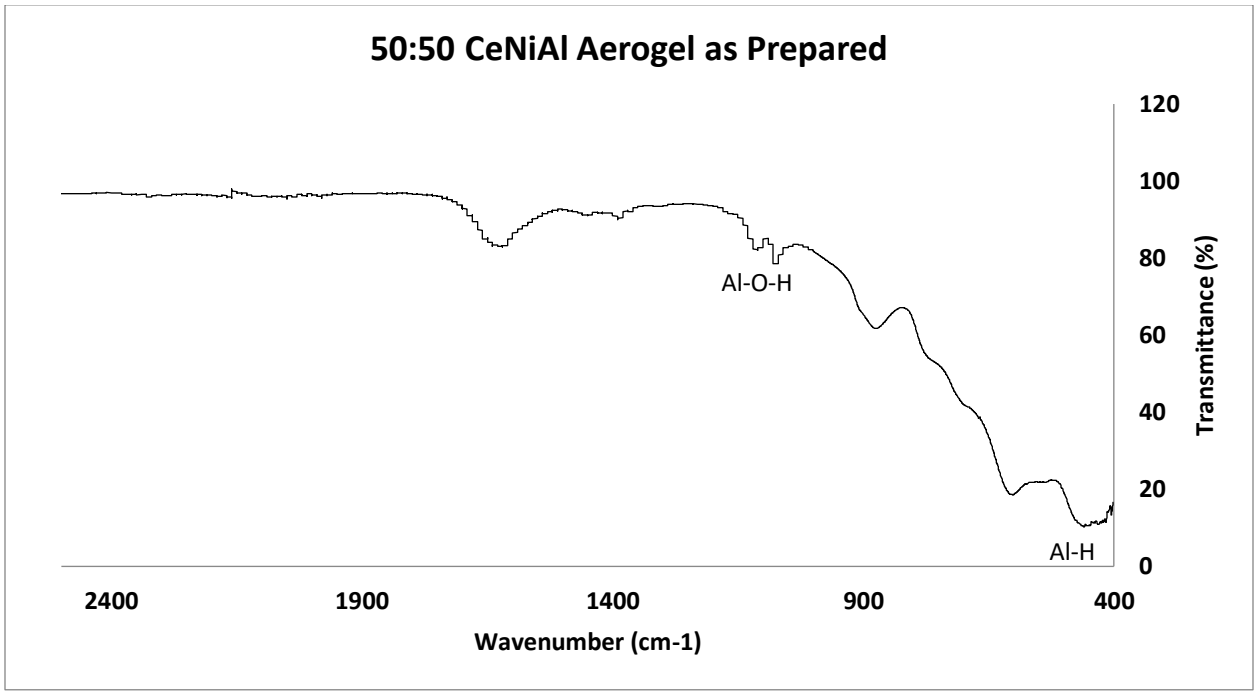

Figure 7. The IR spectrum of 50:50 CeNiAl aerogel before heat treatment.

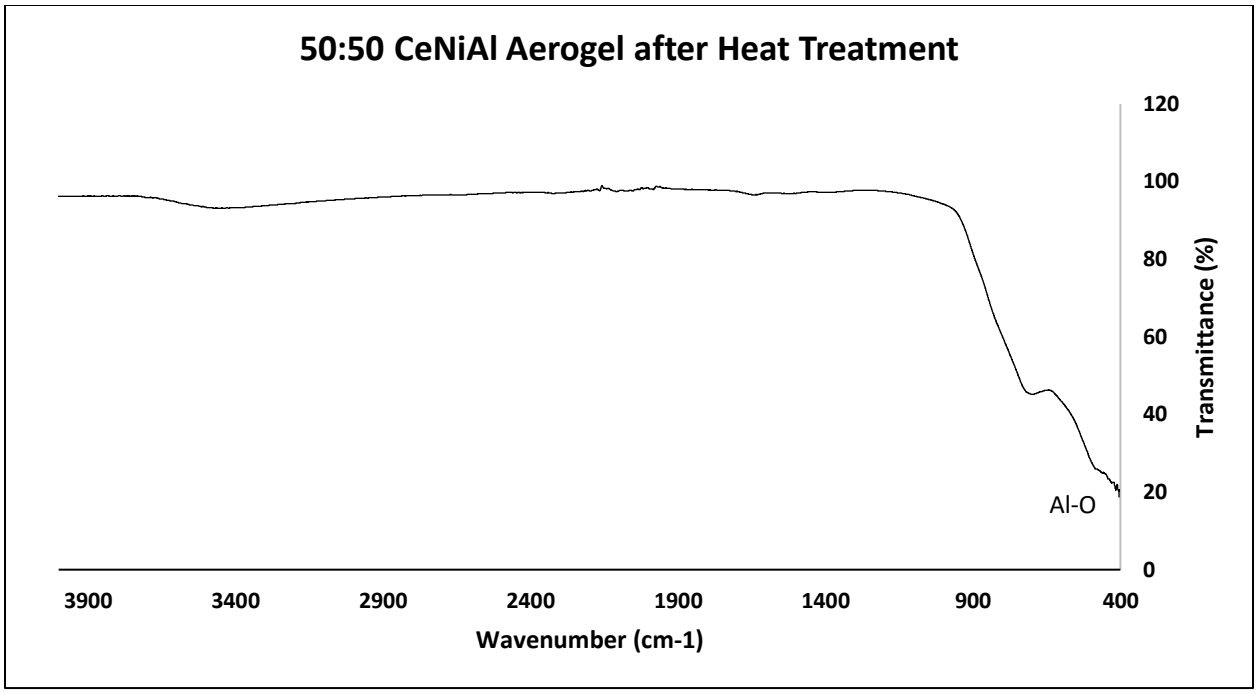

Figure 8. The IR spectrum of 50:50 CeNiAl aerogel after heat treatment.

In Figure 7, the IR spectrum of 50:50 CeNiAl aerogel before heat treatment Al-O-H and Al-H stretches can be identified at around 1000 cm^{-1} and 460 cm^{-1} respectively.[2] In Figure 8, an Al-O stretch can be observed at approximately 450 cm^{-1}.[2]

The IR spectra of 75:25 CeNiAl aerogel as prepared and after heat treatment can be observed in Figures 9 and 10, respectively.

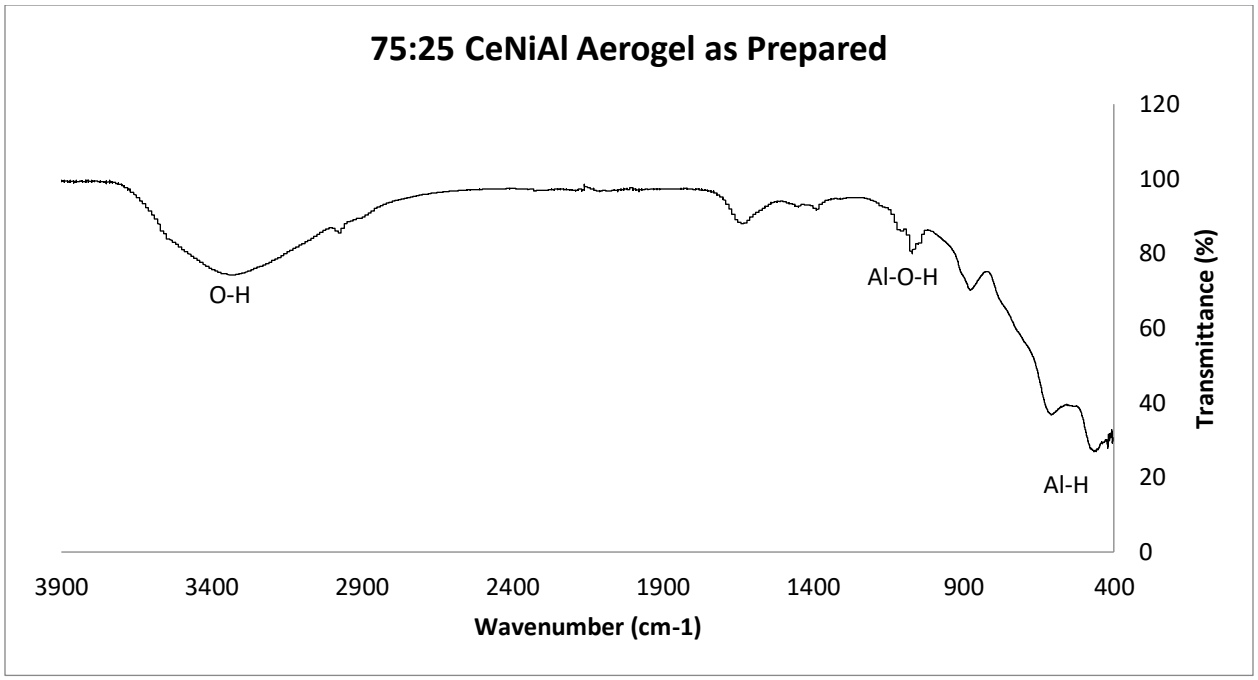

Figure 9. The IR spectrum of 75:25 CeNiAl aerogel before heat treatment.

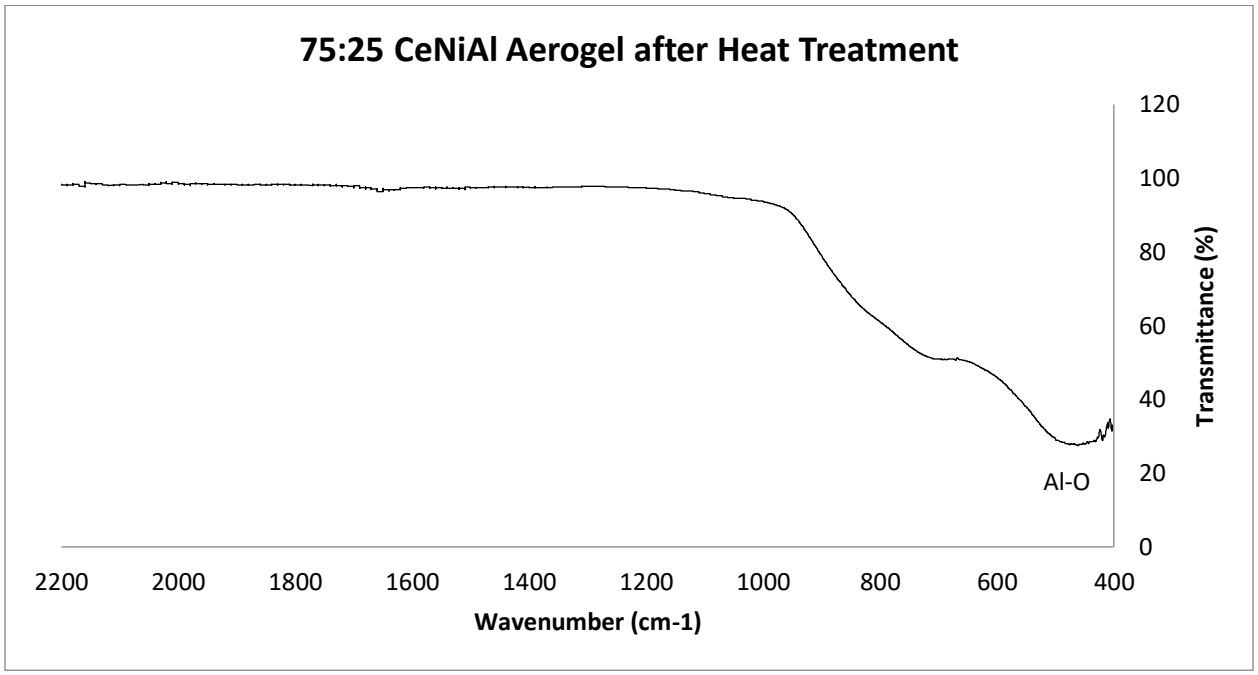

Figure 10. The IR spectrum of 75:25 CeNiAl aerogel after heat treatment.

In Figure 9, an O-H stretch attributed to water can be identified at around 3400 cm^{-1}, an Al-H stretch around 460 cm^{-1}, and an Al-O-H stretch can be identified at around 1000 cm^{-1} for 75:25 CeNiAl aerogel before heat treatment.[2] The width of the O-H stretch indicates that the O-H groups are undergoing considerable hydrogen bonding. After heat treatment, the O-H stretch disappeared, and an Al-O stretch can be identified at around 450 cm^{-1}.[2]

The IR spectra of 25:75 CeNiAl aerogel as prepared and after heat treatment can be observed in Figures 11 and 12 respectively.

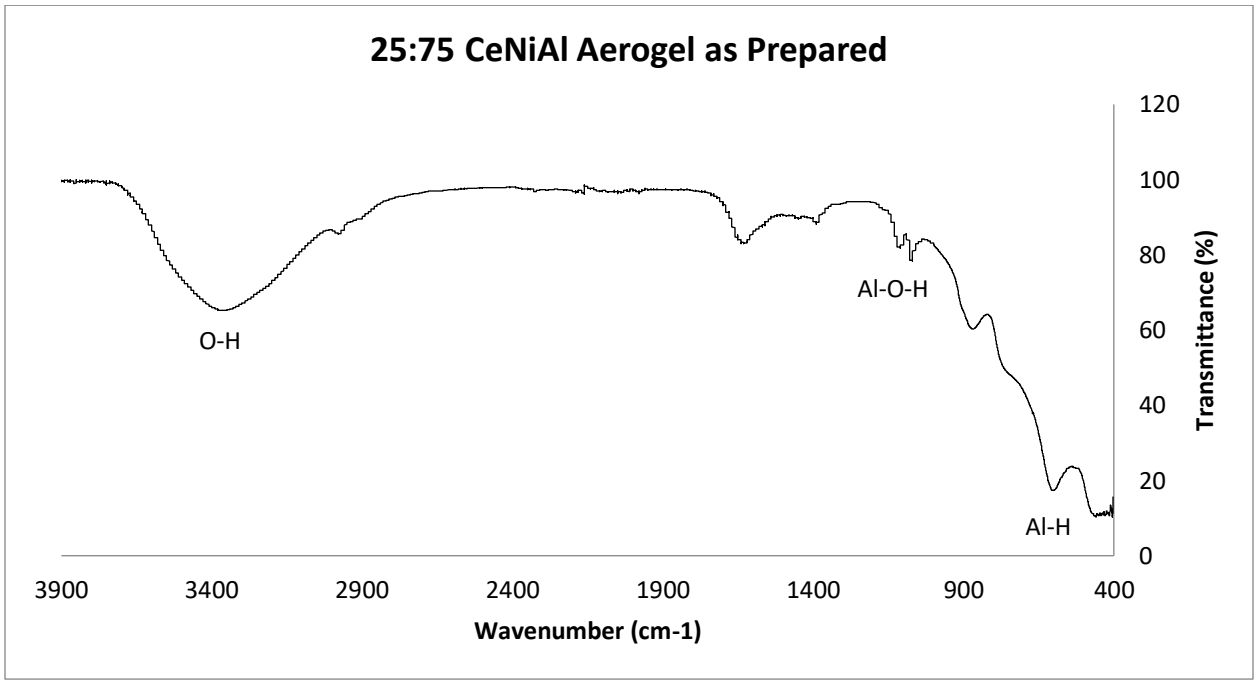

Figure 11. The IR spectrum of 25:75 CeNiAl aerogel before heat treatment.

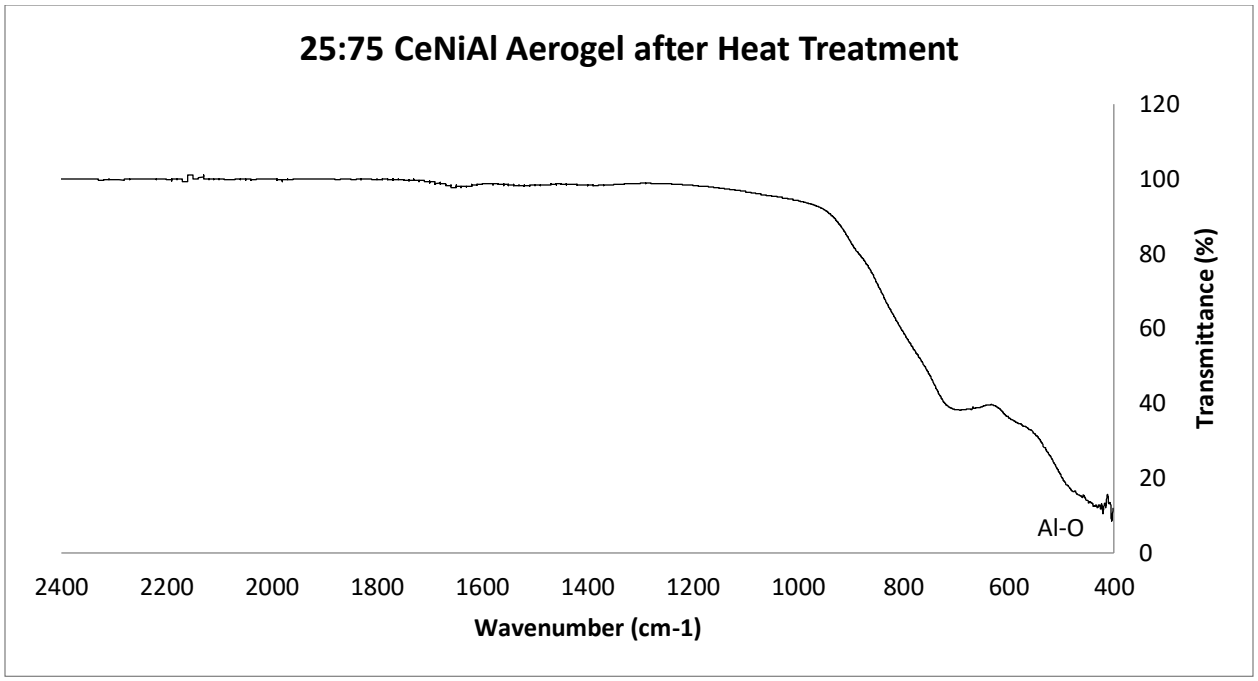

Figure 12. The IR spectrum of 25:75 CeNiAl aerogel after heat treatment.

In Figure 11, similar to the 75:25 CeNiAl aerogel before heat treatment IR spectrum, a broad O-H stretch attributed to water can be identified at around 3400 cm^{-1}, and an Al-O-H stretch can be identified at around 1000 cm^{-1} for 25:75 CeNiAl aerogel.[2] After heat treatment, the O-H stretch disappeared, and an Al-O stretch can be identified at around 500 cm^{-1} in Figure 12.[2]

The IR spectra of 3x-50:50 CeNiAl aerogel as prepared and after heat treatment can be observed in Figures 13 and 14, respectively.

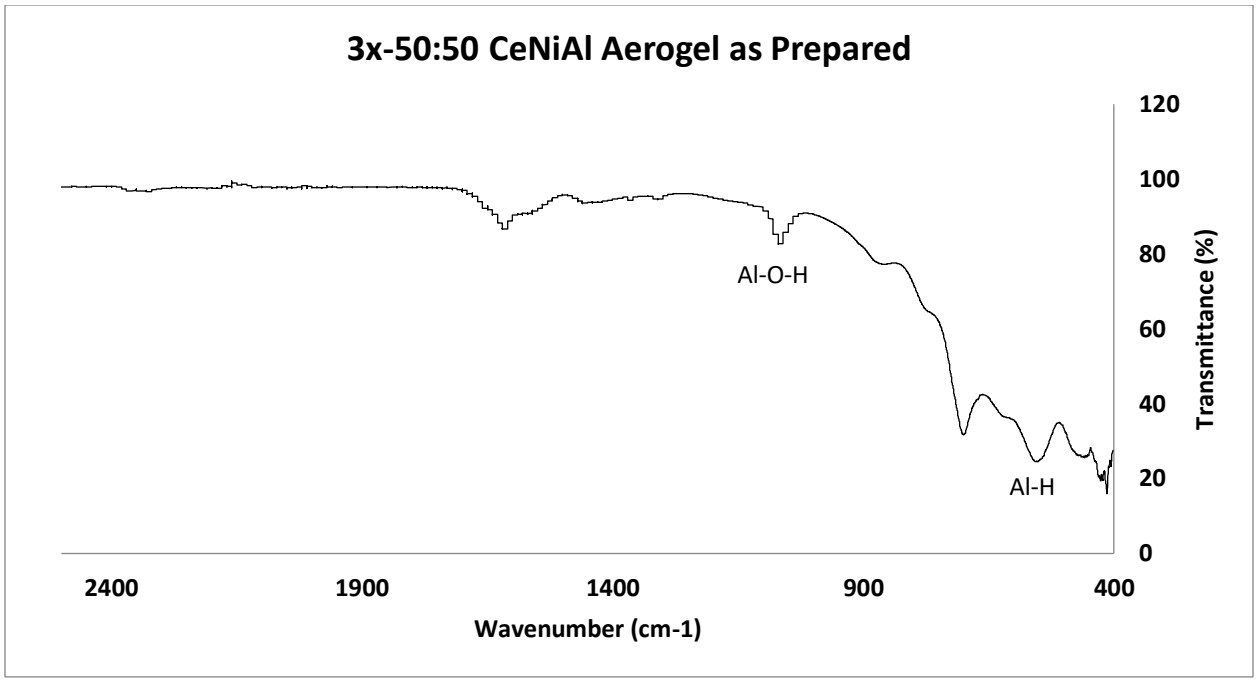

Figure 13. The IR spectrum of 3x-50:50 CeNiAl aerogel before heat treatment.

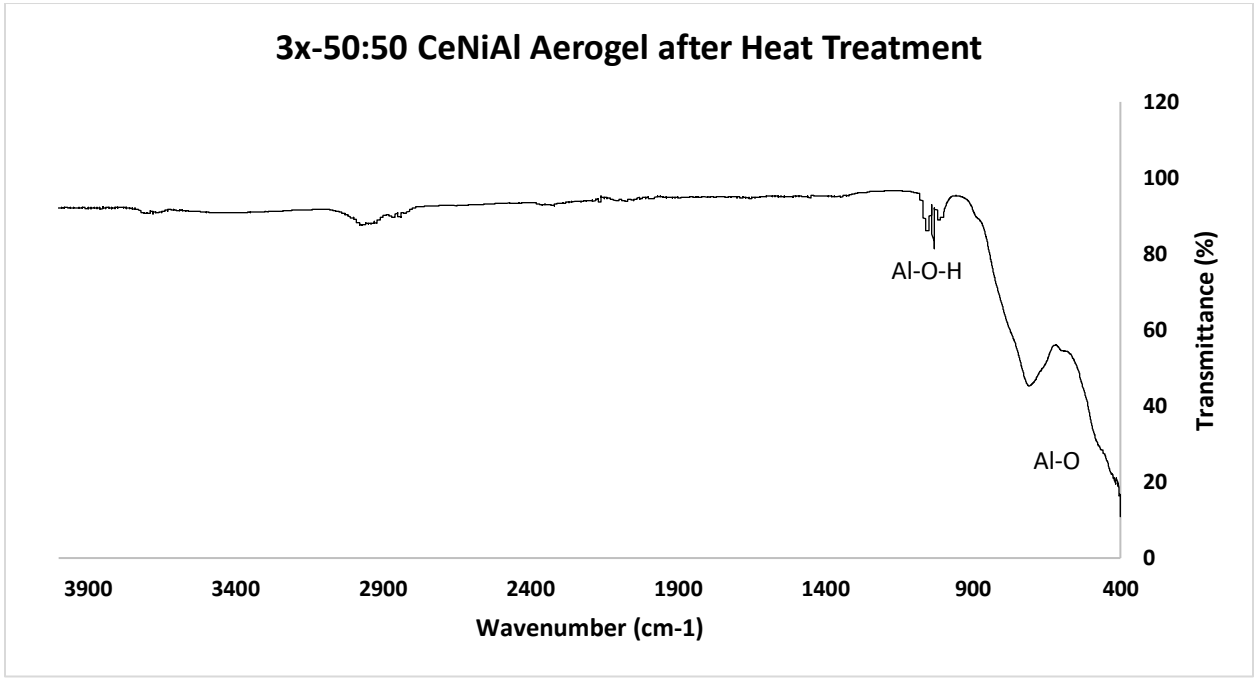

Figure 14. The IR spectrum of 3x-50:50 CeNiAl aerogel after heat treatment.

In Figure 13, the spectrum of 3x-50:50 CeNiAl aerogel before heat treatment is almost identical to the 50:50 CeNiAl aerogel spectrum shown in Figure 7, where an Al-

O-H stretch can be identified at around 1000 cm^{-1} and an Al-H stretch can be identified at around 460 cm^{-1}.[2] Similar to the 50:50 CeNiAl aerogel IR spectrum after heat treatment (Figure 8), the IR spectrum of 3x-50:50 CeNiAl aerogel after heat treatment (Figure 14) includes an Al-O stretch at approximately 460 cm^{-1}.

The IR spectra of NiAl aerogel as prepared and after heat treatment can be observed in Figures 15 and 16, respectively.

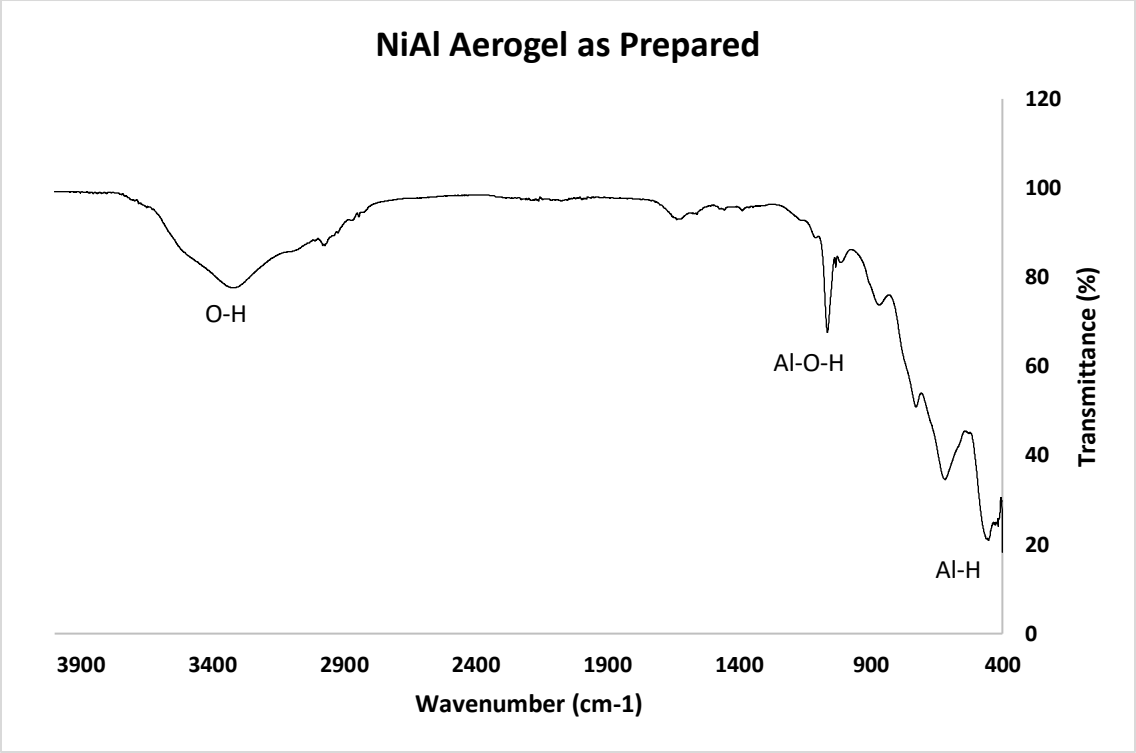

Figure 15. The IR spectrum of NiAl aerogel before heat treatment.

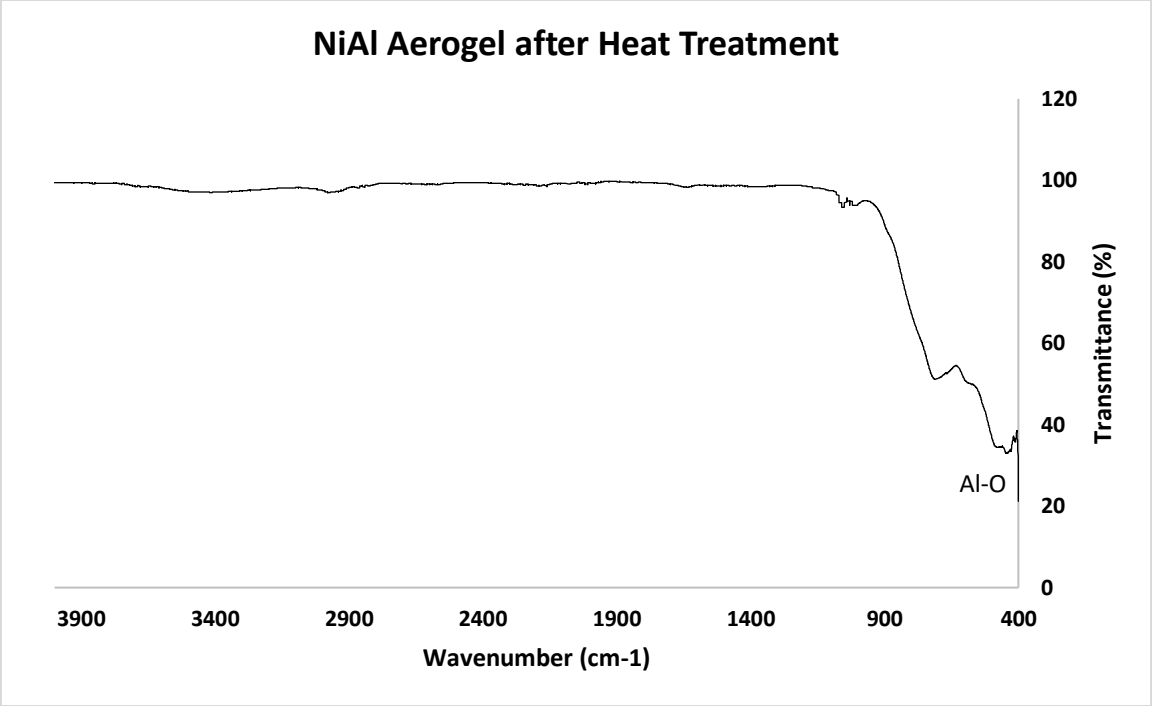

Figure 16. The IR spectrum of NiAl aerogel after heat treatment.

In Figure 15, the spectrum of the as-prepared NiAl aerogel sample contains an O-H stretch at approximately 3400 cm^{-1} attributed most likely to water. This stretch can be observed previously in 75:25 CeNiAl aerogel and 25:75 CeNiAl aerogel before heat treatment. Additionally, in Figure 15, Al-O-H and Al-H stretches at approximately 1000 cm^{-1} and 450 cm^{-1}, respectively, can be observed in the NiAl aerogel before treatment.[2] After heat treatment (Figure 16), the O-H stretch disappeared, and an Al-O stretch at approximately 460 cm^{-1} can be identified.[2]

The IR spectra of 50:50 CeNiSi aerogel as prepared and after heat treatment can be observed in Figures 17 and 18 respectively.

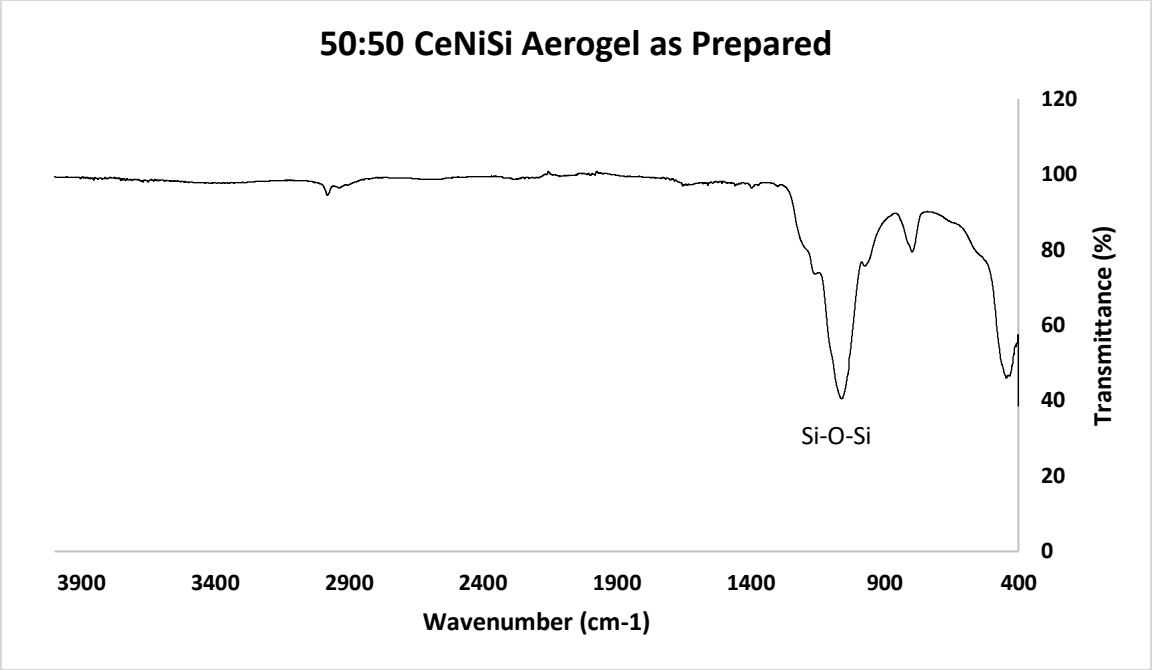

Figure 17. The IR spectrum of 50:50 CeNiSi aerogel before heat treatment.

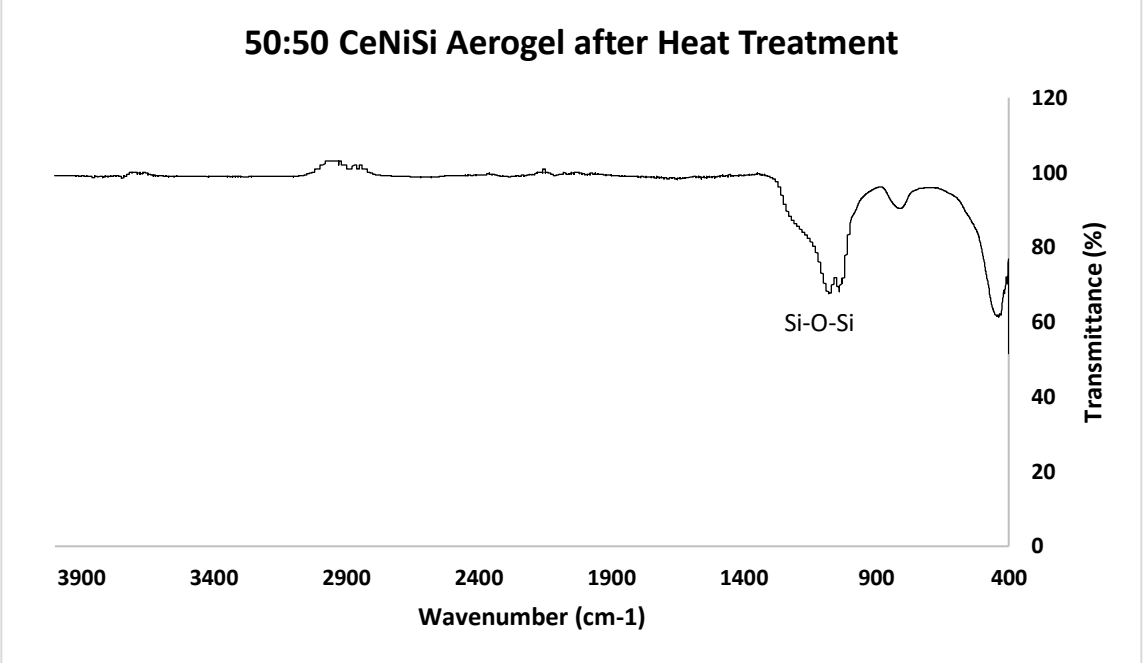

Figure 18. The IR spectrum of 50:50 CeNiSi aerogel after heat treatment.

In Figures 17 and 18, a Si-O-Si stretch can be observed at approximately 1000 cm^{-1} for the 50:50 CeNiSi aerogel sample before and after heat treatment.[2] In Figure 18, after heat treatment, it can be observed that the Si-O-Si peak is not as intense as the same peak before heat treatment. The intensity of the Si-O-Si peak is likely due to the change in the % transmittance to how well each sample was in contact with the ATR crystal.

Across the aerogel samples, it can be observed that the unheated aerogels contain adsorbed solvent, evidenced by the O-H stretch at approximately 3400 cm^{-1}. The expected signals of Al-O-H, Al-H, and Al-O can be observed for the alumina-based aerogel samples. The same can be said for the silica-based aerogel sample, where the IR spectra contained Si-O-Si signals. The shape of the peaks in the alumina-based aerogels differs somewhat before and after heat treatment, which likely indicates some structural change. From the expected signals, the conclusion made from these IR spectra were that alumina-based and silica-based aerogels were successfully synthesized.

3.3. X-ray Powder Diffraction (XRD)

The following figures are the XRD patterns for the synthesized aerogels. In Figures 19, 20, and 21, the XRD patterns for 50:50 CeNiAl aerogel as prepared, post heat treatment, and post UCAT testing can be observed, respectively.

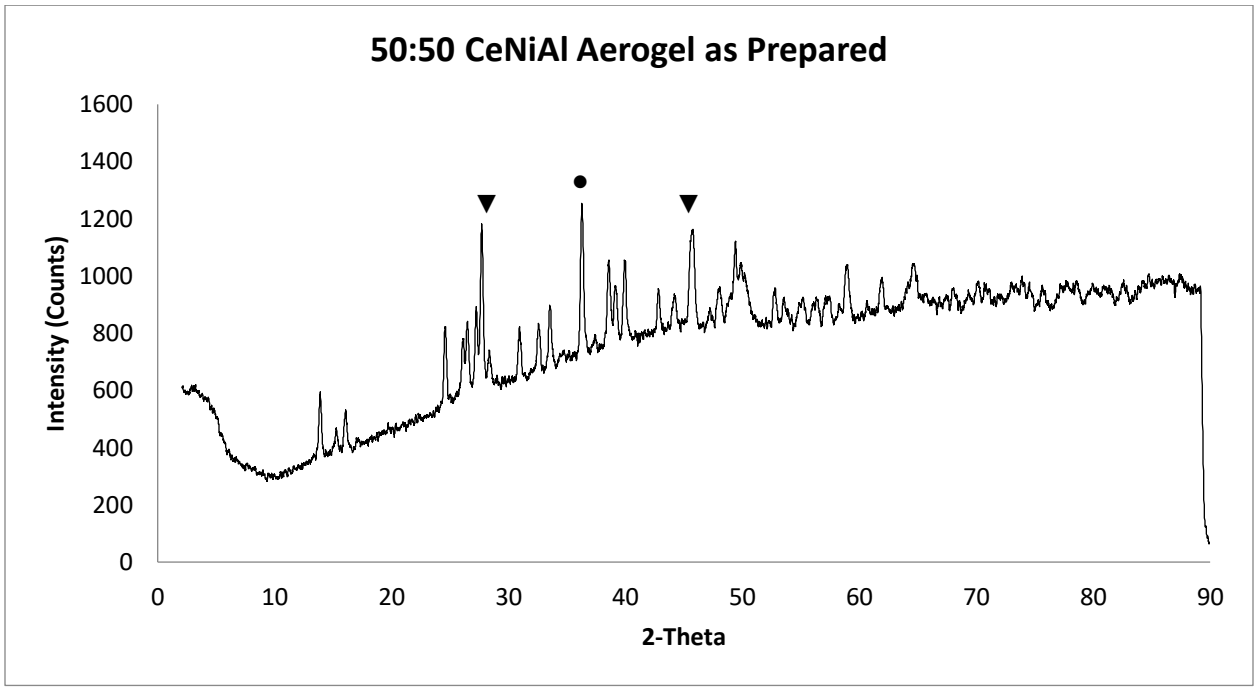

Figure 19. The XRD pattern of 50:50 CeNiAl aerogel before heat treatment; triangle indicates peaks attributed to cerium(IV) oxide and circle indicates peaks attributed to nickel(II) oxide.

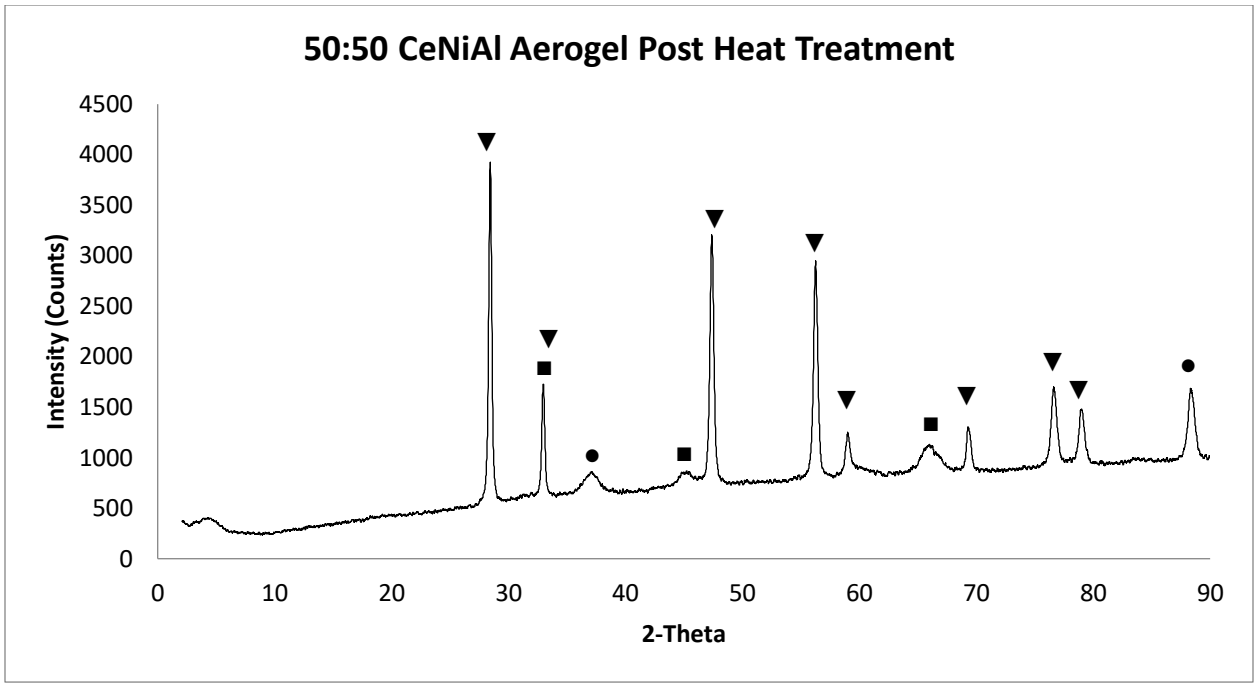

Figure 20. The XRD pattern of 50:50 CeNiAl aerogel after heat treatment; triangles indicate peaks attributed to cerium(IV) oxide, squares indicate peaks attributed gamma alumina, and circles indicate peaks attributed to nickel(II) oxide.

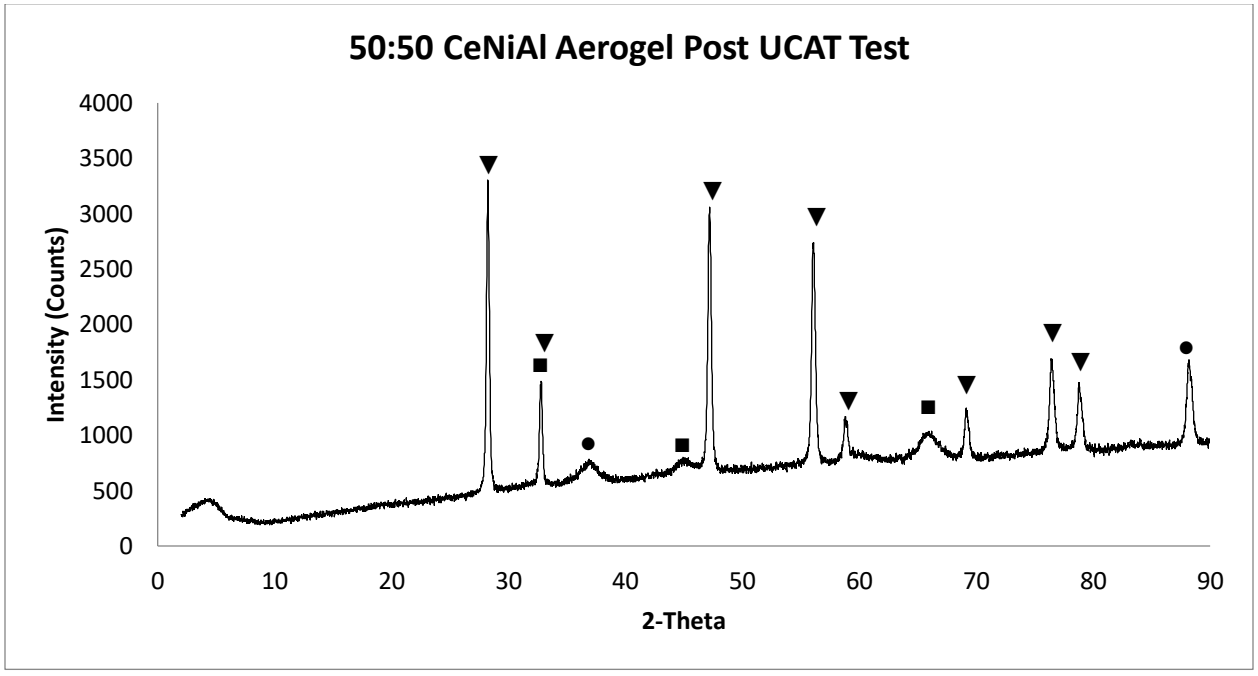

Figure 21. The XRD pattern of 50:50 CeNiAl aerogel after UCAT testing; triangle indicates peaks attributed to cerium(IV) oxide, square indicates peaks attributed gamma alumina, and circle indicates peaks attributed to nickel(II) oxide.

In Figure 20, the signal-to-noise ratio for the 50:50 CeNiAl aerogel sample improved after heat treatment. Also, there have clearly been structural changes in the aerogel sample because many peaks seen for the as-prepared aerogel sample (Figure 19), no longer appear after heat-treatment. For the heat-treated samples, peaks attributed to cerium(IV) oxide, gamma alumina, and nickel(II) oxide can be observed. The cerium(IV) oxide and nickel(II) oxide peaks can be identified based on previous work by Luisa Posada[1] and Ziyi Zhong.[3] In Figure 21, the 50:50 CeNiAl aerogel after UCAT testing has the same XRD pattern as the sample after heat treatment. This means the sample did not undergo chemical changes after UCAT testing.

. The XRD patterns for 75:25 CeNiAl aerogel as prepared, post heat treatment, and post UCAT testing can be observed in Figures 22, 23, and 24, respectively.

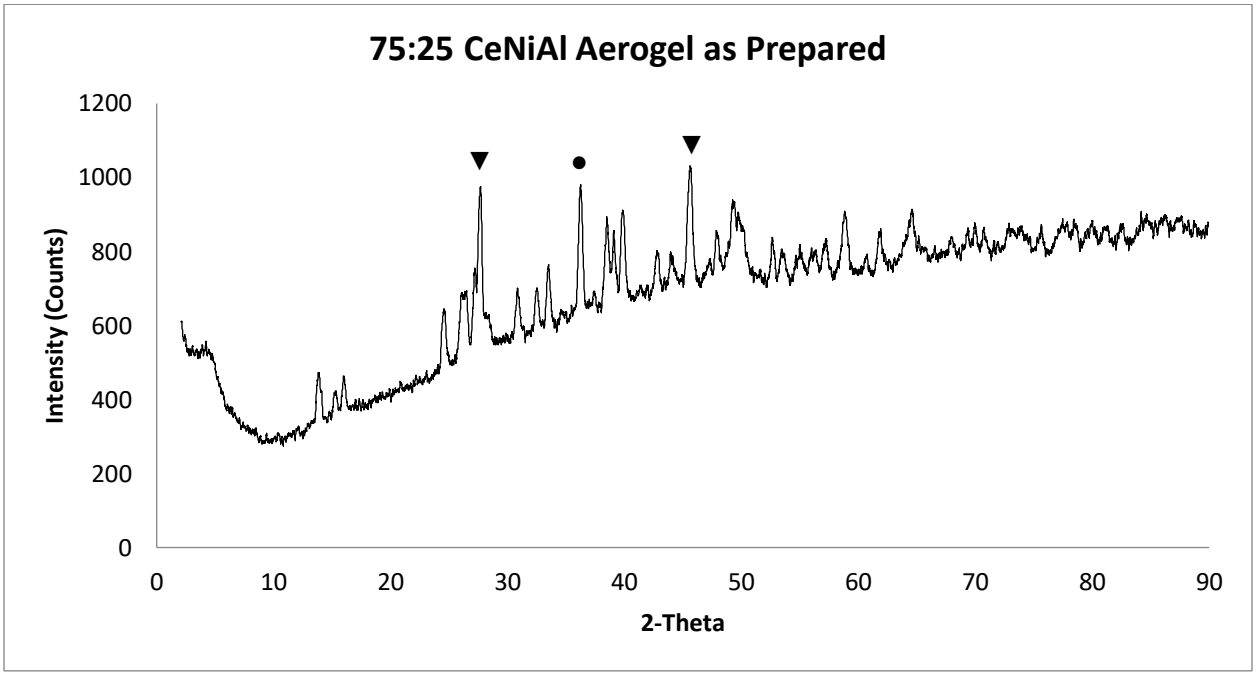

Figure 22. The XRD patterns of 75:25 CeNiAl aerogel before heat treatment; triangle indicates peaks attributed to cerium(IV) oxide and circle indicates peaks attributed to nickel(II) oxide.

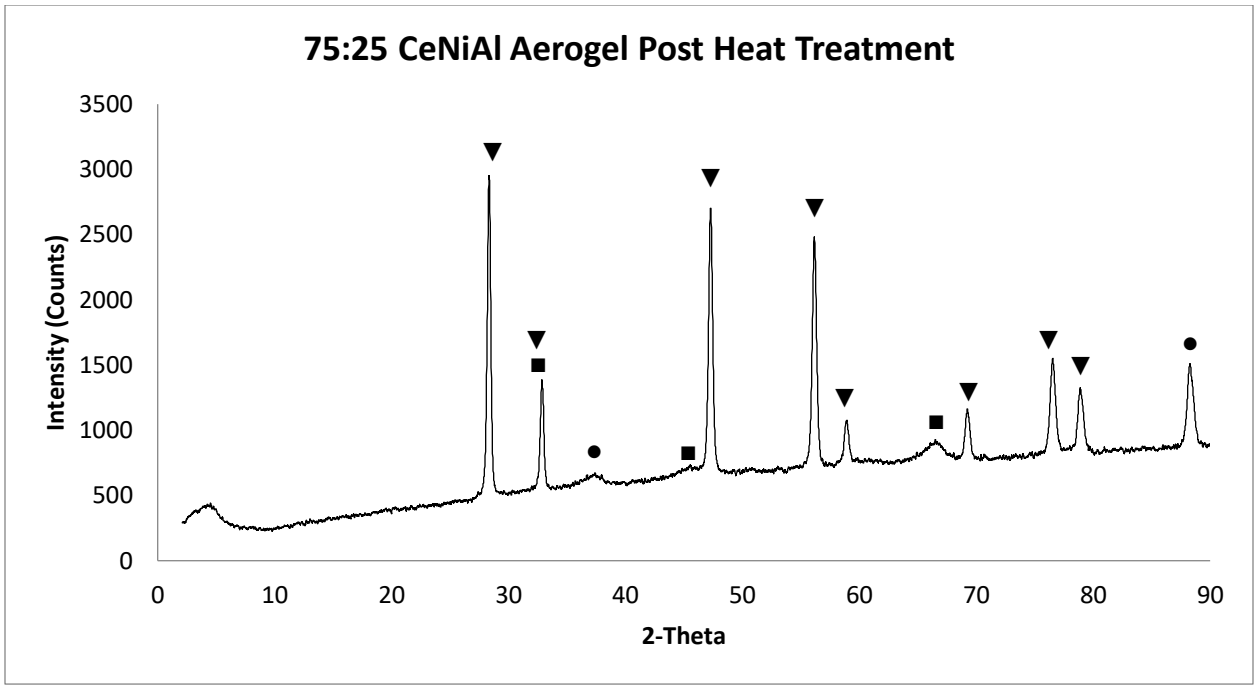

Figure 23. The XRD patterns of 75:25 CeNiAl aerogel after heat treatment; triangle indicates peaks attributed to cerium(IV) oxide, square indicates peaks attributed gamma alumina, and circle indicates peaks attributed to nickel(II) oxide.

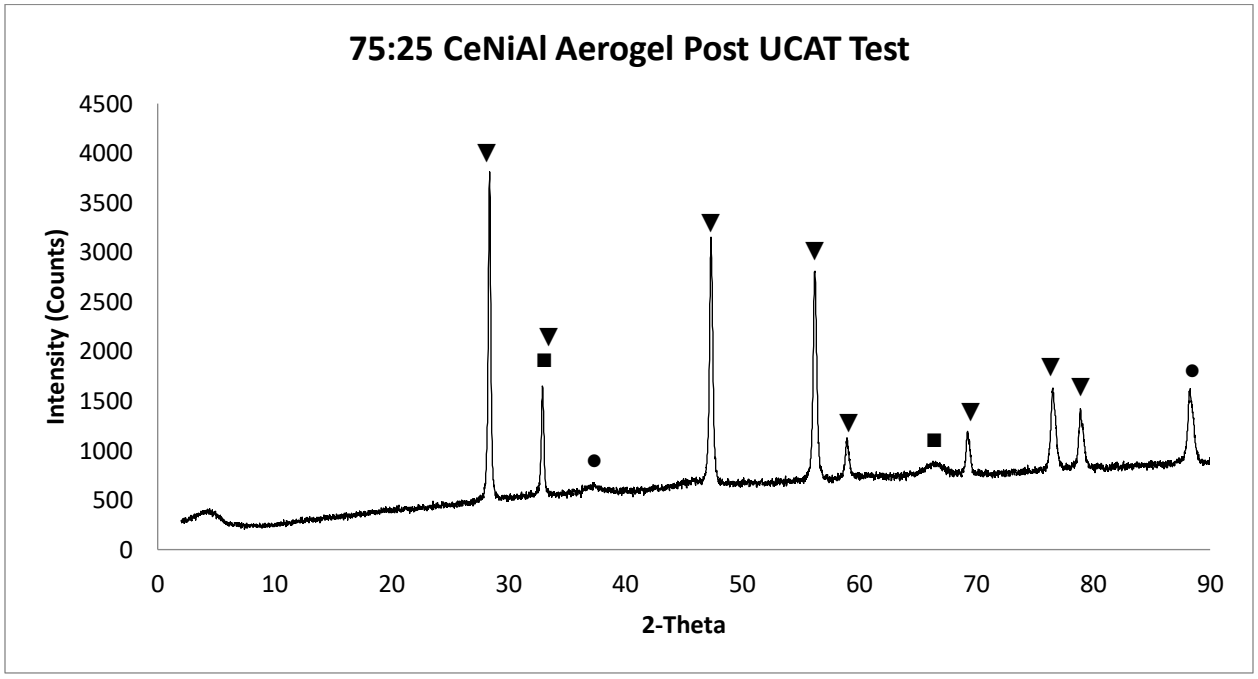

Figure 24. The XRD patterns of 75:25 CeNiAl aerogel after UCAT testing; triangle indicates peaks attributed to cerium(IV) oxide, square indicates peaks attributed gamma alumina, and circle indicates peaks attributed to nickel(II) oxide.

The XRD pattern of the 75:25 CeNiAl aerogel before heat treatment shown in Figure 22 has similar results to the 50:50 CeNiAl aerogel sample shown in Figure 19. It is clear that structural changes have occurred as in the 75:25 CeNiAl sample. The signal-to-noise ratio was poor before heat treatment for the 75:25 CeNiAl aerogel sample, and the signal-to-noise ratio improved after heat treatment. Peaks due to cerium(IV) oxide, gamma alumina, and nickel(II) oxide can be found in the XRD pattern of 75:25 CeNiAl aerogel sample after heat treament. Like the 50:50 CeNiAl sample, the 75:25 CeNiAl XRD pattern after UCAT testing has the same pattern as the 75:25 CeNiAl aerogel XRD pattern after heat treatment.

The XRD patterns for 25:75 CeNiAl aerogel as prepared, post heat treatment, and post UCAT testing can be observed in Figures 25, 26, and 27, respectively.

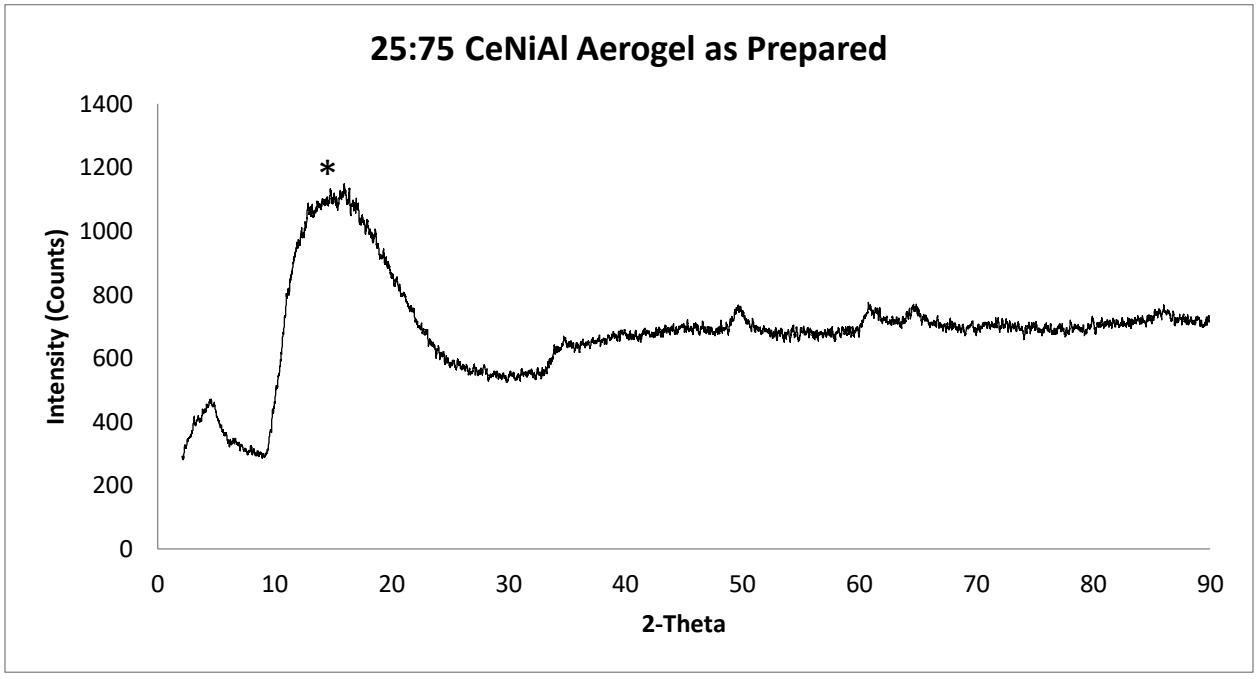

Figure 25. The XRD patterns of 25:75 CeNiAl aerogel before heat treatment; asterisk indicates peak attributed to silica.

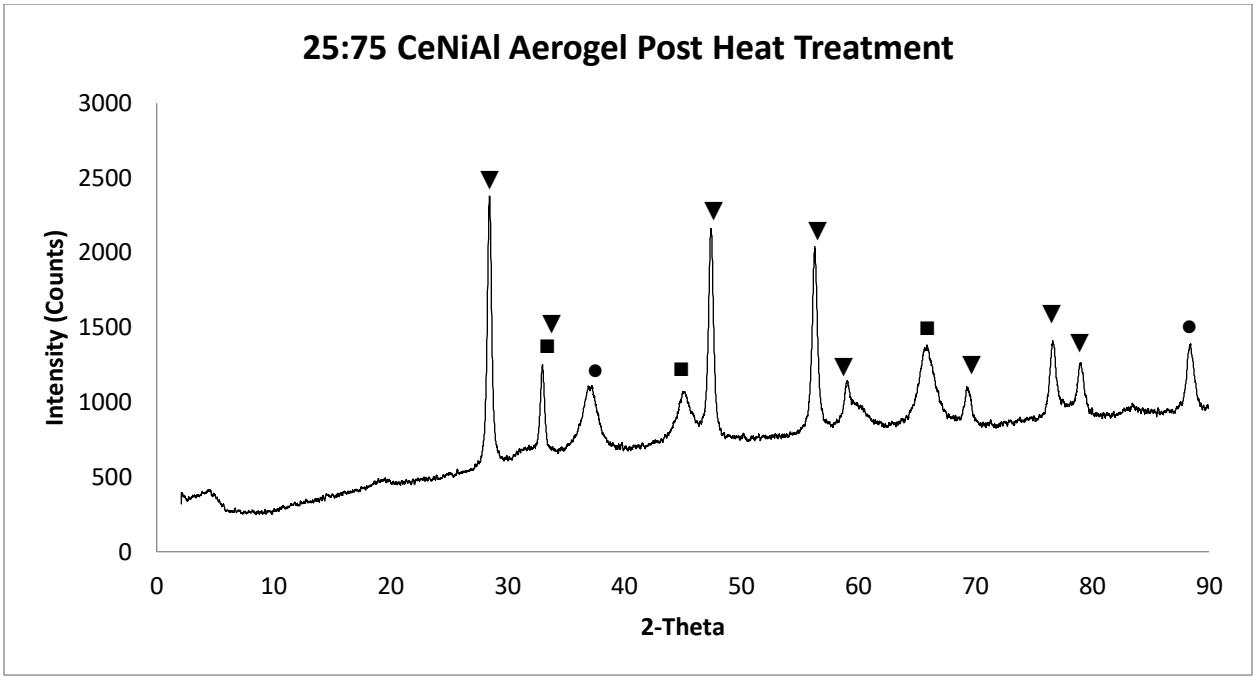

Figure 26. The XRD patterns of 25:75 CeNiAl aerogel after heat treatment; triangle indicates peaks attributed to cerium(IV) oxide, square indicates peaks attributed gamma alumina, and circle indicates peaks attributed to nickel(II) oxide.

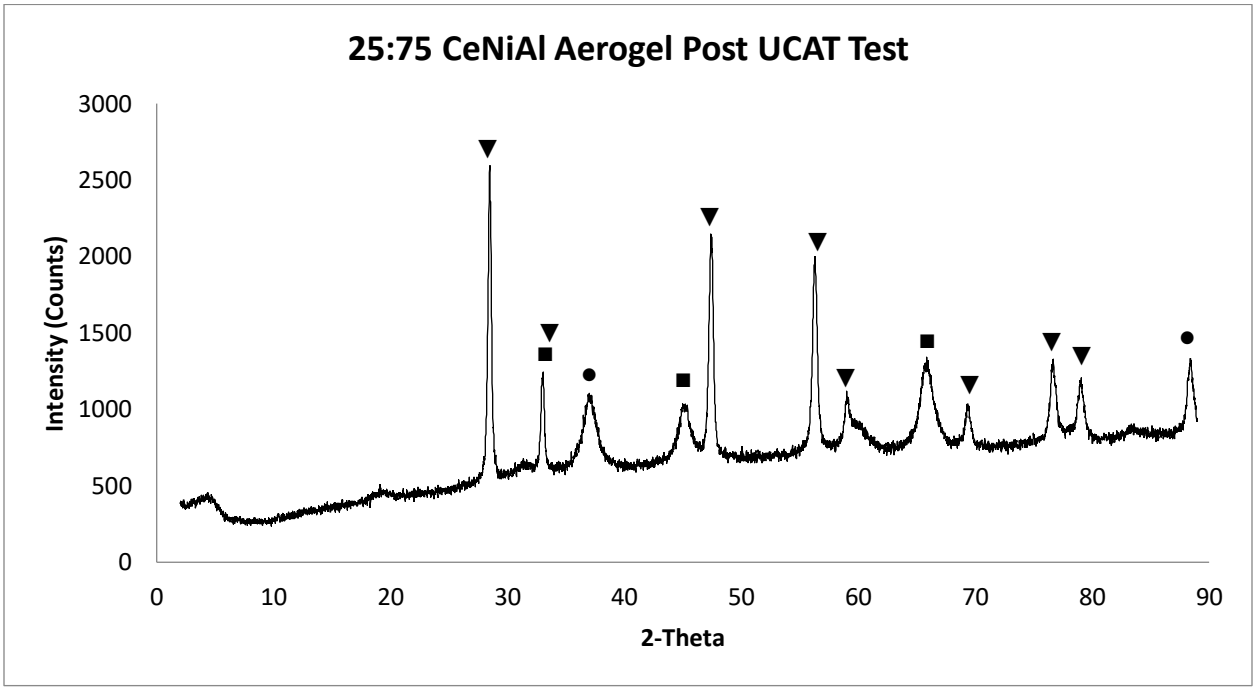

Figure 27. The XRD patterns of 25:75 CeNiAl aerogel after UCAT testing; triangle indicates peaks attributed to cerium(IV) oxide, square indicates peaks attributed gamma alumina, and circle indicates peaks attributed to nickel(II) oxide.

In Figure 25, a silica peak from the silica plate holder can be observed between 10 to 20 degrees for 25:75 CeNiAl aerogel before heat treament. Similar peaks to the 50:50 CeNiAl aerogel sample after heat treament can be identified in Figure 26. In Figure 26. more intense peaks attributed to gamma alumina around 32, 48, and 68 degrees can be observed. Additionally, peaks attributed to nickel(II) oxide around 38 and 88 degrees can be observed. These peaks in the 25:75 CeNiAl sample appeared to be more intense compared to the 50:50 CeNiAl and 75:25 CeNiAl aerogel samples. An explanation, besides the improvement of the signal-to-noise ratio, can be that the greater nickel-to-cerium mole ratio in the 25:75 CeNiAl aerogel leads to a more intense signal. Observed in Figure 27, the 25:75 CeNiAl aerogel after UCAT testing has the same XRD pattern as the sample after heat treatment.

The XRD patterns for 3x-50:50 CeNiAl aerogel as prepared, post heat treatment, and post UCAT testing can be observed in Figures 28, 29, and 30 respectively.

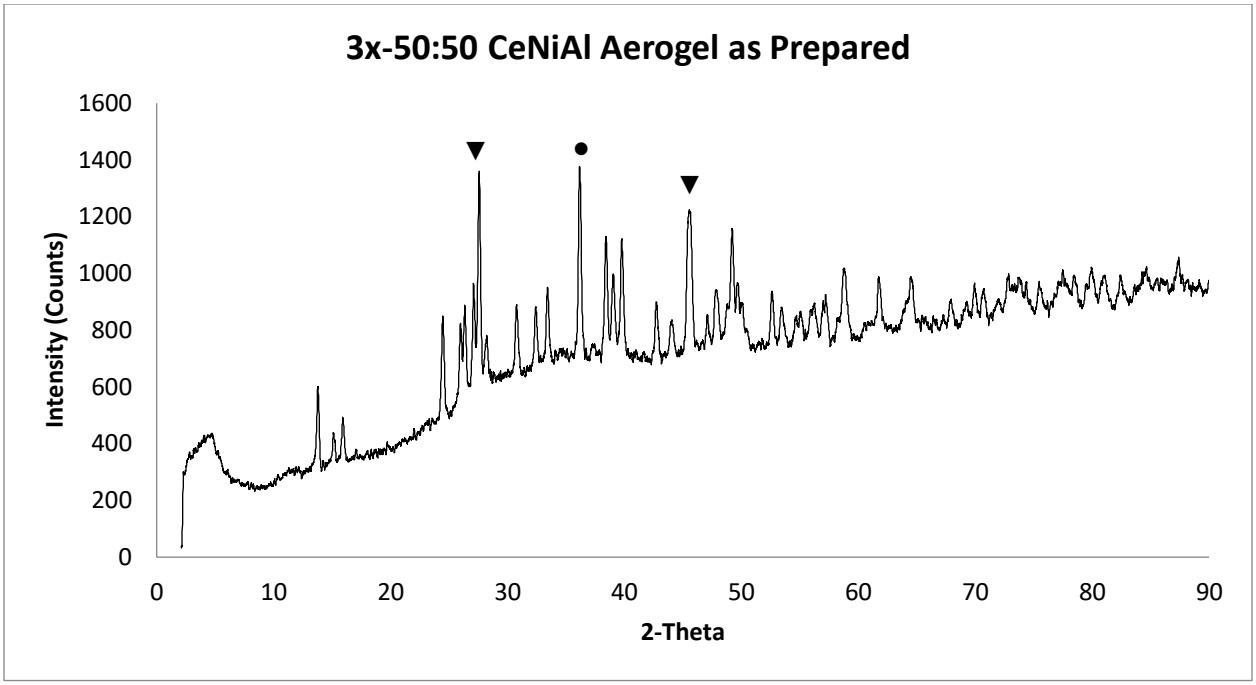

Figure 28. The XRD patterns of 3x-50:50 CeNiAl aerogel before heat treatment; triangle indicates peaks attributed to cerium(IV) oxide and circle indicates peaks attributed to nickel(II) oxide.

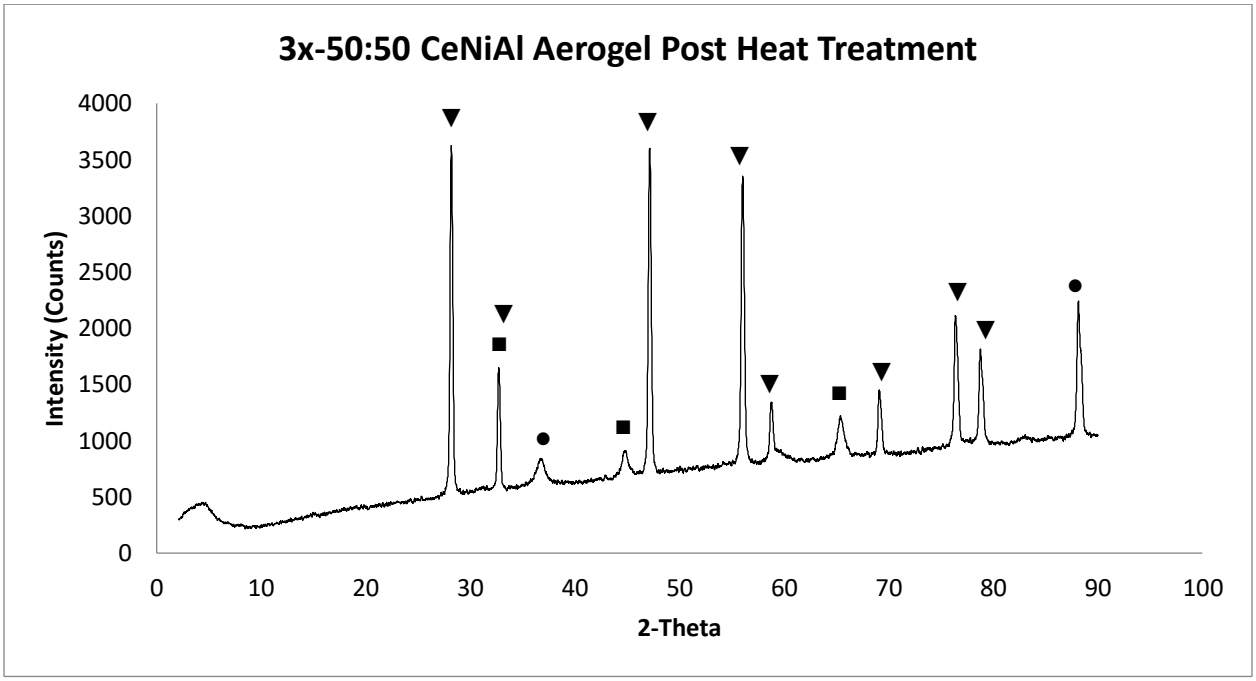

Figure 29. The XRD patterns of 3x-50:50 CeNiAl aerogel after heat treatment; triangle indicates peaks attributed to cerium(IV) oxide, square indicates peaks attributed gamma alumina, and circle indicates peaks attributed to nickel(II) oxide.

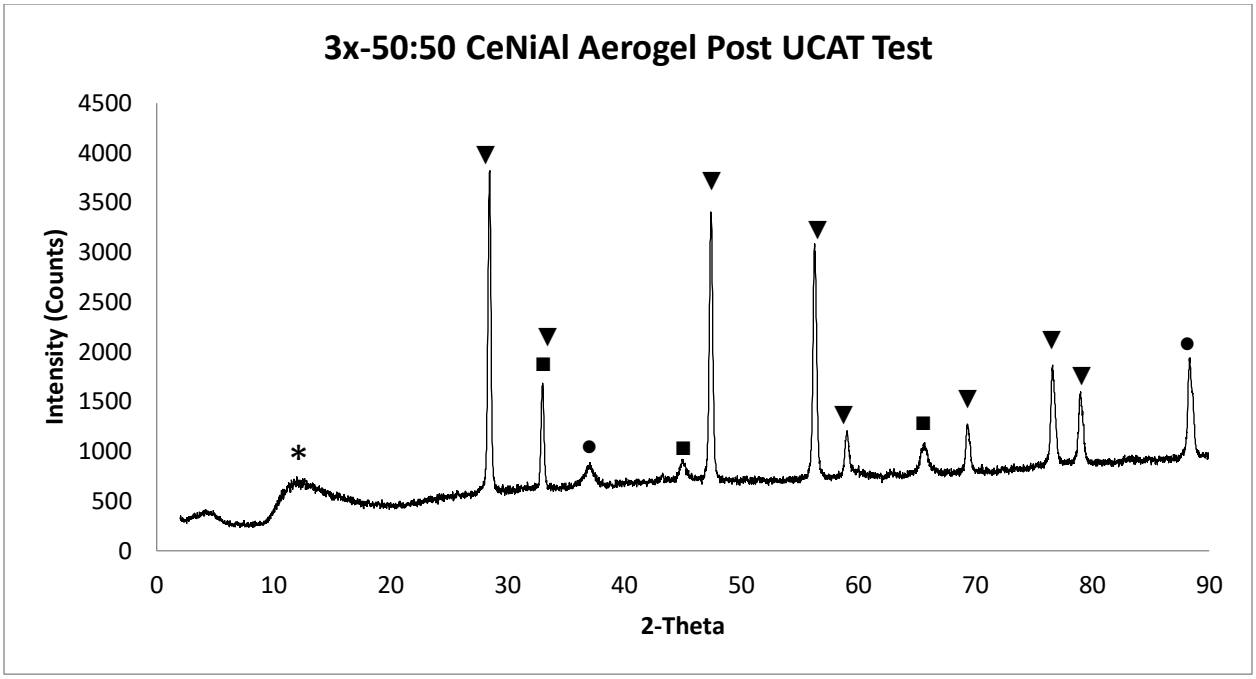

Figure 30. The XRD patterns of 3x-50:50 CeNiAl aerogel after UCAT testing; triangle indicates peaks attributed to cerium(IV) oxide, square indicates peaks attributed gamma alumina, and circle indicates peaks attributed to nickel(II) oxide.

In Figure 30, the XRD pattern of the 3x-50:50 CeNiAl aerogel after UCAT testing has the same XRD pattern as the sample after heat treatment, observed in Figure 29. As shown in Figures 28, 29, and 30, the 3x-50:50 CeNiAl aerogel has a very similar XRD pattern to the 50:50 CeNiAl aerogel sample shown in Figure 19, 20, and 21. This was expected because the nickel to cerium mole ratio is identical to the 50:50 CeNiAl aerogel. This shows that the structure does not appear to depend on the amount of Ni and Ce present in the aerogels for the 50:50 CeNiAl and 3x-50:50 CeNiAl aerogel samples.

The XRD patterns for NiAl aerogel as prepared, post heat treatment, and post UCAT testing can be observed in Figures 31, 32, and 33, respectively.

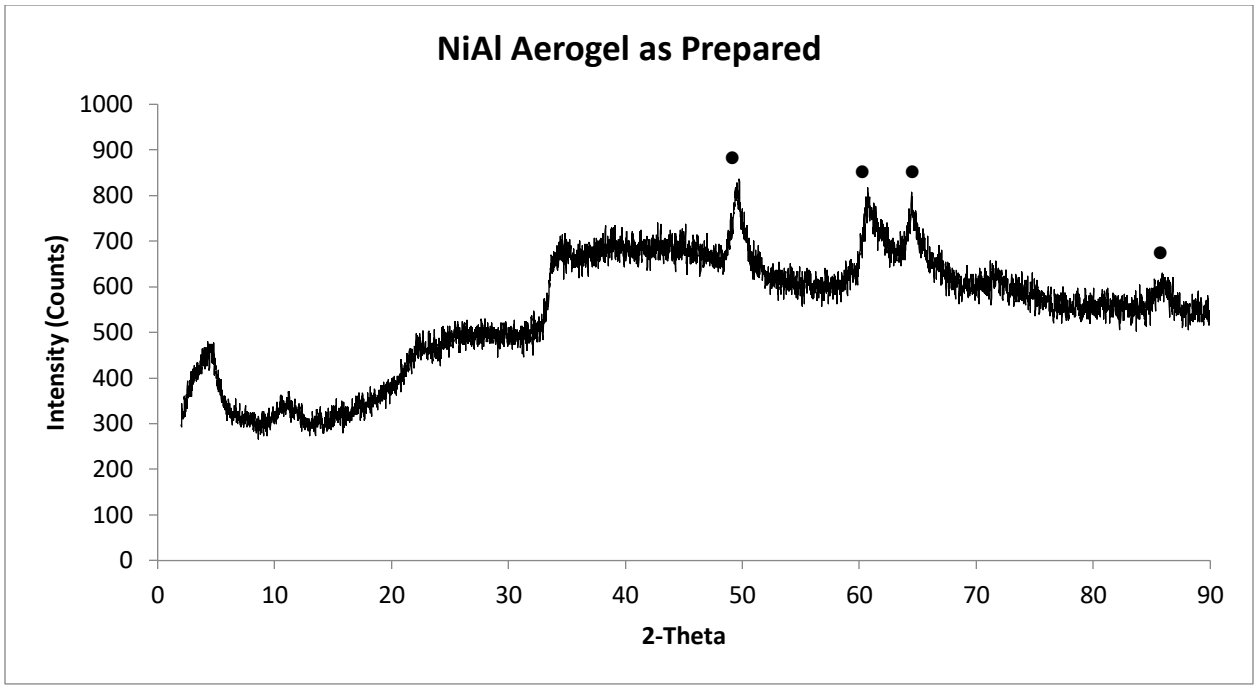

Figure 31. The XRD patterns of NiAl aerogel before heat treatment; circle indicates peaks attributed to nickel(II) oxide.

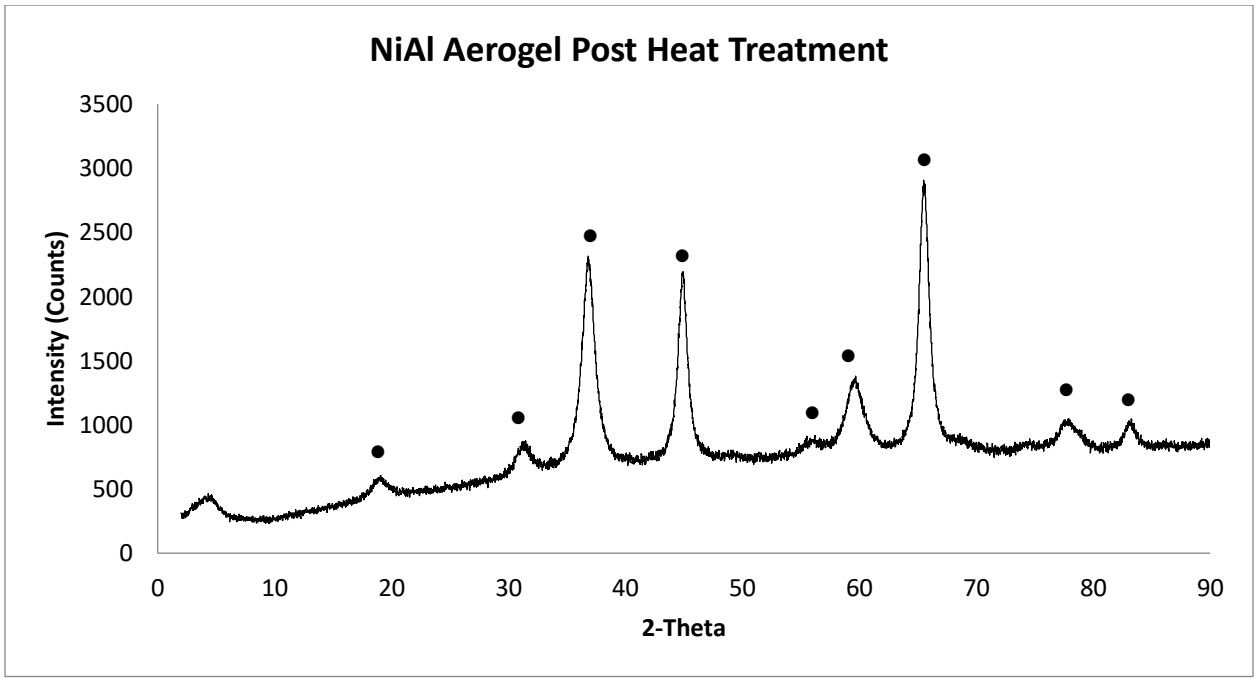

Figure 32. The XRD patterns of NiAl aerogel after heat treatment; circle indicates peaks attributed to nickel(II) oxide.

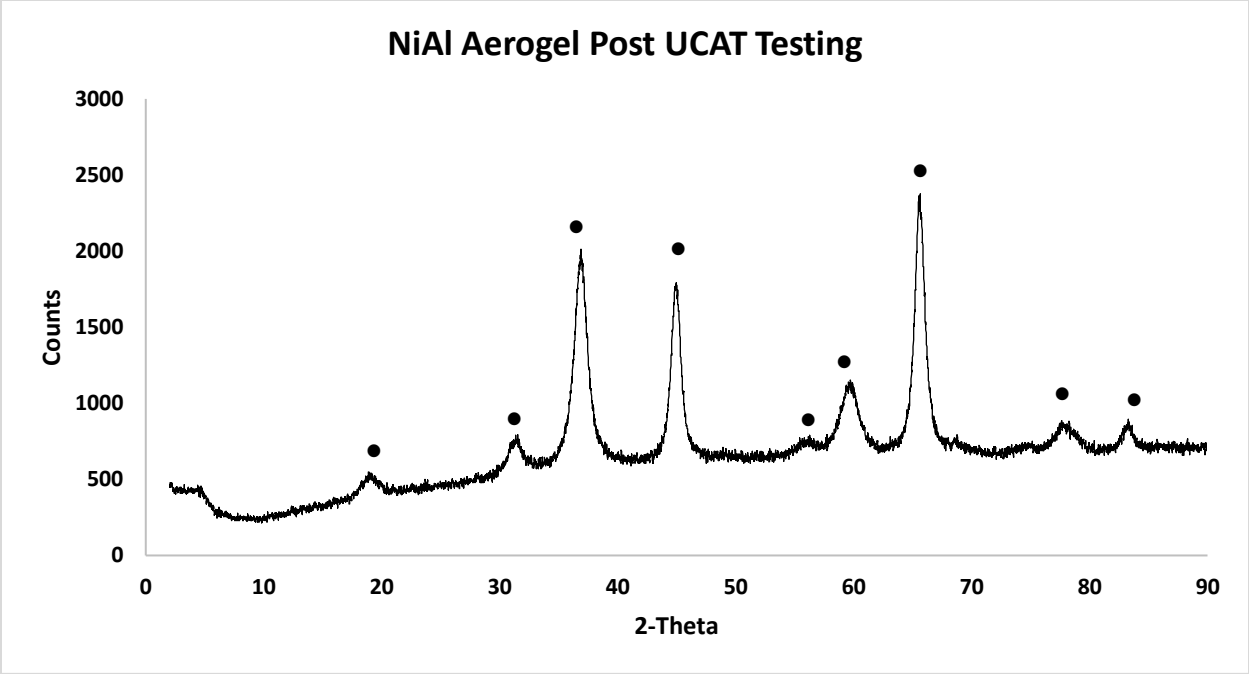

Figure 33. The XRD patterns of NiAl aerogel after UCAT testing; circle indicates peaks attributed to nickel(II) oxide.

In Figure 31, the signal-to-noise ratio of NiAl aerogel before heat treatment is lower than the XRD pattern of the aerogel sample after heat treatment (Figure 32). Peaks attributed to nickel(II) oxide can be observed across the NiAl aerogel XRD patterns. The peaks attributed to nickel(II) oxide around 38 and 88 degrees can be observed in Figures 32 and 33, and those peaks can be seen in the CeNiAl aerogels. The pattern of NiAl aerogel after heat treatment and after UCAT testing in Figures 32 and 33 agrees with a published literature value by Ziyi Zong.[3]

The XRD patterns for 50:50 CeNiSi aerogel as prepared, post heat treatment, and post UCAT testing can be observed in Figures 34, 35, and 36, respectively.

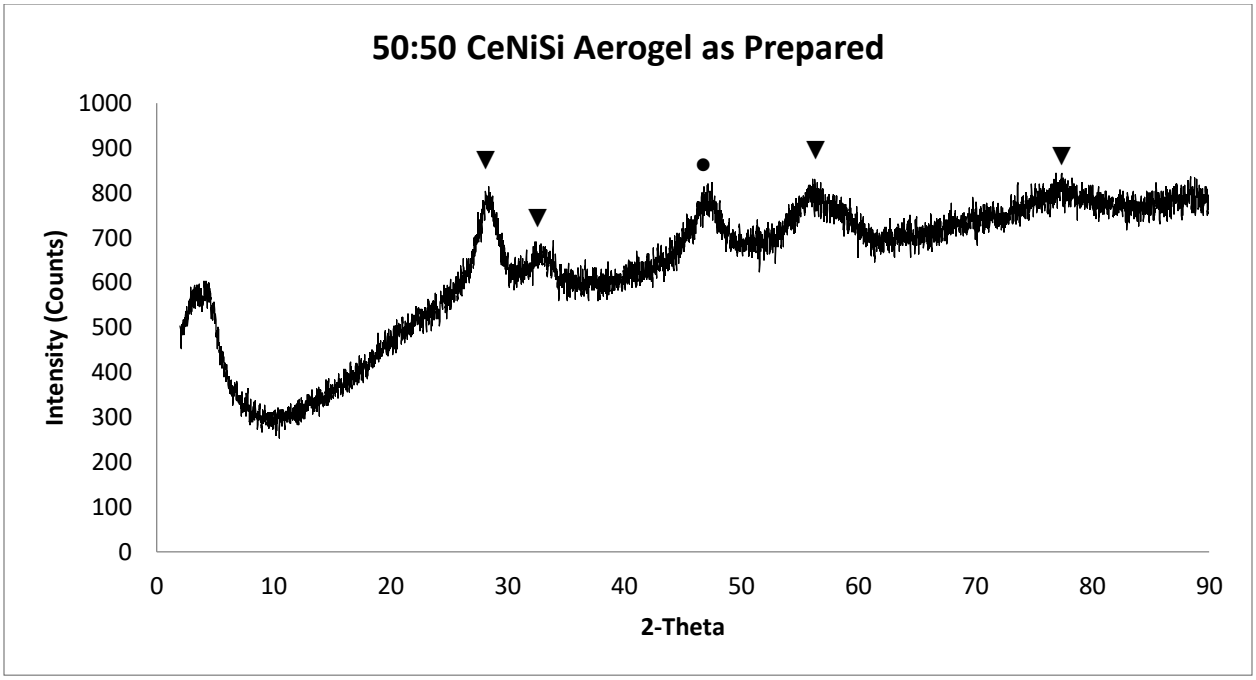

Figure 34. The XRD patterns of 50:50 CeNiSi aerogel before heat treatment; triangle indicates peaks attributed to cerium(IV) oxide and circle indicates peaks attributed to nickel(II) oxide.

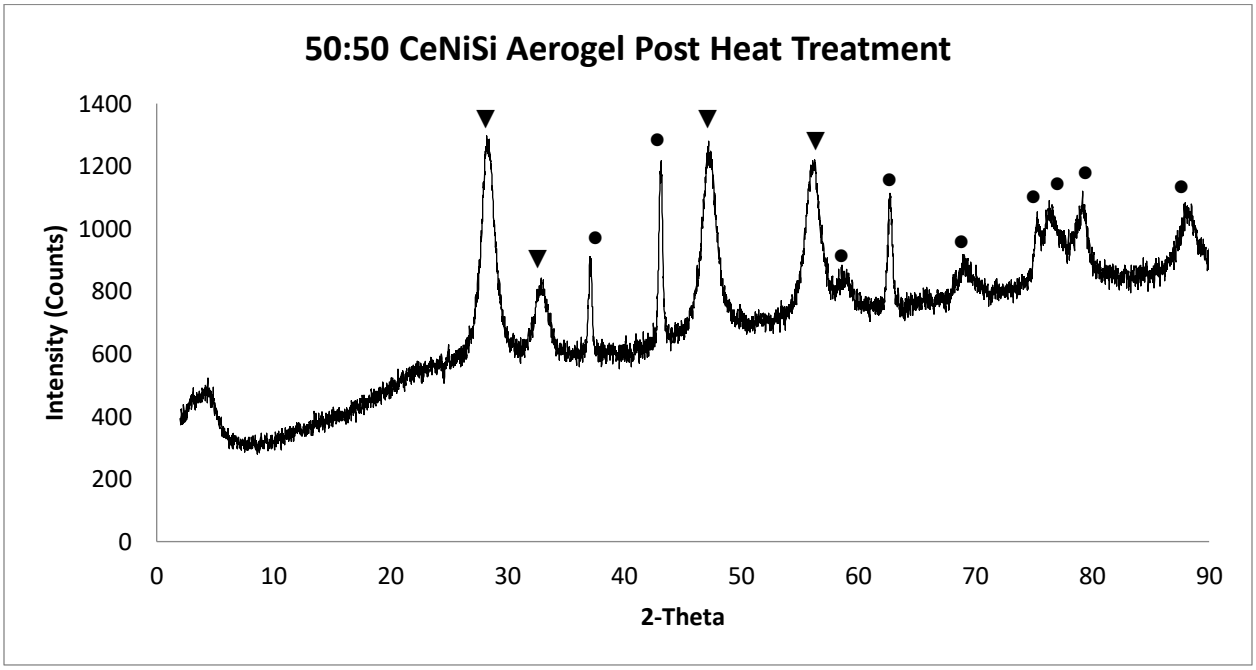

Figure 35. The XRD patterns of 50:50 CeNiSi aerogel after heat treatment; triangle indicates peaks attributed to cerium(IV) oxide and circle indicates peaks attributed to nickel(II) oxide.

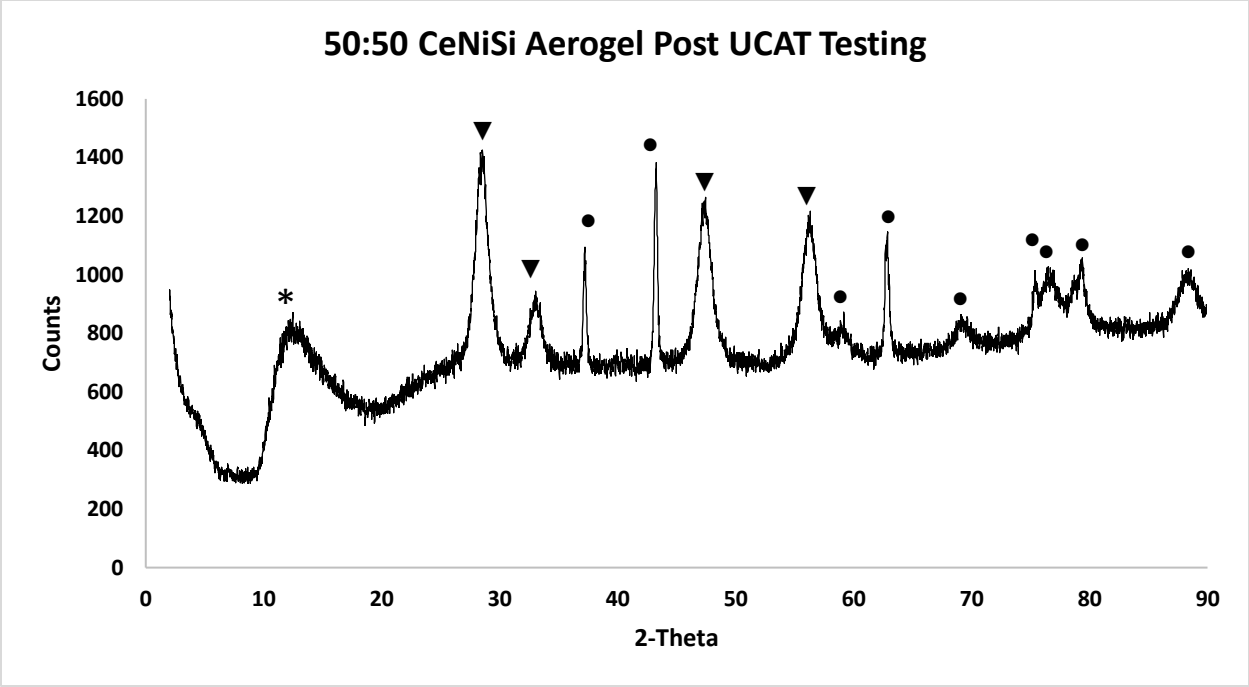

Figure 36. The XRD patterns of 50:50 CeNiSi aerogel after UCAT testing; triangle indicates peaks attributed to cerium(IV) oxide and circle indicates peaks attributed to nickel(II) oxide.

Observed in Figure 34, the 50:50 CeNiSi aerogel XRD pattern shows peaks attributed to cerium(IV) oxide and nickel(II) oxide. The peaks attributed to cerium(IV) oxide were identified from prior works done on ceria-containing aerogels by Lusia Posada.[1] Peaks attributed to cerium(IV) oxide and nickel(II) oxide can be observed in the sample after heat treatment and after UCAT testing. Observed in Figures 35 and 36, the XRD patterns of 50:50 CeNiSi aerogel after UCAT testing is the same as for the sample after heat treatment. The signal-to-noise ratio of the 50:50 CeNiSi improved after heat treatment compared to the sample before heat treatment.

To summarize, the signal-to-noise ratio of the XRD patterns of CeNiAl, NiAl, and CeNiSi aerogels improved after heat treatment compared to the samples before heat treatment. Most of the peaks can be identified as attributed to cerium(IV) oxide, gamma

alumina, and/or nickel(II) oxide from previous works by Luisa Posada[1] and Ziyi Zhong.[3] The signal-to-noise ratio of the silica-based aerogel is overall lower than the alumina-based aerogels. However, peaks also disappeared after heat treatment. This means there may be a structural and chemical changes to the aerogels during heat treatment. Observed for all the aerogel samples, the XRD patterns of the aerogel samples after UCAT testing are identical to the aerogel samples after heat treatment. It can be concluded there was not additional structural and chemical change in the metal-containing aerogels after UCAT testing. This stability means the catalytic metal-containing aerogels has potential as a heterogeneous catalysis for automotive exhaust.

3.4. Scanning Electron Microscopy (SEM) and Electron-Dispersive X-ray Spectroscopy (EDX).

The SEM images of the CeNiAl, NiAl, and CeNiSi aerogel samples were taken at various magnifications. To help identify the chemical composition of nanoparticles observed in the SEM images of the CeNiAl samples, EDX was utilized. The SEM and EDX images of 50:50 CeNiAl samples after heat treatment and after UCAT testing can be viewed in Figures 37 and 38.

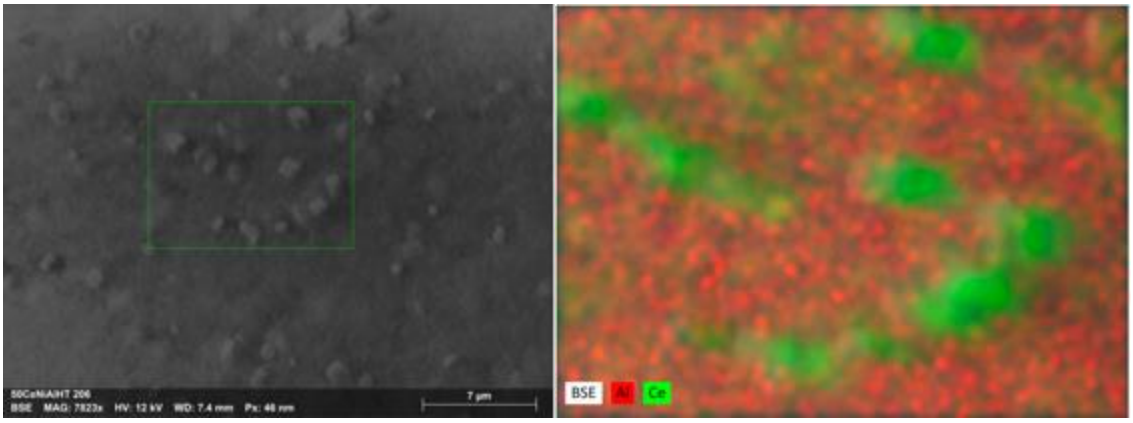

Figure 37. The image on the left is an SEM image of 50:50 CeNiAl aerogel after heat treatment (scale bar = 7 µm), and the image on the right is the EDX image of the area indicated; red indicates aluminum and green indicates cerium.

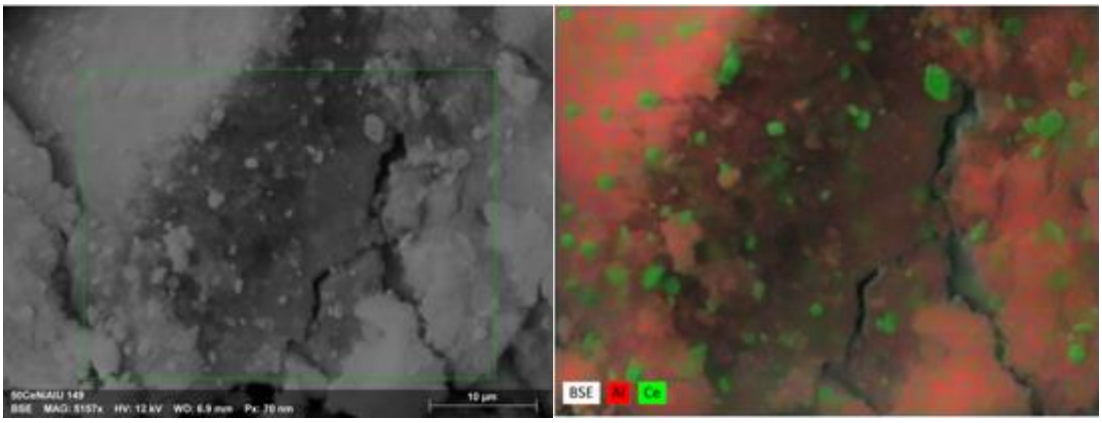

Figure 38. The image on the left is an SEM image of 50:50 CeNiAl aerogel after heat-treatment and UCAT testing (scale bar = 10 µm), and the image on the right is the EDX image of the selected region; red indicates aluminum and green indicates cerium.

As observed in Figure 37, small (ca. 1 µm), cubic like particles can be identified for the 50:50 CeNiAl aerogel sample after heat treatment for the SEM image at 8-µm magnification. The particles were determined to be cerium-containing (shown as bright green spots on the image) through EDX imaging. Similar particles were observed in the 50:50 aerogels after UCAT testing (Figure 38).

The SEM and EDX images of 75:25 CeNiAl samples after heat treatment and after UCAT testing can be viewed in Figures 39 and 40.

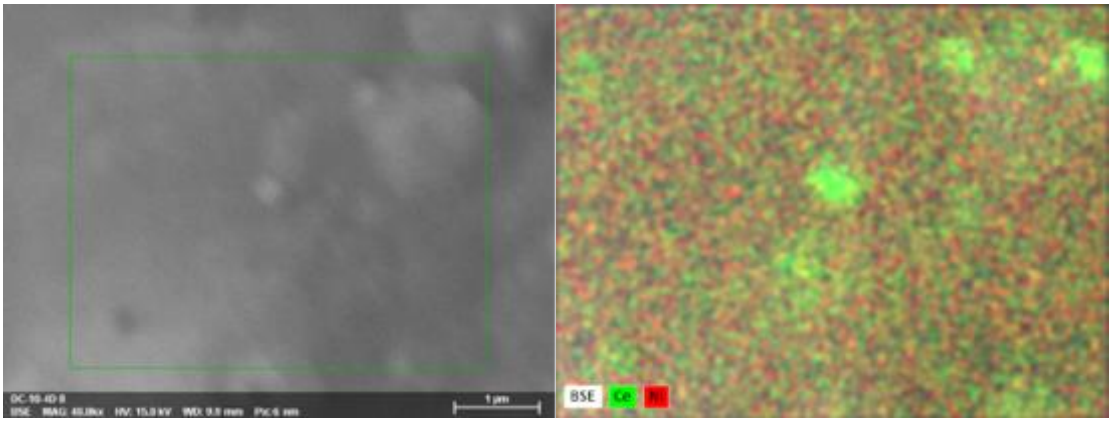

Figure 39. The image on the left is an SEM image of 75:25 CeNiAl aerogel after heat treatment (scale bar = 1 µm), and the image on the right is the EDX image; red indicates aluminum and green indicates cerium.

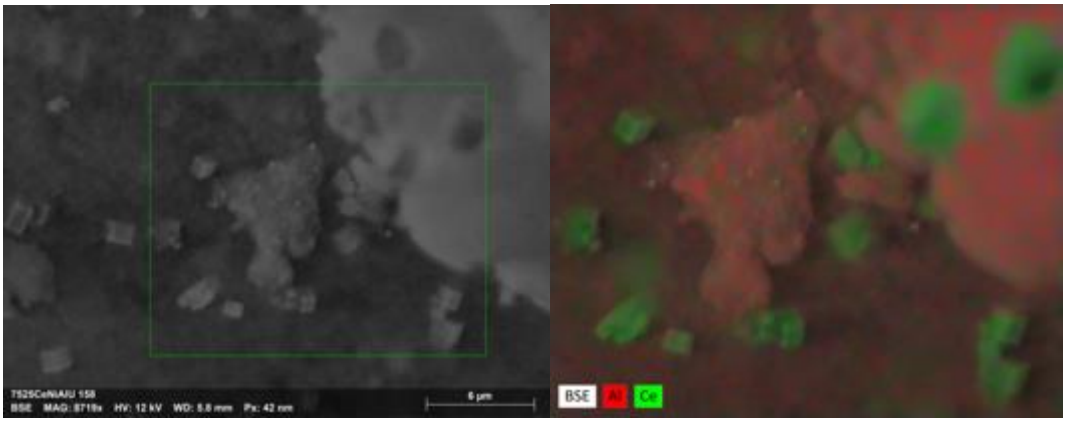

Figure 40. The image on the left is an SEM image of 75:25 CeNiAl aerogel after UCAT testing (scale bar = 6 µm), and the image on the right is the EDX image; red indicates aluminum and green indicates cerium.

In Figure 39, similar size and shape particles observed in the 50:50 CeNiAl aerogel sample can be observed in the 75:25 CeNiAl aerogel. Cerium-containing particles were identified at 1-µm magnification for the 75:25 CeNiAl aerogel sample after heat treatment with EDX imaging. A clearer SEM image of the cubic like cerium-containing particles can be observed at 6-µm magnification in the 75:25 CeNiAl sample after UCAT testing (Figure 40).

The SEM and EDX images of 25:75 CeNiAl samples after heat treatment and after UCAT testing can be viewed in Figures 41, 42, and 43.

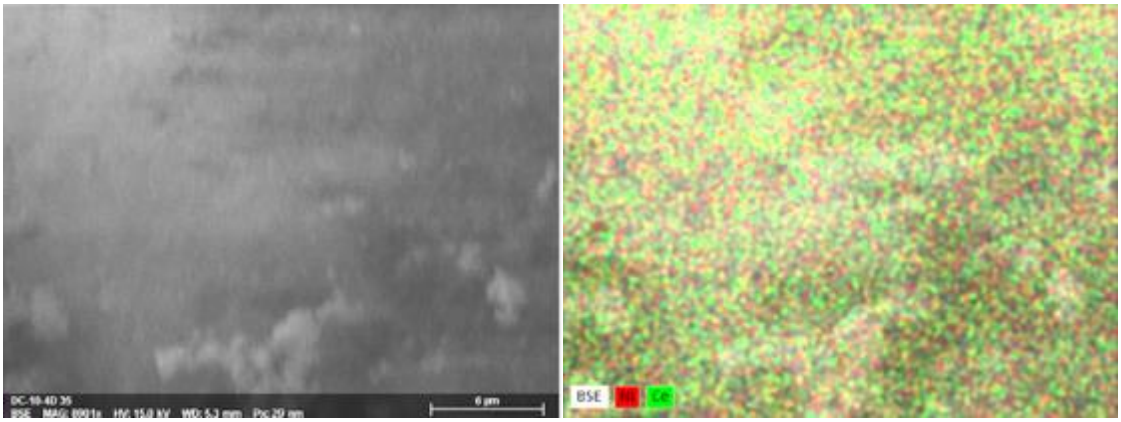

Figure 41. The image on the left is an SEM image of 25:75 CeNiAl aerogel after heat treatment (scale bar = 6 µm), and the image on the right is the EDX image; red indicates aluminum and green indicates cerium.

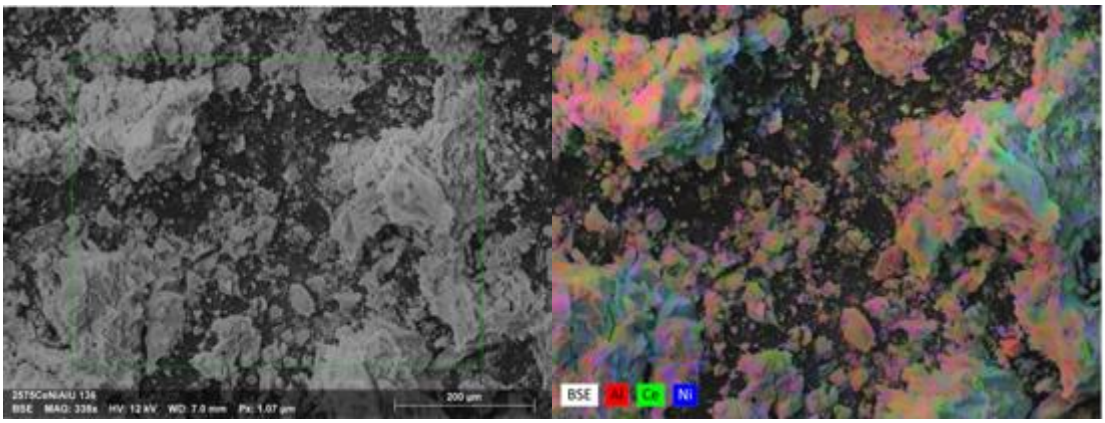

Figure 42. The image on the left is an SEM image of 25:75 CeNiAl aerogel after UCAT testing (scale bar = 200 µm), and the image on the right is the EDX image; red indicates aluminum, green indicates cerium, and blue indicates nickel.

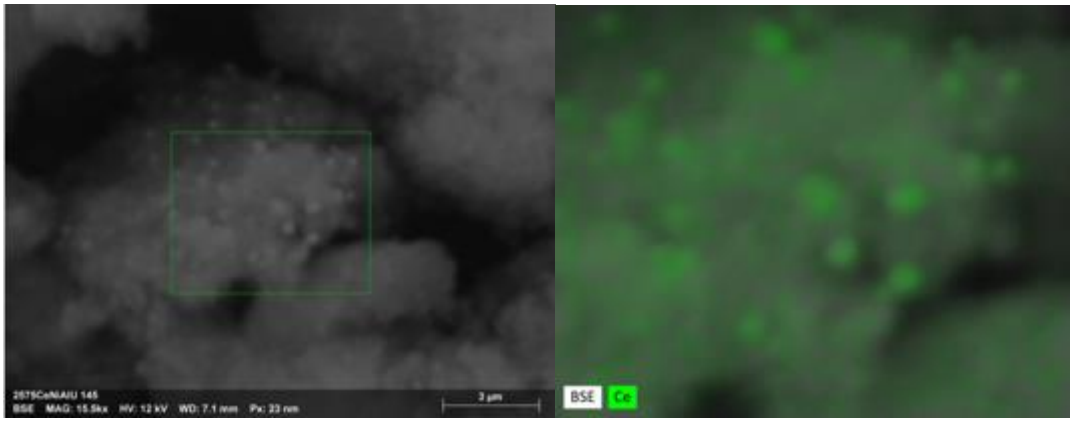

Figure 43. The image on the left is an SEM image of 25:75 CeNiAl aerogel after UCAT testing (scale bar = 3 µm), and the image on the right is the EDX image; green indicates cerium.

The cerium-containing particles were difficult to locate in the 25:75 CeNiAl sample after heat treatment as observed in Figure 41. The poor differentiation between the elements with EDX can be due to the blurry SEM image. However, slightly more distinct (ca. 1 µm), cerium-containing particles can be observed in the sample after UCAT testing at 3-µm magnification shown in Figure 43. Unlike the 50:50 CeNiAl and 75:25 CeNiAl samples, nickel-containing particles can also be observed in the 25:75 CeNiAl sample after UCAT testing at 200 µm magnification in Figure 42. The 25:75 CeNiAl contained more nickel salt than the 50:50 CeNiAl and 75:25 CeNiAl sample. Therefore, the nickel-containing particles may be easier to observe in the 75:25 CeNiAl.

The SEM and EDX images of 3x-50:50 CeNiAl samples after heat treatment and after UCAT testing can be viewed in Figures 44 and 45.

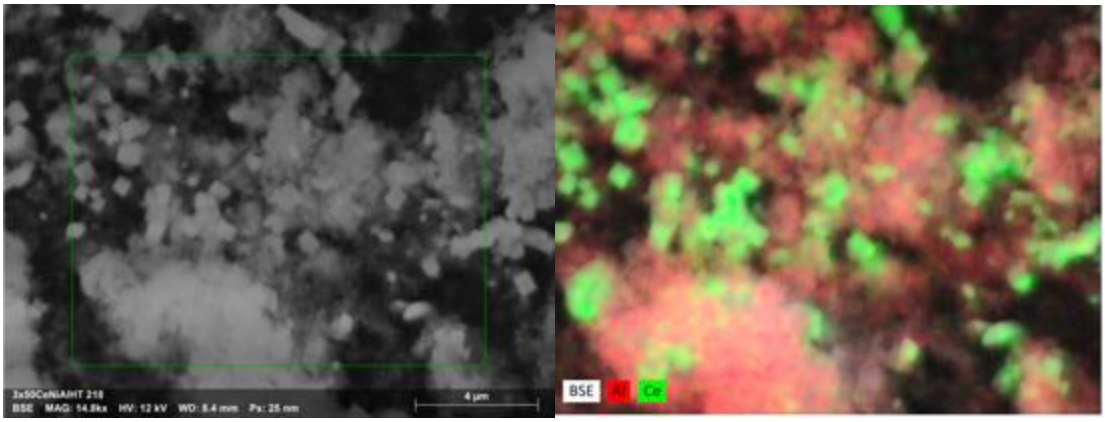

Figure 44. The image on the left is an SEM image of 3x-50:50 CeNiAl aerogel after heat treatment (scale bar = 4 µm), and the image on the right is the EDX image; red indicates aluminum and green indicates cerium.

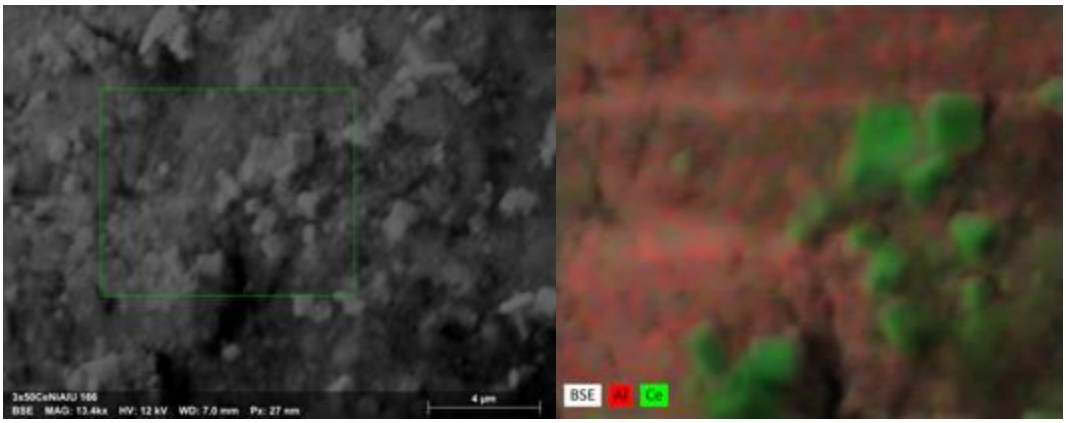

Figure 45. The image on the left is an SEM image of 3x-50:50 CeNiAl aerogel after UCAT testing (scale bar = 4 µm), and the image on the right is the EDX image; red indicates aluminum and green indicates cerium.

In Figure 44, cubic like particles can be identified at 4-µm magnification for the 3x-50:50 CeNiAl aerogel sample after heat treatment. The cubic like particles were identified as cerium-containing particles as observed by the EDX image in Figure 44. Cubic like cerium-containing particles in the 3x-50:50 CeNiAl after UCAT testing can be identified with SEM and EDX imaging.

The SEM and EDX images of NiAl samples after heat treatment can be viewed in Figure 46.

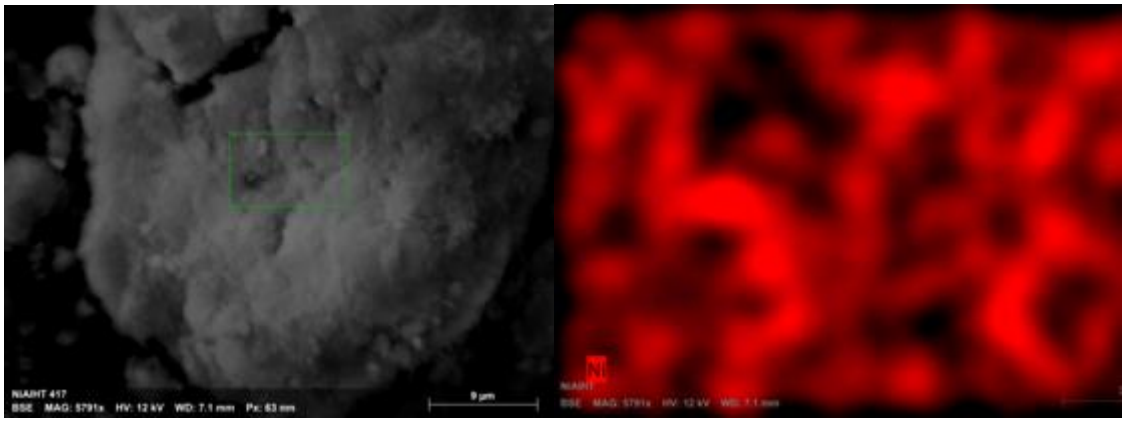

Figure 46. The image on the left is an SEM image of NiAl aerogel after heat treatment (scale bar = 9 µm), and the image on the right is the EDX image; red indicates nickel.

In Figure 46, metal-containing particles could not be observed for the NiAl sample after heat treatment; this differs from the other metal-containing alumina-based aerogels.

The SEM and EDX images of 50:50 CeNiSi samples after heat treatment and UCAT testing can be viewed in Figures 47 and 48.

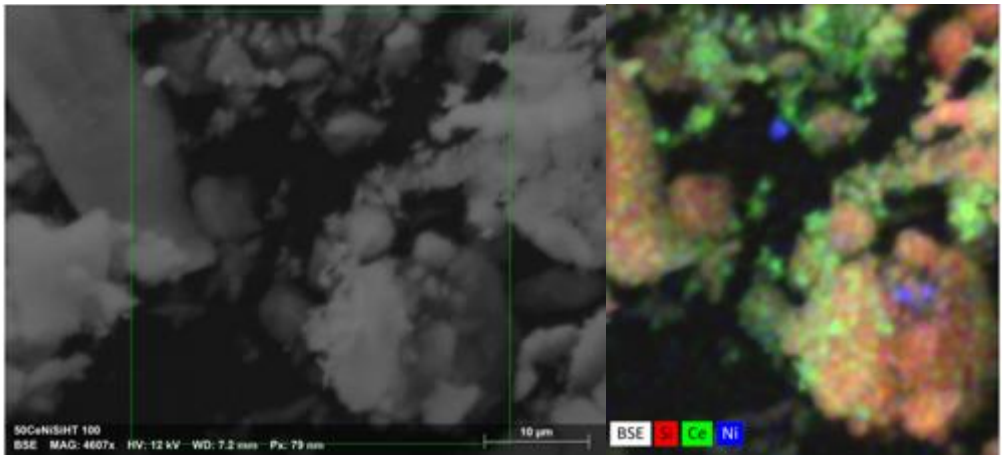

Figure 47. The image on the left is an SEM image of 50:50 CeNiSi aerogel after heat treatment (scale bar = 10 µm), and the image on the right is the EDX image; red indicates silica, green indicates cerium, and blue indicates nickel.

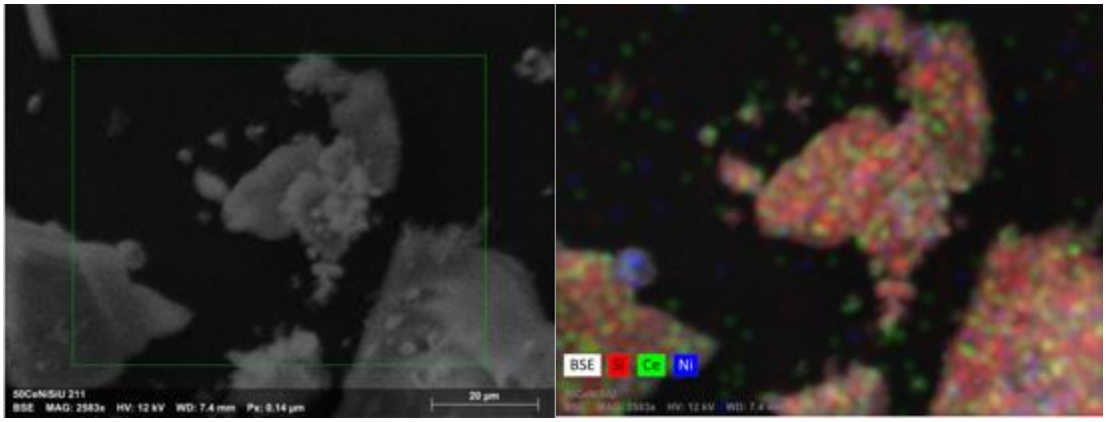

Figure 48. The image on the left is an SEM image of 50:50 CeNiSi aerogel after UCAT testing (scale bar = 20 µm), and the image on the right is the EDX image; red indicates silica, green indicates cerium, and blue indicates nickel.

In Figures 47 and 48, cerium-containing and nickel-containing particles can be observed for the 50:50 CeNiSi sample after heat treatment and after UCAT testing. The nickel-containing particles can be observed more distinctly (ca. 0.5 µm) in the silica-based aerogel than the alumina-based aerogels.

Throughout each of the CeNiAl and CeNiSi SEM images, small particles can be observed. The majority of the small particles contain cerium(IV) oxide based of the EDX images. Similar shaped particles have been observed previously in ceria-containing aerogels.[1] Nickel-containing particles were identified in the 25:75 CeNiAl and 50:50 CeNiSi samples. The nickel-containing particles (ca. 0.5 µm) are smaller than the ceria-containing particles (1 µm); therefore they were more difficult detect by SEM and EDX imaging. It is also possible that the majority of the nickel is incorporated into the alumina aerogel backbone in the CeNiAl aerogels and not present in microcrystalline form as it is in the NiAl aerogels. Based on the SEM and EDX images, majority of the cubic like particles were observed to be cerium-containing particles.

3.5. Union Catalytic Aerogel Testbed (UCAT)

The UCAT was used to evaluate the catalytic activity of each type of metal-containing alumina aerogels. Before UCAT testing, all aerogel samples were placed in a furnace at 800˚C, for approximately 24 h. The heat treatment is to prevent the samples from changing structure during the catalytic test runs. Each aerogel sample is catalytically tested three times at temperatures ranging from 200˚C to 600˚C at an increment of 50˚C.

The catalytic performance of HC (propane), NO, and CO gas of 50:50 CeNiAl heat-treated aerogel under the conditions of with air and without air can be observed in Figures 49, 50, and 51, respectively. The average conversion of HC, NO, and CO gas by 50:50 CeNiAl heat-treated aerogel can be observed in Figure 52.

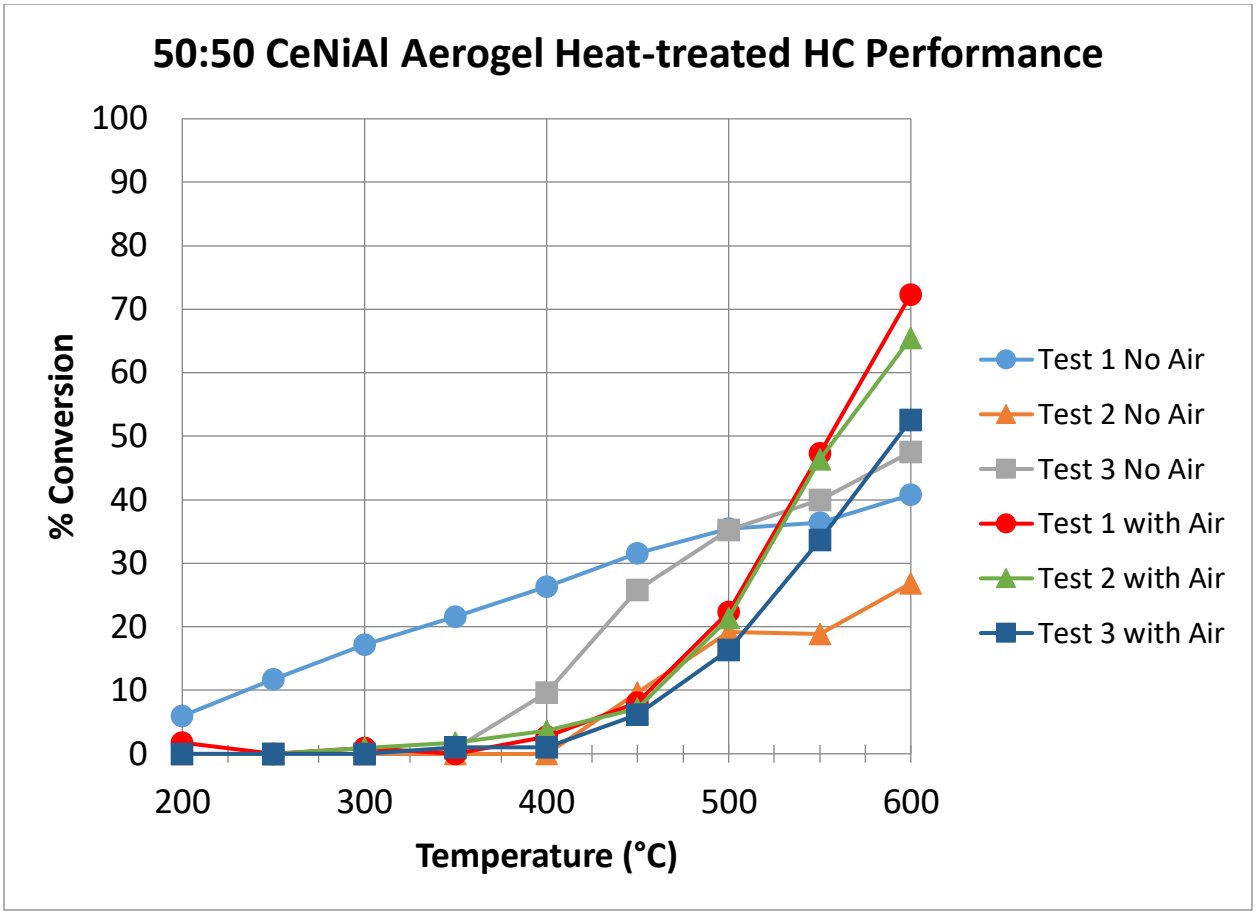

Figure 49. The percent conversion of HC by 50:50 CeNiAl heat-treated aerogel as a function of temperature: lines provided as guide to the eye.

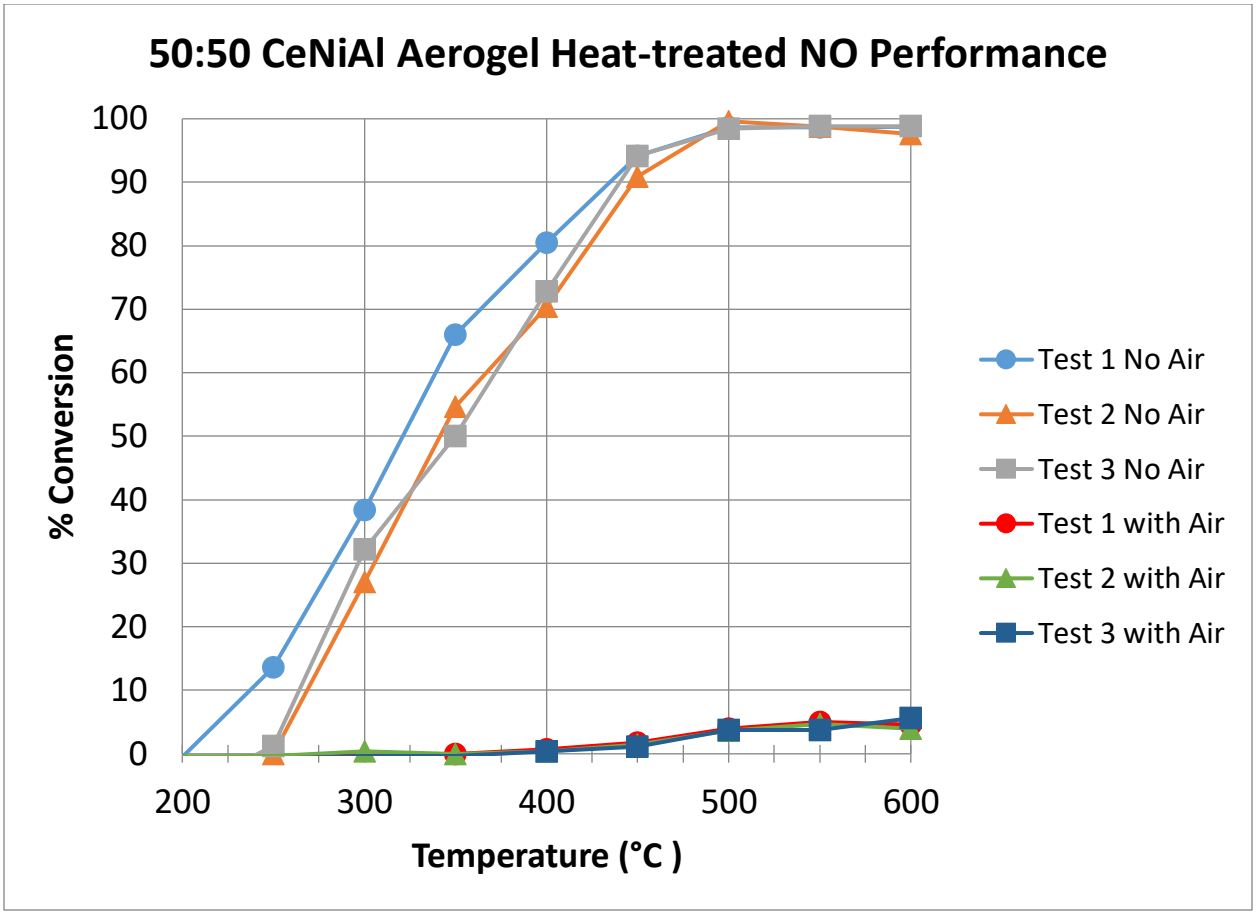

Figure 50. The percent performance of NO by 50:50 CeNiAl heat-treated aerogel as a function of temperature: lines provided as guide to the eye.

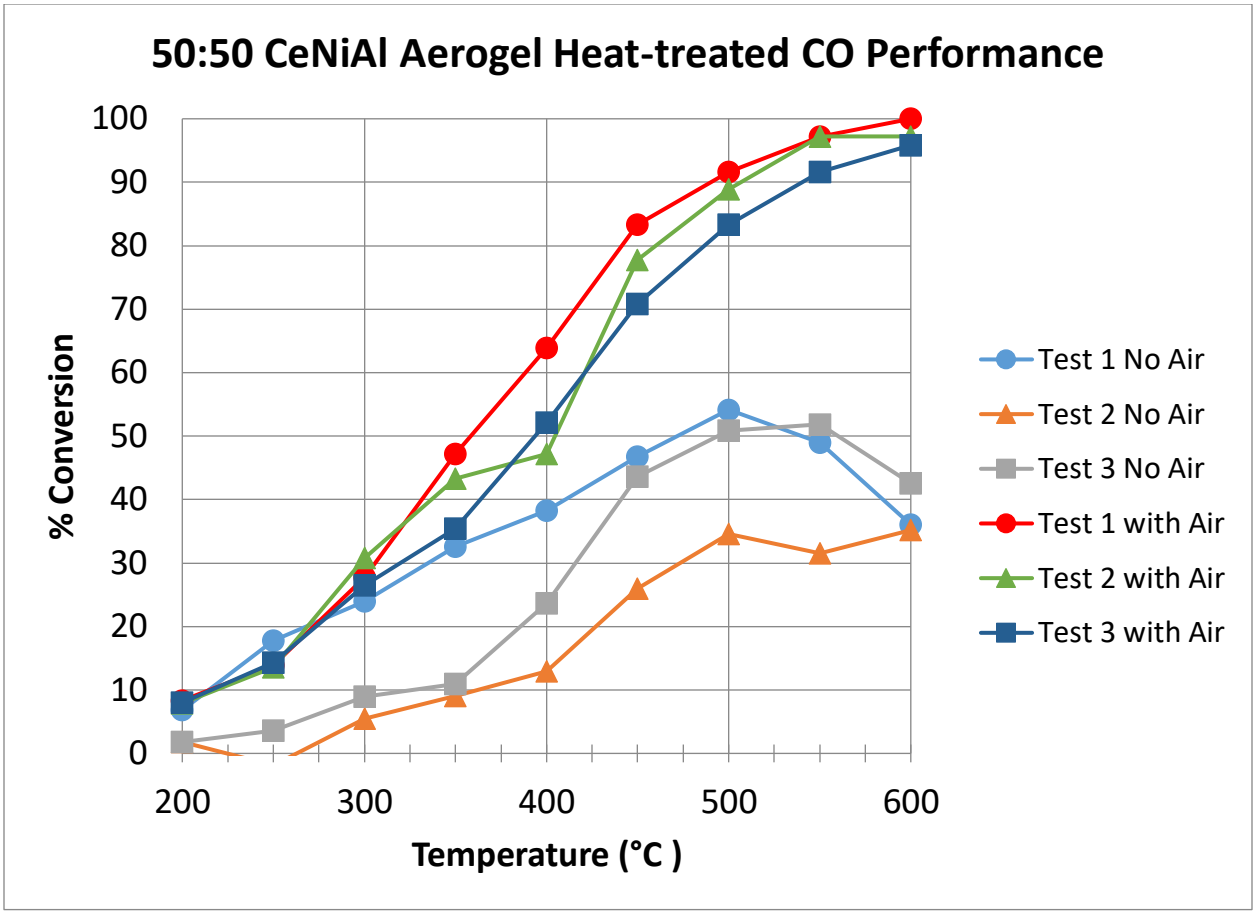

Figure 51. The percent performance of CO by 50:50 CeNiAl heat-treated aerogel as a function of temperature: lines provided as guide to the eye.

The conversion of HC by 50:50 CeNiAl observed in Figure 49 is not consistent throughout the three test runs. Unlike the 50:50 CeNiAl heat-treated aerogel HC catalytic test, the NO performance over the three test runs is consistent (Figure 50). The final conversion of CO for 50:50 CeNiAl heat-treated under with-air condition is consistent. However, it can be observed in Figure 51 that under without-air condition, the highest conversion rate of CO ranges from 30-50% conversion at 500˚C, whereas under with-air condition, the highest conversion of CO is at 600˚C.

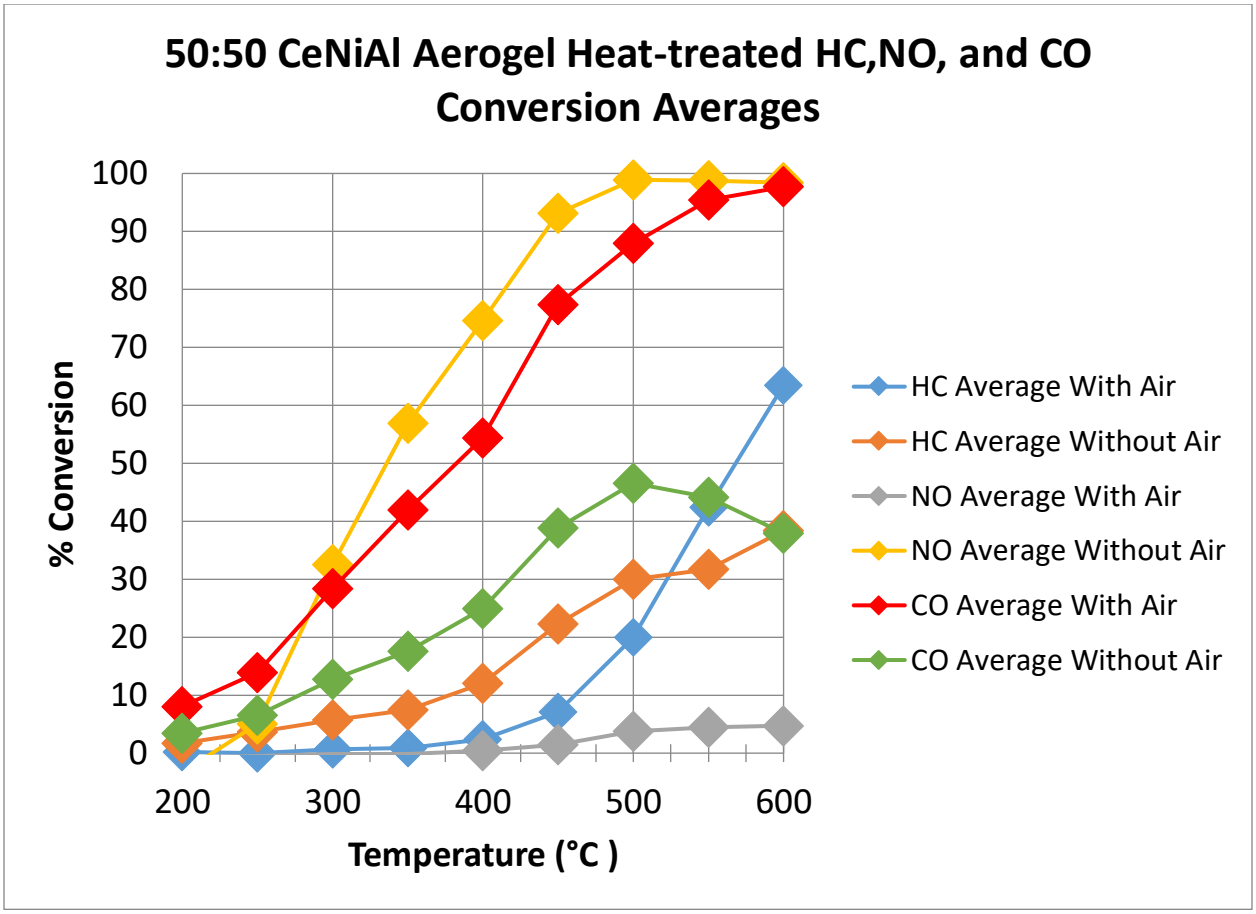

Figure 52. The average catalytic performance of 50:50 CeNiAl heat-treated aerogel for HC, NO, CO gas: lines provided as guide to the eye.

For each gas conversion averages, standard deviations in percentage of gas conversion between the three runs were calculated. Based on the three runs of the 50:50 CeNiAl sample, under without-air conditions, HC has a 38% +/- 9% conversion, NO has a 98.4 +/- 0.5% conversion, and CO has a 38 +/- 3% conversion. The light-off temperature for HC gas under without-air conditions was around 580˚C and approximately 350˚C for NO gas. Under with-air conditions, HC has a 64 +/- 8% conversion, and NO has a 4.7% +/- 0.7% conversion, and CO has a 98% +/- 2% conversion. The light-off temperature for CO gas under with-air conditions was approximately 380˚C. Under without -air conditions, each of the three major pollutants was being converted to some extent, with approximately 100% conversion of NO gas and 38% conversion for HC and CO gas.

Under with-air conditions, HC gas and CO gas were being converted, but NO gas was not converted.

The catalytic performance of HC, NO, and CO gas of 75:25 CeNiAl heat-treated aerogel under the conditions of with air and without air can be observed in Figure 53, 54, and 55, respectively. The average conversion of HC, NO, and CO gas by 75:25 CeNiAl heat-treated aerogel can be observed in Figure 56.

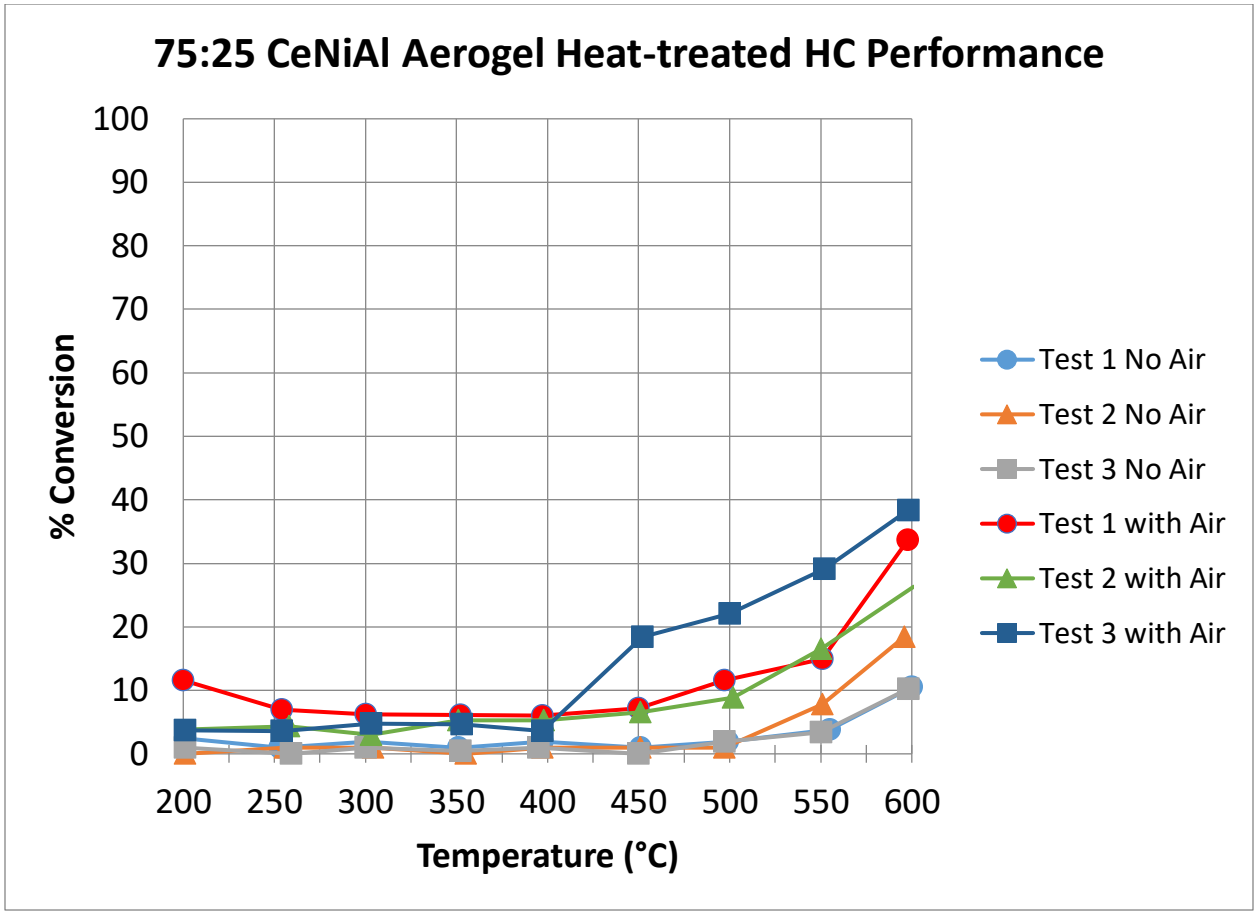

Figure 53. The percent conversion of HC by 75:25 CeNiAl heat-treated as a function of temperature: lines provided as guide to the eye.

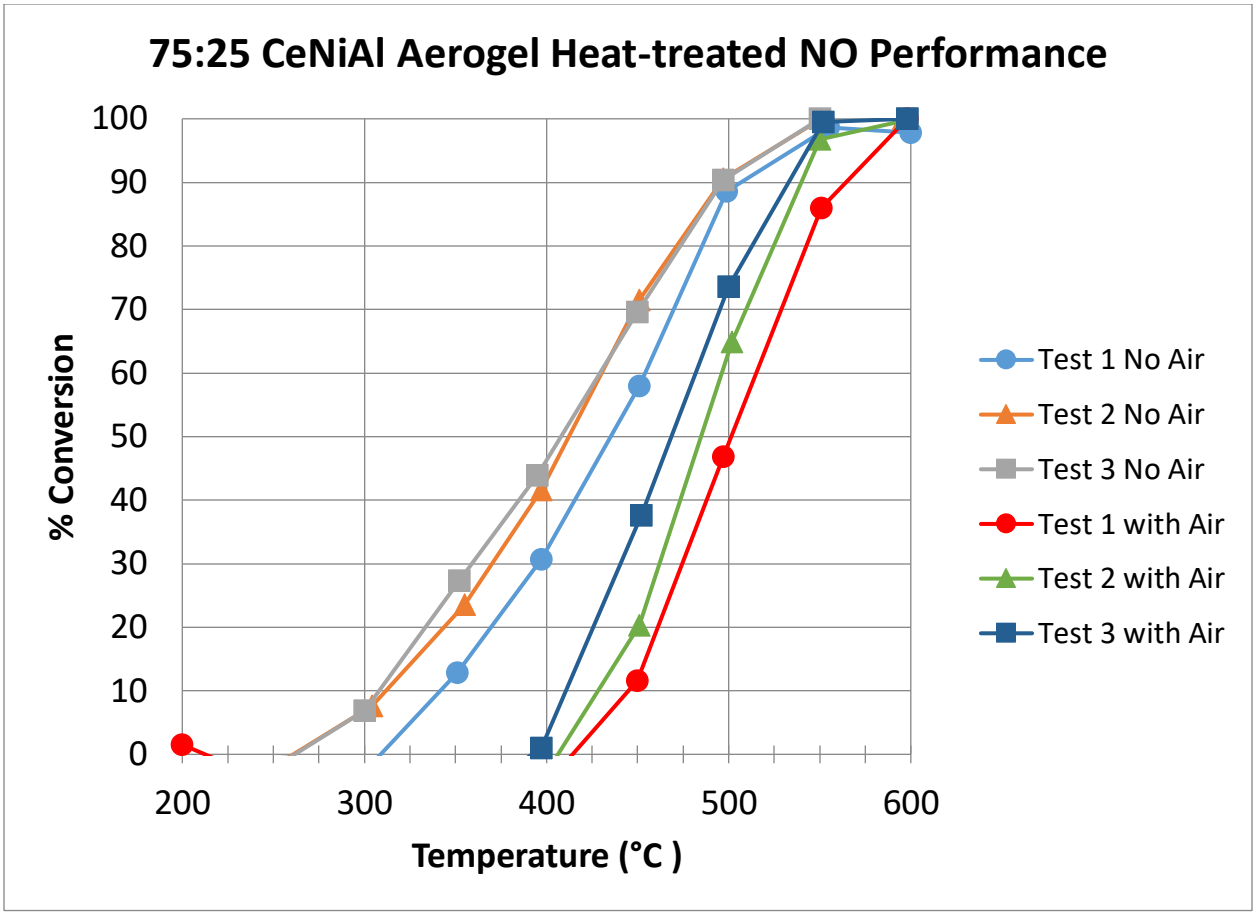

Figure 54. The percent conversion of NO by 75:25 CeNiAl heat-treated as a function of temperature: lines provided as guide to the eye.

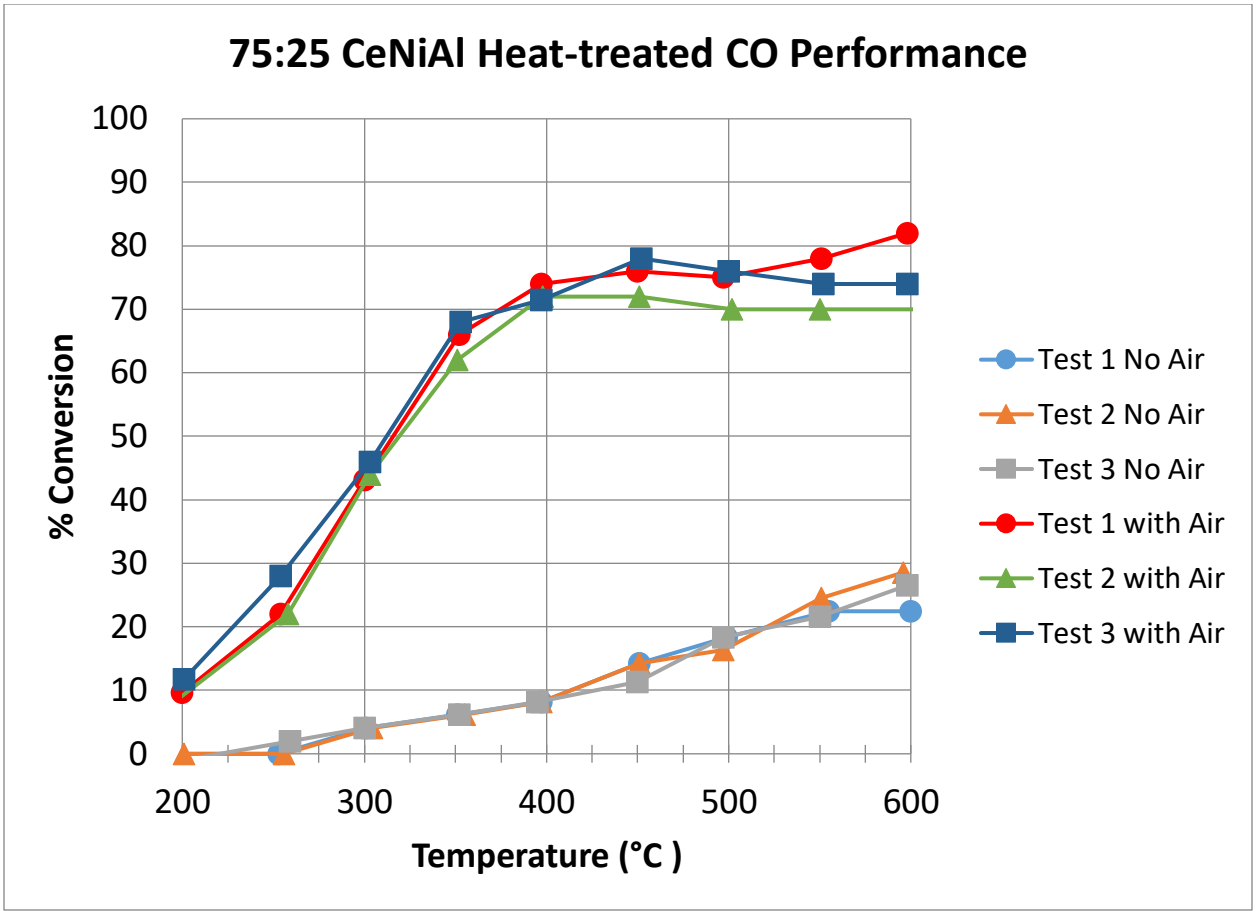

Figure 55. The percent conversion of CO by 75:25 CeNiAl heat-treated as a function of temperature: lines provided as guide to the eye.

Shown in Figure 53, under with-air and without-air conditions, the HC conversion of 75:25 CeNiAl heat-treated aerogel was below 40% conversion at the 600˚C. The overall conversion for HC of 75:25 CeNiAl heat-treated aerogel was lower than the 50:50 CeNiAl heat-treated sample. In Figure 54, it can be observed that the 75:25 CeNiAl heat-treated aerogel have approximately 100% conversion of NO under with-air and without-air conditions. In Figure 55, it can be observed that the overall conversion of CO for 75:25 CeNiAl heat-treated ranges from 70-80% under the with-air condition. On the other hand, the aerogel sample has an approximate range of 20-30% conversion of CO gas under the without-air condition.

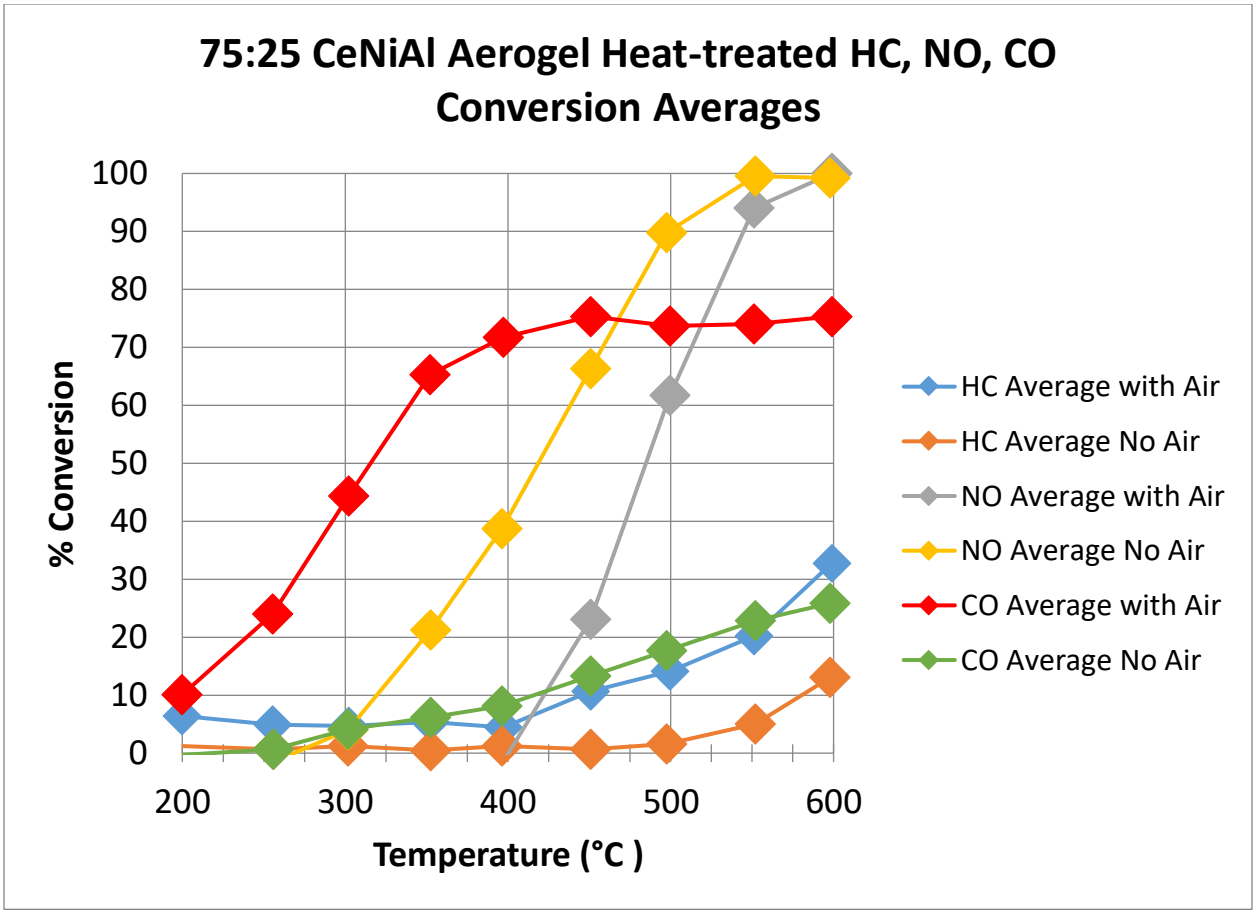

Figure 56. The average catalytic performance of 75:25 CeNiAl heat-treated for HC, NO, CO gas: lines provided as guide to the eye.

The standard deviation in percentage of gas conversion between the three runs were calculated for each gas conversion average. In Figure 56, the average conversion of 75:25 CeNiAl heat-treated aerogel for HC, NO, and CO gas can be observed. Under without-air conditions, HC has a 13% +/- 4% conversion, NO has a 99 +/- 1% conversion, and CO has a 26 +/- 3% conversion. The light-off temperature for NO gas under without-air conditions was around 410˚C. Under with-air conditions, HC has a 33 +/- 5% conversion, NO has a 100% conversion, and CO has a 75% +/- 5% conversion. The light-off temperature under with-air conditions was approximately 300˚C for CO and 380˚C for NO. Under without-air and with-air conditions, all three major pollutants were being

converted to some extent, with approximately 100% conversion of NO gas under both conditions.

The catalytic performance of HC, NO, and CO gas of 25:75 CeNiAl heat-treated aerogels under with-air and without-air conditions can be observed in Figure 57, 58, and 59. respectively. The average conversion of HC, NO, and CO gas of 25:75 CeNiAl heat-treated aerogel can be observed in Figure 60.

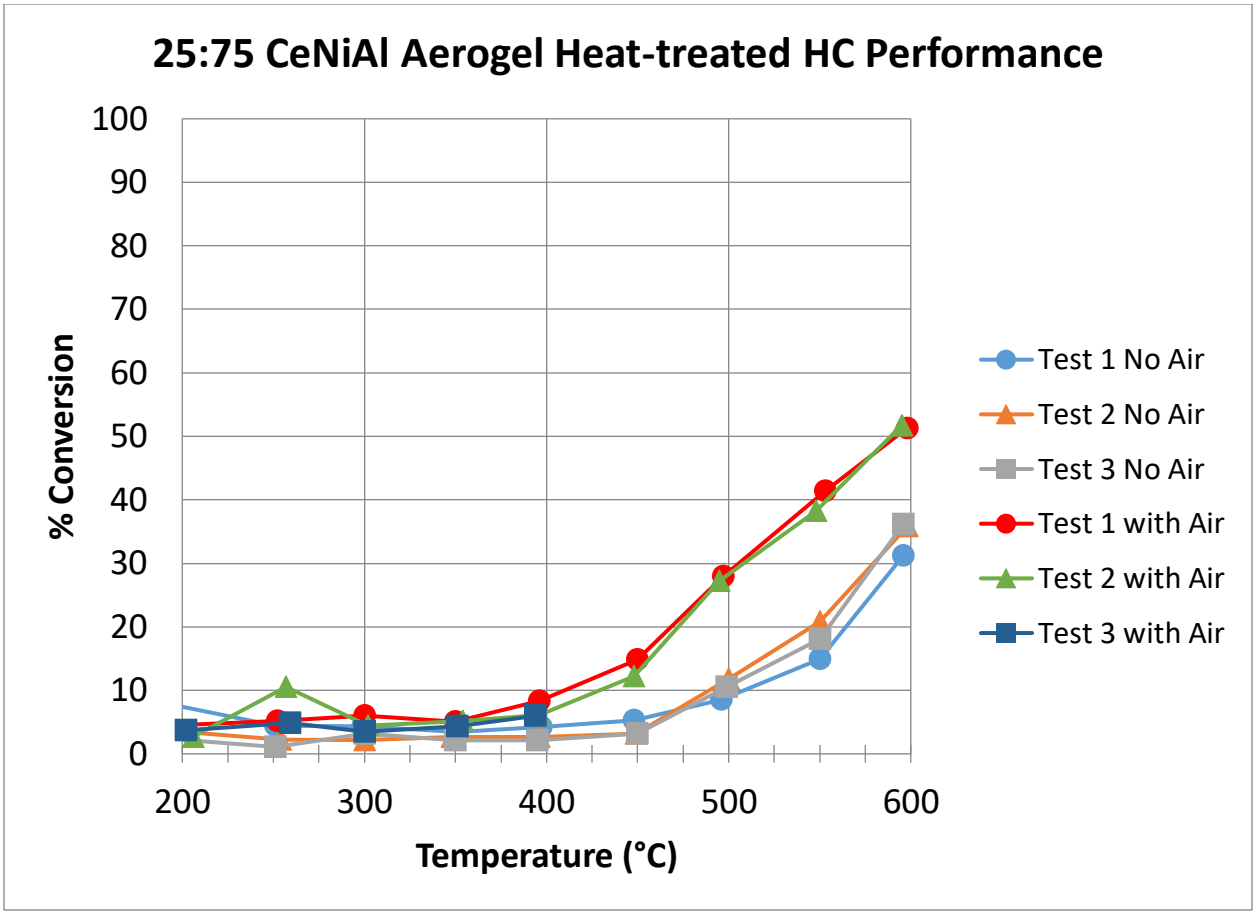

Figure 57. The percent conversion of HC by 25:75 CeNiAl heat-treated as a function of temperature: lines provided as guide to the eye.

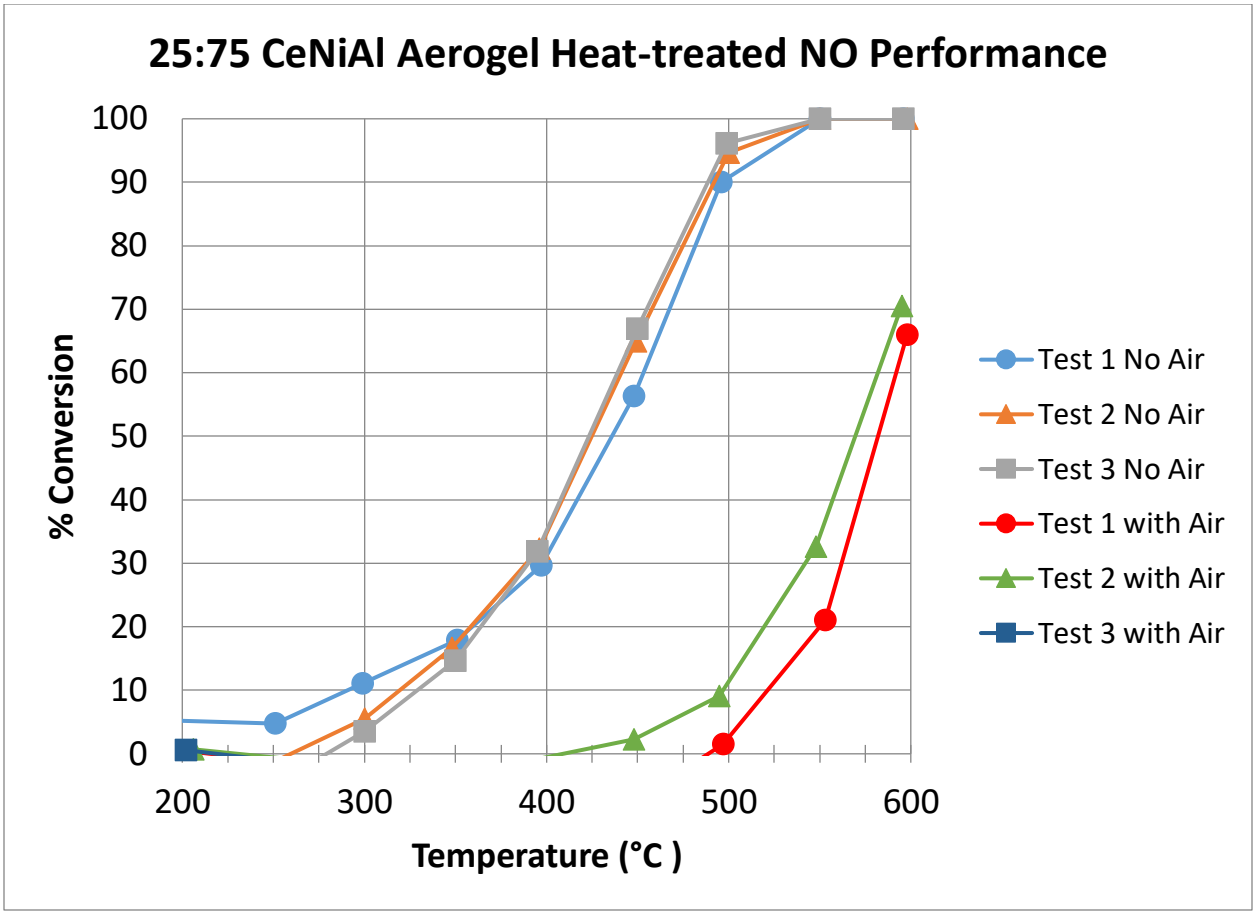

Figure 58. The percent conversion of NO by 25:75 CeNiAl heat-treated as a function of temperature: lines provided as guide to the eye.

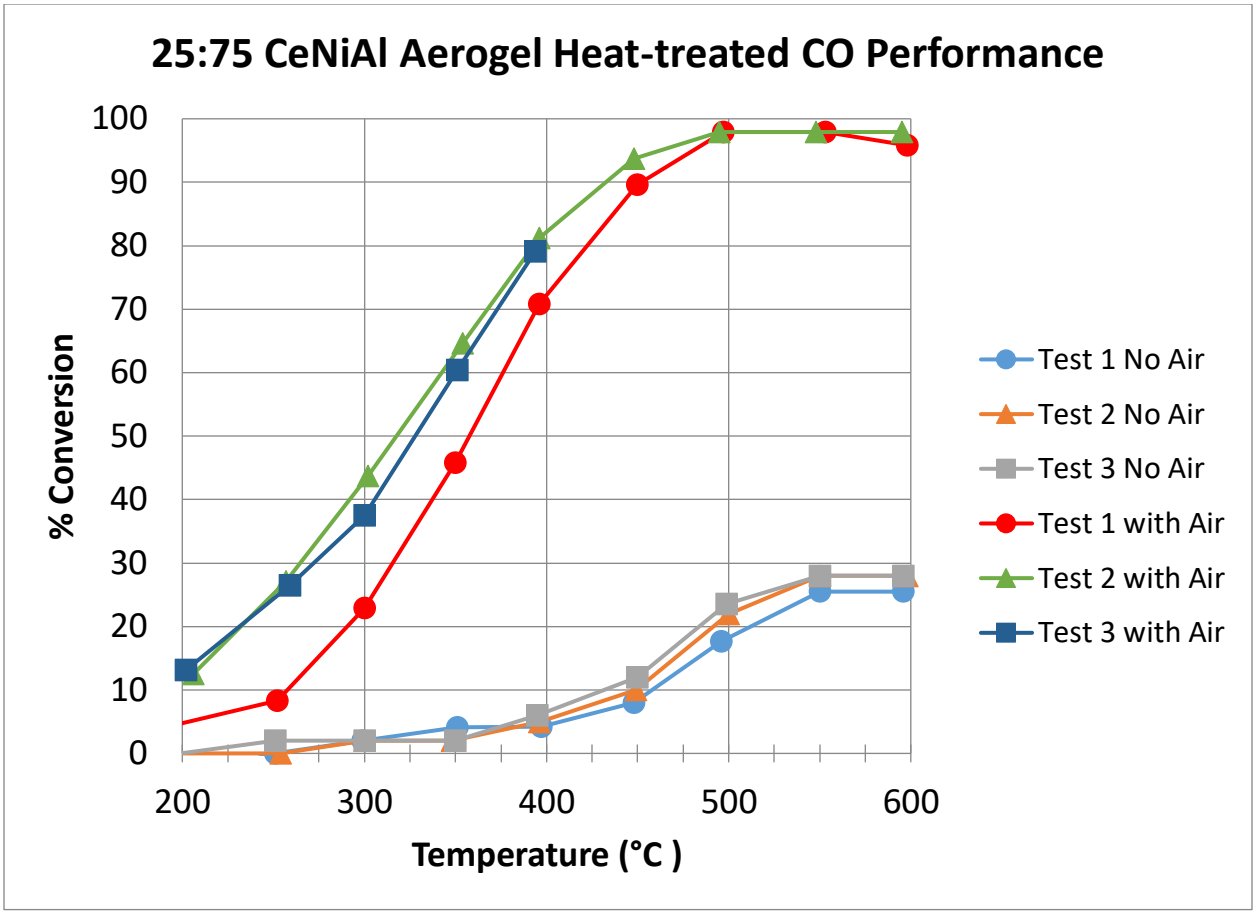

Figure 59. The percent conversion of CO by 25:75 CeNiAl heat-treated as a function of temperature: lines provided as guide to the eye.

In Figure 57, it can be seen that the results are consistent between all three test runs. Under without air condition, the HC conversion was approximately 30% at 600˚C. Under with air condition, the HC conversion is approximately 50% at 600˚C. The three-test run NO performance is consistent as shown in Figure 58. The NO gas has an approximate of 100% at 550˚C under without air condition, and approximately 78% conversion of NO gas under with air condition. Like the other test-runs for 25:75 CeNiAl heat-treated, the results are consistent as observed in Figure 59. CO gas has an approximate 30% conversion at 600˚C under with air condition, and approximately 100% at 500˚C under without air condition.

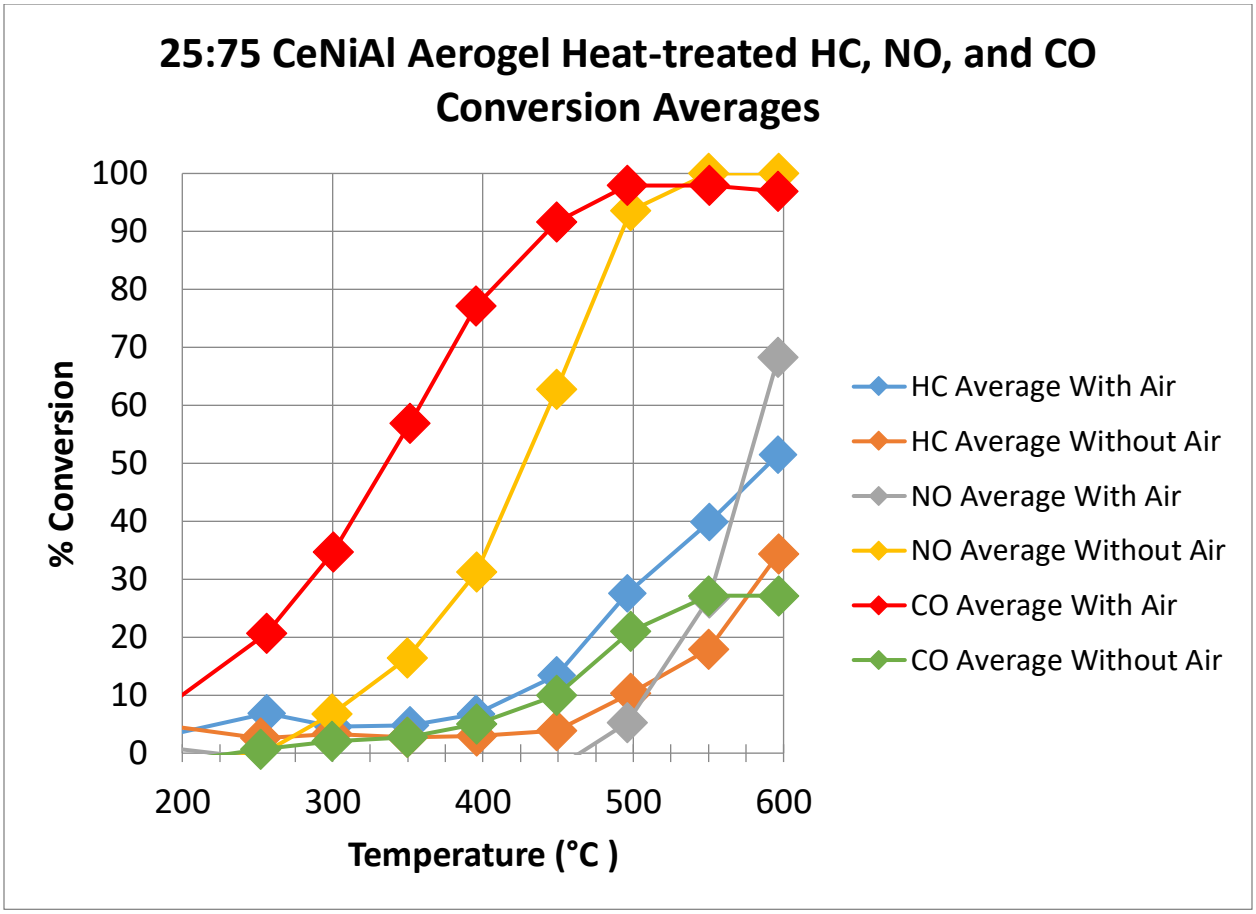

Figure 60. The average catalytic performance of 25:75 CeNiAl heat-treated for HC, NO, CO gas: lines provided as guide to the eye.

The standard deviations in percentage of gas conversion between the three runs were calculated for each gas conversion averages. Under without air conditions, HC has a 34% +/- 2% conversion, NO has a 100% conversion, and CO has a 27 +/- 1% conversion. The light-off temperature for NO gas under without air conditions was around 420˚C. Under with air conditions, HC has a 51.5 +/- 0.2% conversion, and NO has a 68% +/0 2%% conversion, and CO has a 97% +/- 1% conversion. Under with air condition, the light-off temperature for HC gas was approximately 600˚C. The light-off temperature for NO and CO gas was 560˚C and 330˚C respectively. Under without air and with air conditions, all the three-major pollutants were being converted to some extent, with approximately a

100% conversion of NO and CO gas under without air condition and with air respectively.

The catalytic performance of HC, NO, and CO gas of 3x-50:50 CeNiAl heat-treated under the conditions of with air and without air can be observed in Figure 61, 62, and 63 respectively. The average performance of HC, NO, and CO gas of 3x-50:50 CeNiAl heat-treated can be observed in Figure 64. For only 3x-50:50 CeNiAl samples, only two full UCAT test runs were performed.

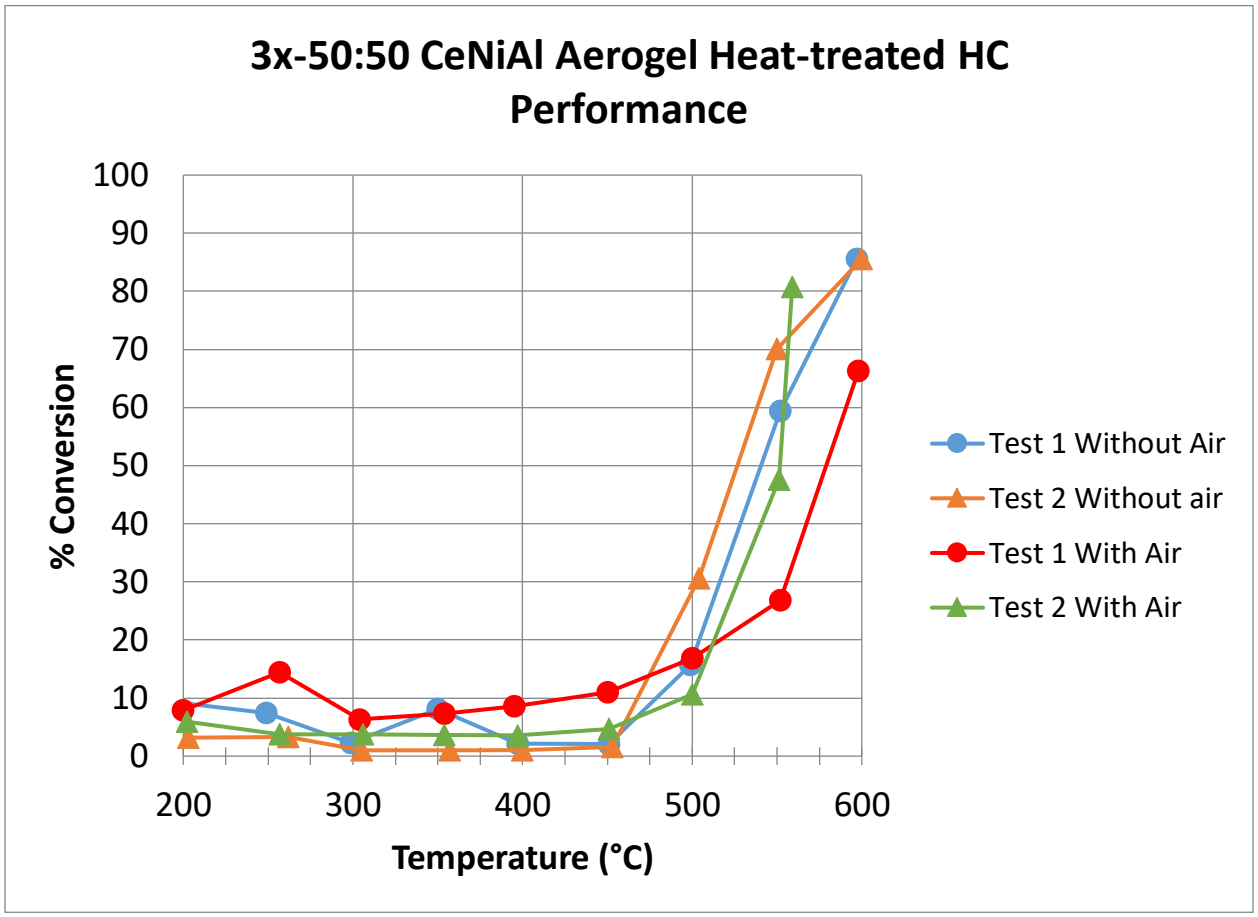

Figure 61. The percent conversion of HC by 3x-50:50 CeNiAl heat-treated as a function of temperature: lines provided as guide to the eye.

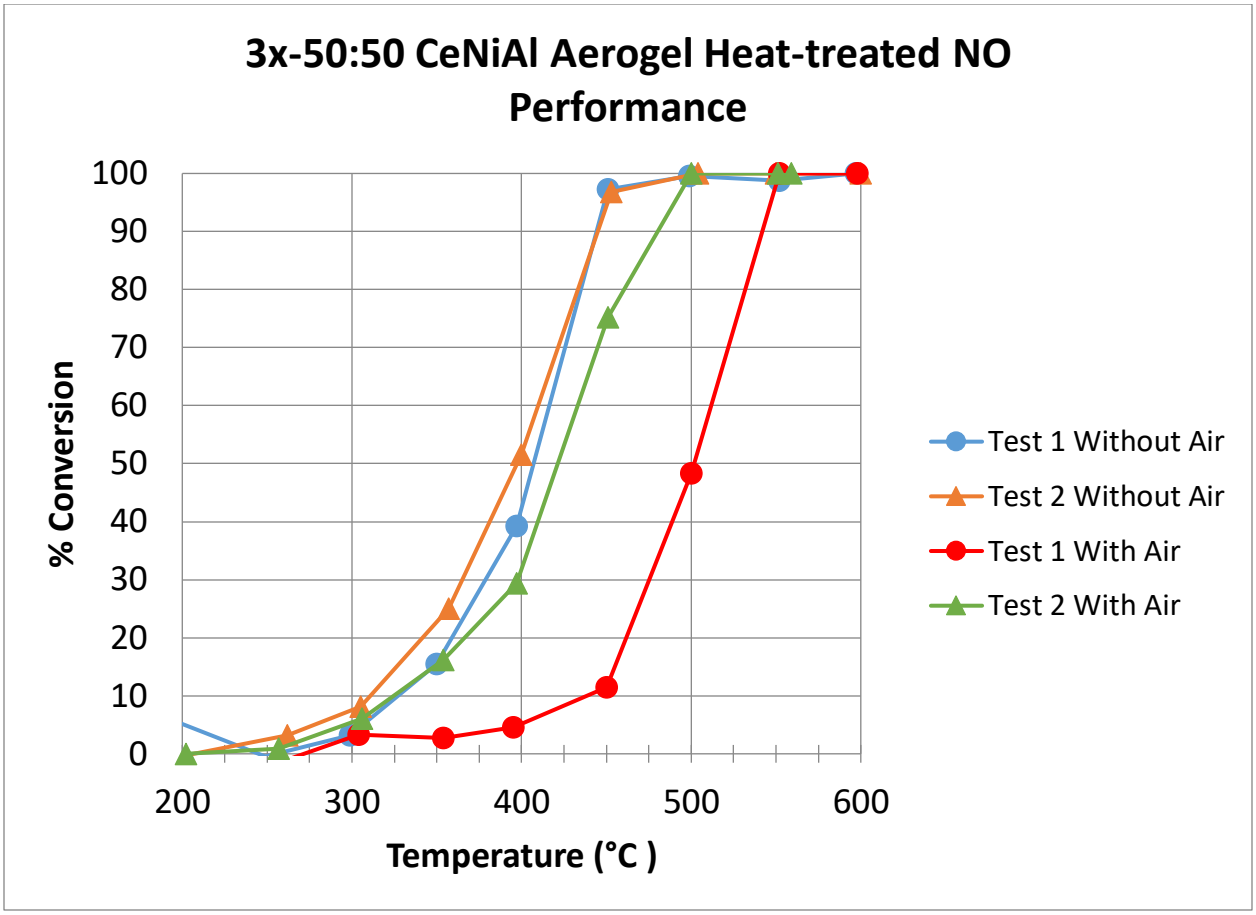

Figure 62. The percent conversion of NO by 3x-50:50 CeNiAl heat-treated as a function of temperature: lines provided as guide to the eye.

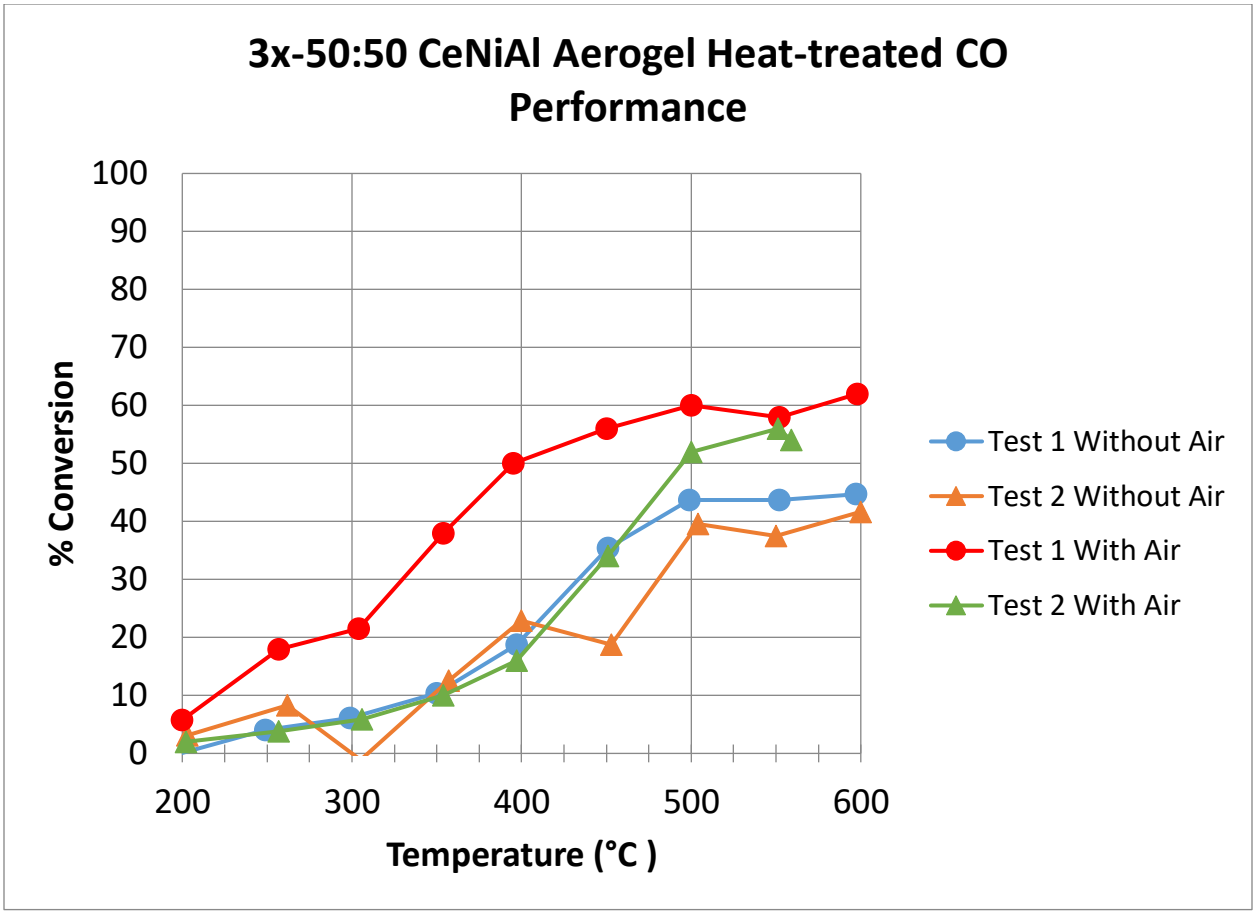

Figure 63. The percent conversion of CO by 3x-50:50 CeNiAl heat-treated as a function of temperature: lines provided as guide to the eye.

In Figures 61, it can be observed that the two test runs for 3x-50:50 CeNiAl heat-treated under with air and without air is not completely consistent. The 3x-50:50 CeNiAl heat-treated aerogel showed conversions of HC under both conditions. The HC gas conversion reached as high as approximately 85% conversion for the test run without air condition, and it reached approximately 65% HC conversion with air condition. The light-off temperature for the 3x-50:50 CeNiAl heat-treated sample is approximately 550˚C under both conditions. Like the 3x-50:50 CeNiAl heat-treated aerogel HC performance, the aerogel also converted NO under with air and without air conditions. Under both conditions, the aerogel reached approximately 100% NO conversion at 450˚C. The light-

off temperature observed in Figure 62 for both aerogels is approximately 400˚C. Shown in Figure 63. the aerogel converted CO under with and without air conditions. Under both conditions, the CO conversion ranged between 40%-60%. Observed in Figure 63, the CO conversion for 3x-50:50 CeNiAl under both conditions seemed to flat-lined after 500˚C.

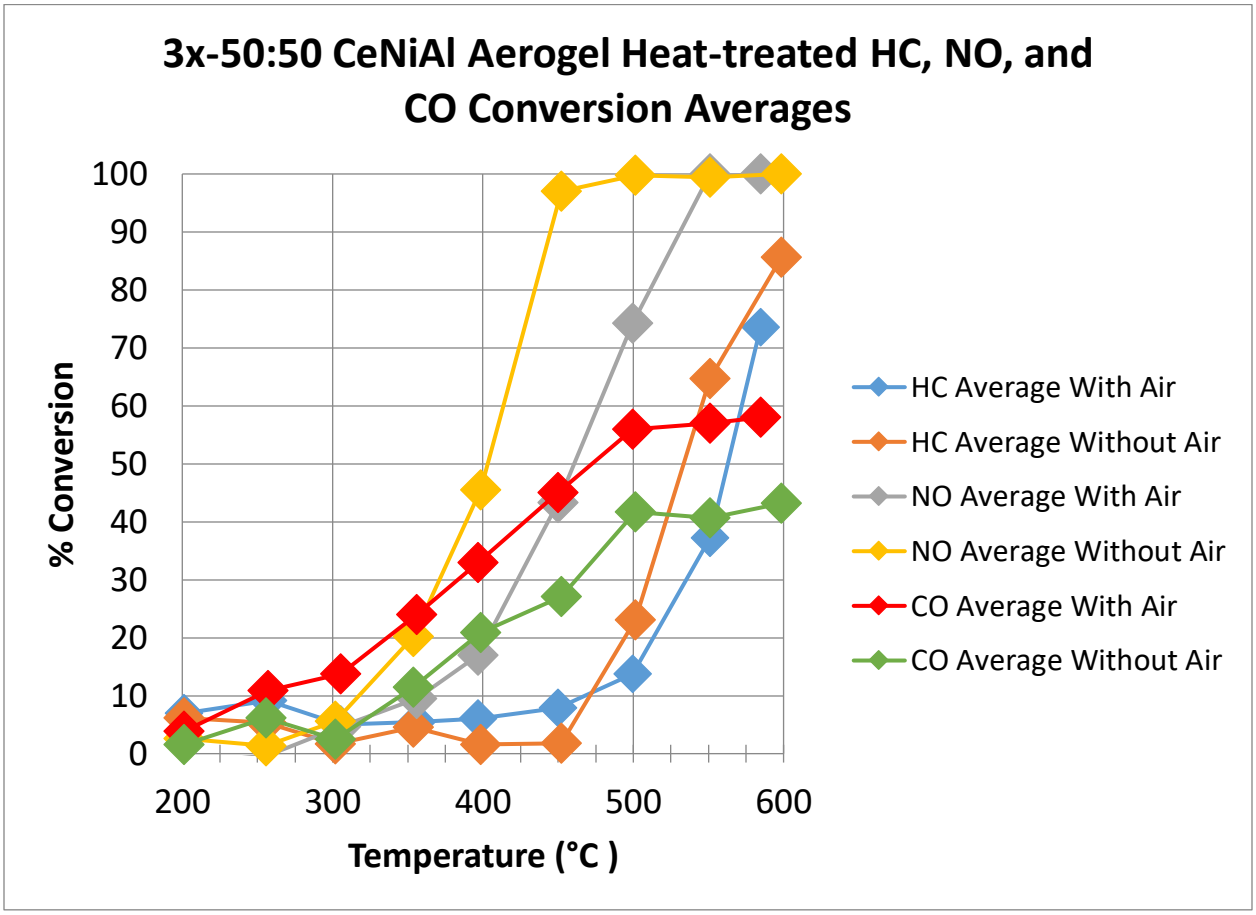

Figure 64. The average catalytic performance of 3x-50:50 CeNiAl heat-treated for HC, NO, CO gas: lines provided as guide to the eye.

The standard deviations in percentage of gas conversion between the three runs were calculated for each gas conversion averages. Under without air conditions, HC has an 85.6% conversion, NO has a 100% conversion, and CO has a 43 +/- 2% conversion. The light-off temperature for HC and NO gas under without air condition was around 525˚C and 400˚C. Under with air conditions, HC has a 78 +/- 11% conversion, and NO has a

100 conversion, and CO has a 58% +/- 4% conversion. Under with air condition, the light-off temperature for HC was approximately 550˚C. The light NO and CO gas was approximately 450˚C and 475˚C respectively. Under without air and with air conditions, all the three-major pollutants were being converted to some extent as observed in Figure 64.

The tabulated average conversion of HC, NO, and CO gas under with-air and without-air conditions for 50:50 CeNiAl, 75:25 CeNiAl, 25:75 CeNiAl, and 3x-50:50 CeNiAl can be found in Table 5. The aerogel samples were also compared with previous work on cerium-containing aerogels by Luisa Posada.[1]

Samples	HC with Air	HC without Air	NO with Air	NO without Air	CO with Air	CO without Air
CeAl[1]	84%	0%	0%	99%	100%	30%
25:75 CeNiAl	51.5% +/- 0.2%	34% +/- 2%	68% +/- 2%	100%	97% +/- 1%	27% +/- 1%
50:50 CeNiAl	64 +/- 8%	38% +/- 9%	4.7% +/- 0.7%	98.4 +/- 0.5%	98% +/- 2%	38 +/- 3%
3x-50:50 CeNiAl	78 +/- 11%	85.6%	100%	100%	58% +/- 4%	43% +/-2%
75:25 CeNiAl	33% +/- 5%	13% +/- 4%	100%	99% +/- 1%	75% +/- 5%	26% +/- 3%

Table 5. The conversion of HC, NO, and CO gas under with-air and without-air conditions for CeAl, 25:75 CeNiAl, 50:50 CeNiAl, 3x-50:50 CeNiAl, and 75:25 CeNiAl aerogels.

Observed in Table 5, under with-air condition, all the CeNiAl aerogel samples underperformed compared to CeAl aerogels. 3x-50:50 has a higher conversion of HC compared to 25:75 CeNiAl aerogels. However, there was not a trend in increasing conversion of HC gas under with-air conditions in increasing cerium or nickel metals. All the CeNiAl aerogels converted HC gas under without-air conditions, unlike CeAl aerogels. Under without-air conditions, 25:75 CeNiAl and 50:50 CeNiAl aerogels converted HC gas nearly the same amount with 34% +/- 2% and 38% +/- 9% respectively. 3x-50:50 CeNiAl also converted HC the same amount under both conditions with 78 +/-11 % under with air and 85.6% without air. The CeNiAl aerogels converted the HC gas less than half under without-air conditions compared to the aerogels with air conditions. The 50:50 CeNiAl gas did not have a significant amount of NO conversion, but the 3x-50:50 CeNiAl has approximately 100% NO conversion under with-air conditions. It can be observed in Table 5 that the conversion of NO increased with higher amounts of cerium metal under with air conditions. All the aerogel samples had approximately 100% conversion of NO gas under without air conditions. All the aerogels had nearly 100% conversion of CO gas under with-air conditions, with the exception of 75:25 CeNiAl, which had 75% +/- 5% CO conversion. Under without air condition, 25:75 CeNiAl and 75:25 CeNiAl had almost identical CO conversion with 27% +/- 1% and 26 +/- 3% conversion respectively. The 50:50 CeNiAl and 3x-50:50 CeNiAl also had almost identical CO conversion under with-air condition with 38% +/- 3% and 43% +/-2%, respectively. The conversion of NO gas under with air conditions was surprising because it was not expected that NO will be reduced when oxygen is present. Observed in Table 5, it does not appear that nickel salt is enhancing the catalytic

performance of cerium salt because there was not an increase in conversion for HC and CO gas under both conditions. However, the presence of nickel helped convert NO gas under both conditions, which is favorable for the performance of a catalytic aerogel.

Looking at the various mole ratio of cerium and nickel metals in CeNiAl aerogels, there does not appear to be a trend for any of the gas pollutants. The only consistent gas conversion was NO gas under without-air condition, where all the metal-containing aerogel samples had a 100% NO conversion. There may be a certain amount of cerium and nickel metal required for optimal HC, NO, and CO conversion. However, the CeNiAl seem to be a better catalytic aerogel than CeAl aerogels because the CeNiAl aerogels converted all the gas pollutants to a certain extent in both conditions. The viability of CeNiAl aerogels for automotive exhaust conversion is still in question because the light-off temperature for all the samples was ca. 400˚C or higher.

Reference

1. Luisa Posada. “Fabrication and Characterization of Ceria-Containing Aerogels.” Senior Thesis, Union College, 2017.

2. ChemLibre Texts. Infrared Spectroscopy Absorption Table. https://chem.libretexts.org/Reference/Reference_Tables/Spectroscopic_Parameters/Infrared_Spectroscopy_Absorption_Table (accessed June 10, 2019).

3. Ziyi Zhong, Yitzhak Mastai, Yuri Koltypin, Yanming Zhao, and Aharon Gedanken. “Sonochemical Coating of Nanosized Nickel on Alumina Submicrospheres and the Interaction between the Nickel and Nickel(II) oxide with the Substrate.” *Chem. Mater.* **1999**, 11, 2350-2359

Conclusions and Future Work

Cerium-nickel-alumina, nickel-alumina, and cerium-nickel-silica aerogels were successfully synthesized and characterized. All the wet gels were made via the co-precursors method, and the aerogels were made by the rapid supercritical extraction (RSCE) of the solvents process with a hydraulic hot press. All the aerogels were heat-treated, and color, volume, and mass changes were noticed for all the aerogels. This suggests a chemical and structural change in the aerogels during heat treatment.

The IR spectra of all the alumina-based aerogels as prepared showed the presence of Al-O-H and Al-H peaks. Some alumina-based aerogels as prepared showed the presence of O-H stretch: 75:25 CeNiAl, 25:75 CeNiAl, and NiAl. After heat treatment, the O-H stretch disappeared, which suggested the excess solvents that were either left behind after the RSCE method or adsorbed from the atmosphere were expelled from the aerogels. Peaks attributed to Al-O were also observed in the alumina-based aerogels after heat treatment. For the silica-based aerogel, peaks attributed to Si-O-Si before and after heat treatment were observed. The overall conclusion from the IR spectra was that alumina-based and silica-based aerogels were successfully synthesized.

The XRD data revealed majority of the peaks attributed to cerium(IV) oxide and nickel(II) oxide after heat treatment and after UCAT testing for the cerium-nickel-containing aerogels. Cerium(IV) oxide peaks were identified in previous experiments by Luisa Posada, and nickel(II) oxide peaks were identified by the literature from Ziyi Zhong. In the alumina-based aerogels, boehmite alumina peaks were present after heat treatment and after UCAT testing. In the silica-based aerogels, silica peaks were present after heat treatment and after UCAT testing. Observed across all the XRD patterns, peaks

disappeared from the XRD pattern of the aerogels that had been present before heat treatment. Compared to the XRD patterns of the aerogels after heat treatment, the XRD patterns remained identical for the aerogel samples after UCAT testing. This suggested the aerogels gone through structural change after heat treatment, but the aerogels remained the same after UCAT testing. The unchanged XRD patterns after UCAT testing for the metal-containing-aerogels means the aerogels potentially have the temperature stability needed in an automotive exhaust catalyst. Further study on the structural changes that occur during heat treatment could be undertaken with the newly purchased XRD. XRD patterns of the aerogel samples will be taken as during *in situ* heat treatment of aerogel samples.

The SEM and EDX images revealed cubic like particles mostly associated with cerium(IV) oxide in all the cerium-nickel-containing aerogels. Rarely were nickel-containing particles identified, with the exception of the 25:75 CeNiAl and 50:50 CeNiSi samples. This suggested the majority of the nickel might have been incorporated into the alumina backbone and not present in the microcrystalline form. The same result was observed for the NiAl aerogels. Another suggestion is that the nickel-containing crystals are too small to be imaged with the SEM used in this experiment.

The catalytic performance from the UCAT tests showed promising conversion of NO gas for CeNiAl aerogels under without-air conditions, where at 600˚C all the aerogels reached 100% NO conversion. The same can be said for the CeNiAl aerogels for CO gas under with-air conditions. Under both conditions, all the CeNiAl aerogels converted the gas pollutants to a certain extent, where the lowest conversion of gases were HC and CO under without air conditions. Overall, it is advantageous for the CeNiAl to convert the

gas pollutants under both conditions. Although the CeNiAl converted the gas pollutants in both conditions to a certain extent, the light-off temperature for the HC, NO, and CO gases were approximately 400˚C or higher. Compared to the CeAl aerogels, the CeNiAl aerogels converted HC gas under with air and No gas with air. Further catalytic testing needs to be done on NiAl and CeNiSi aerogels to understand why the aerogels converted the pollutants under both conditions and the catalytic performance of silica-based aerogels compared to alumina-based aerogels.